NAVAL
POSTGRADUATE
SCHOOL

MONTEREY, CALIFORNIA

THESIS

**THE MODIFICATION OF HOMER SOFTWARE
APPLICATION TO PROVIDE THE UNITED STATES
MARINE CORPS WITH AN ENERGY PLANNING TOOL**

by

Alexis R. Harvey

December 2012

Thesis Advisor:	Sherif Michael
Second Advisor:	Daniel Nussbaum

Approved for public release, distribution is unlimited

THIS PAGE INTENTIONALLY LEFT BLANK

REPORT DOCUMENTATION PAGE		*Form Approved OMB No. 0704-0188*

Public reporting burden for this collection of information is estimated to average 1 hour per response, including the time for reviewing instruction, searching existing data sources, gathering and maintaining the data needed, and completing and reviewing the collection of information. Send comments regarding this burden estimate or any other aspect of this collection of information, including suggestions for reducing this burden, to Washington headquarters Services, Directorate for Information Operations and Reports, 1215 Jefferson Davis Highway, Suite 1204, Arlington, VA 22202-4302, and to the Office of Management and Budget, Paperwork Reduction Project (0704-0188) Washington DC 20503.

1. AGENCY USE ONLY *(Leave blank)*	2. REPORT DATE December 2012	3. REPORT TYPE AND DATES COVERED Master's Thesis	
4. TITLE AND SUBTITLE The Modification of HOMER Software Application to Provide the United States Marine Corps with an Energy Planning Tool		5. FUNDING NUMBERS	
6. AUTHOR(S) Alexis R. Harvey			

7. PERFORMING ORGANIZATION NAME(S) AND ADDRESS(ES)
    Naval Postgraduate School
    Monterey, CA 93943-5000
		8. PERFORMING ORGANIZATION REPORT NUMBER	

9. SPONSORING /MONITORING AGENCY NAME(S) AND ADDRESS(ES)
    N/A
		10. SPONSORING/MONITORING
		     AGENCY REPORT NUMBER	

11. SUPPLEMENTARY NOTES The views expressed in this thesis are those of the author and do not reflect the official policy or position of the Department of Defense or the U.S. Government. IRB Protocol number: N/A.

12a. DISTRIBUTION / AVAILABILITY STATEMENT Approved for public release, distribution is unlimited	12b. DISTRIBUTION CODE

13. ABSTRACT (maximum 200 words)

The Marine Corps is getting back to its expeditionary roots, becoming lighter, leaner, and conversely ever more dependent on power. Until recently, expeditionary power planning has been an afterthought in the Marine Corps. HOMER (Hybrid Optimization Model for Electric Renewables) is a software tool that will enable Logistics Marines to conduct detailed planning to provide efficient expeditionary power. The focus of this thesis is the addition of Marine Corps systems into HOMER. Specific investigations include an analysis of SPACES compared to a control system, and rapid-discharge heat testing of lithium ion batteries. Results include performance specifications for SPACES entry into HOMER and partial validation of the use of the Kinetic Battery Model for Lithium Ion Batteries.

14. SUBJECT TERMS HOMER, Model, Logistics, Solar Array, SPACES, Kinetic Battery Model, Lithium Ion Battery			15. NUMBER OF PAGES 152
			16. PRICE CODE
17. SECURITY CLASSIFICATION OF REPORT Unclassified	18. SECURITY CLASSIFICATION OF THIS PAGE Unclassified	19. SECURITY CLASSIFICATION OF ABSTRACT Unclassified	20. LIMITATION OF ABSTRACT UU

NSN 7540-01-280-5500

THIS PAGE INTENTIONALLY LEFT BLANK

THE MODIFICATION OF HOMER SOFTWARE APPLICATION TO PROVIDE THE UNITED STATES MARINE CORPS WITH AN ENERGY PLANNING TOOL

Alexis R. Harvey
Captain, United States Marine Corps
B.S., United States Naval Academy, 2003

Submitted in partial fulfillment of the
requirements for the degree of

MASTER OF SCIENCE IN ELECTRICAL ENGINEERING

from the

**NAVAL POSTGRADUATE SCHOOL
December 2012**

Author: Alexis R. Harvey

Approved by: Dr. Sherif Michael
                Thesis Advisor

                Dr. Daniel Nussbaum
                Thesis Co-Advisor

                Dr. Clark Robertson
                Chair, Department of Electrical Engineering
                Graduate School of Engineering and Applied
                Science

THIS PAGE INTENTIONALLY LEFT BLANK

ABSTRACT

The Marine Corps is getting back to its expeditionary roots, becoming lighter, leaner, and conversely ever more dependent on power. Until recently, expeditionary power planning has been an afterthought in the Marine Corps. HOMER (Hybrid Optimization Model for Electric Renewables) is a software tool that will enable Logistics Marines to conduct detailed planning to provide efficient expeditionary power. The focus of this thesis is the addition of Marine Corps systems into HOMER. Specific investigations include an analysis of SPACES compared to a control system and rapid-discharge heat testing of lithium ion batteries. Results include performance specifications for SPACES entry into HOMER and partial validation of the use of the Kinetic Battery Model for Lithium Ion Batteries.

THIS PAGE INTENTIONALLY LEFT BLANK

TABLE OF CONTENTS

THIS PAGE INTENTIONALLY LEFT BLANK

LIST OF FIGURES

xii

THIS PAGE INTENTIONALLY LEFT BLANK

LIST OF TABLES

THIS PAGE INTENTIONALLY LEFT BLANK

LIST OF ACRONYMS AND ABBREVIATIONS

AC	Alternating Current
A	Amps
Ah	Amp-hours
AM	Air Mass
AMMPS	Advanced Medium Mobile Power Systems
BJT	Bipolar Junction Transistor
BMS	Battery Management System
C	Battery Capacity (Ah)
CIGS	Copper-Indium-Gallium-Di-Selenide
CMC	Commandant of the Marine Corps
DC	Direct Current
ECU	Environmental Control Unit
ELF	Extremely Low Frequency
E2O	Expeditionary Energy Office
EM	Electromagnetic
eV	Electron Volts
ExFOB	Experimental Forward Operating Base
FF	Fill Factor
FOB	Forward Operating Base
GREENS	Ground Renewable Expeditionary Energy System
HOMER	Hybrid Optimization Model for Electric Renewables
I-V	Current-Voltage
JP	Jet Propellant
KBM	Kinetic Battery Model
kW	Kilowatt
kWh	Kilowatt-hour
Li^+	Lithium Ion
LIB	Lithium Ion Battery
LiFePO4	Lithium Iron Phosphate

MEP	Mobile Electric Power
MP	Maximum Power
MPPT	Maximum Power Point Tracker
NASA	National Aeronautics and Space Administration
NAVSEA	Naval Sea Systems Command
NPC	Net Present Cost
NPS	Naval Postgraduate School
NREL	National Renewable Energy Laboratory
ONR	Office of Naval Research
PV	Photovoltaic
SOC	State of Charge
SPACES	Solar Portable Alternative Communications Energy System
TQG	Tactical Quiet Generator
USMC	United States Marine Corps
V	Voltage
V_{OC}	Open Circuit Voltage
W	Watt
Wh	Watt-hour

EXECUTIVE SUMMARY

As the United States Marine Corps seeks to return to its expeditionary roots, we are confronted by the realization that the modern Marine Corps is more power and energy reliant than ever. As the lethality of each Marine has grown, so has their need to carry more technology, and from radios to night vision devices, the soldiers load keeps growing.

Currently, Marine Corps energy planning for expeditionary power uses peak power to determine the load size for Forward Operating Bases (FOB). A generator is then selected based on the peak power being only 80% of the generator's capacity. Electric loads rarely operate at peak power, resulting in generators experiencing loads at 50% capacity or less almost 80% of their run time. This can cause extra maintenance requirements for diesel generators and forces them to run at the lower end of their efficiency curves, burning more fuel to produce less power.

As the Marine Corps expands its inventory of renewable power sources, expeditionary power planning incorporating those resources into a FOB efficiently becomes a priority. HOMER is a unique software application that is designed to allow users to design a hybrid micro-grid and simulate it in the location it is intended to operate. HOMER (Hybrid Optimization Model for Electric Renewables) then allows the user to optimize the system for performance and cost. HOMER is currently a commercially available tool, and with a few modifications it can become the expeditionary planning tool the Marine Corps needs.

Modifications to HOMER include adding all power systems in the program of record to the component library, the creation and addition of specific unit sized load profiles. These changes will enable a Marine user to design a hybrid micro-grid. Significant changes to HOMER's current capability centers on the optimization feature. HOMER for Marines will enable the optimization a system based on logistics constraints such a fuel, weight, size, and equipment available to transport components. This will empower Marines to create the lightest leanest power system, use less fuel and complete the mission.

The focus of this thesis is on the analysis of the Marine Corps all renewable system SPACES (Solar Portable Alternative Communications energy System) for its performance metrics so that it can be added to the component library of HOMER for Marines. SPACES is a solar system that incorporates a 0.7 m^2 flexible cell solar panel, a DC-to-DC converter, and a lithium ion battery for energy storage.

The lithium ion battery raises several questions on its own. At the time this thesis began, HOMER did not have any lithium batteries in the component library, and it was not entirely clear if the battery model used by HOMER would accurately depict the behavior of lithium ion batteries. As the Marine Corps has added many lithium ion batteries to its inventory, answering this question became central to this thesis.

Related work has shown that the kinetic battery model used by HOMER works well with lithium ion batteries during discharge between 95% and 25% state of charge. Work done in

this thesis used lithium iron phosphate batteries and stressed them by discharging them at high current rates. We suspected that internal temperature affected temperature in quantifiable ways, resulting in a possible temperature corrected KBM.

Results from the work done in this thesis found that SPACES is a very flexible system that enables Marines to power communications systems and charge batteries using a variety of adapter cables. In this investigation, we found the Starpower DC-to-DC controller to be highly efficient and the lithium ion battery to have an excellent roundtrip efficiency. However, the solar panel seemed to have a very low efficiency (6 to 8%) relative to what is currently available on the market (up to 12%). Soon flexible solar cells will be over 16% efficient, and it is the author's opinion that the Marine Corps should be investing in better solar technology as it becomes available to meet its energy requirements.

The lithium ion battery investigation yielded interesting results as well. Experiments were designed to show a correlation between voltage behavior and internal temperature. After 25 battery discharges it seems there is a strong correlation. Additionally, a lithium ion battery at room temperature is easily modeled by the kinetic battery model with deviations between the model and data collected of less than 5 mV. A battery that is well above room temperature (over 40 Celsius) deviates from the kinetic battery model by up to 50 mV, a factor of ten difference. While this makes a strong case for temperature dependence, it is the opinion of the author that HOMER does

not need a temperature corrected battery model at this time. Deviations of 50 mV will not dramatically impact HOMER's energy calculations for a system over the course of a year. Additionally, the batteries in the field will not be discharged at a rate that would increase internal lattice temperature above 40 C very often, eliminating the need for temperature correction at all.

ACKNOWLEDGMENTS

There are many people who helped shape and refine this thesis, and I am grateful to them all. I wish to acknowledge my thesis advisors, Dr. Michael and Dr. Nussbaum, whose advice and input has been critical throughout this process. I wish to thank Maj Newell, who has been a mentor and opened many doors to me in the past year. I wish to thank Dr. Coombe at ONR for seeing potential in this project from the beginning.

I am incredibly grateful to all of the amazing people at the Carderock division of NAVSEA, who invested time and effort into this work. Thank you Dr. House, Dr. Shields, and most especially Dr. Miller; it has been a pleasure and an honor to work with you all.

Thank you to all my editors, whose attention to detail and input shaped this thesis into a document that I am proud of. Finally, thank you to my dedicated spouse, whose endless support and patience helped get this work to the finish line. Thank you all, this would not have been possible without you.

THIS PAGE INTENTIONALLY LEFT BLANK

I. INTRODUCTION

A. MARINE CORPS EXPEDITIONARY POWER REQUIREMENTS

In 2009, General James T. Conway, the 34th Commandant of the Marine Corps (CMC), held the first USMC Energy Summit in Washington, DC. This summit brought to the fore of conversation the Marine Corps' insatiable appetite for fossil fuels as well as the financial and logistical burdens that appetite has on our finite resources. In his opening remarks the CMC said, "I am unsettled by what I now know with regard to our expeditionary capabilities and energy efficiencies…The alarm was set for 5:00 this morning; at 4:00, I was staring at the ceiling thinking about what we are going to do about this problem"[1].

After the summit the CMC sent a team to Afghanistan to study what the Marine Corps was doing right and where we could do things more efficiently. Shortly after the report from this expedition, the CMC created the Expeditionary Energy Office (E2O) [2]. This office was created to "analyze, develop, and direct the Marine Corps' energy strategy in order to optimize expeditionary capabilities across all war-fighting functions" [3].

Since its creation E2O started the Experimental Forward Operating Base (ExFOB) program, which brings emerging technologies and military minds together to solve expeditionary power problems. E2O has completed multiple efficiency studies, including the BOULDAK study in Afghanistan, which collected Marine Corps actual power use data while operating forward. E2O has commissioned work at

NREL to model improving efficiency in field tents and, among many other things, helped shape this thesis [4].

One of the many concerns E2O is confronting is not simply changing how the Marine Corps uses energy but how we plan for energy use and the perception of energy use throughout the entire Marine Corps. The Marine Corps has an energy planning doctrine that determines the size of a generator we bring to a Forward Operating Base (FOB); that doctrine says the peak load requirement can be no more than 80% of the generator's output capability. While this policy ensures the continuity of operations, it effectively hamstrings our operating efficiency. Loads rarely demand peak power and, therefore, Marines are consistently running generators at low power outputs. This burns fuel at the lower end of a generator's efficiency curve and results in higher maintenance requirements [4].

As the Marine Corps shifts away from expeditionary power that relies solely on burning fossil fuels to alternative energy and hybrid power systems, energy planning becomes exponentially more complex, and we were not doing it well to begin with. This is where HOMER Energy LLC may bridge the gap between expeditionary power requirements and planning for efficient power operations [5], [6].

B.   THE ROLE OF HOMER

HOMER (Hybrid Optimization Model for Electric Renewables) is a software application that models hybrid power systems to determine if a micropower system can provide for a particular load and how much the system will cost to install and maintain for the life of the project.

HOMER can design an efficient micro-grid for a user. A power system that exists to supply a specific load is called a micro-grid. A micro-grid can be tied to a grid, or independent of a larger grid system.

HOMER is a unique application that enables a user to build a power system in order to supply a load and model it in a specific location over the course of an average year. This allows the user to quickly determine the most efficient power system configuration for a load. The ability to design a system, test it and then optimize it based on user-defined constraints are just a few of the tools a HOMER user has at their fingertips. Details concerning HOMER software capabilities are discussed in Chapter II.

C.   PURPOSE AND GOALS

The purpose of the work done in this thesis was to work with the individuals at HOMER Energy to create a tool for the Marine Corps to use for expeditionary power planning. The author's role was to provide the team at HOMER Energy with all the data and information they needed to shape HOMER into a user-friendly application. HOMER will enable Logistics Marines to conduct detailed, location specific power planning and incorporate the optimal mix of renewable and conventional power systems to complete a mission. The goals for a Marine Corps specific application are described in Chapter III.

To that end the author examined an all-renewable power systems that are already in the Marine Corps inventory so that they could be integrated into the component library in HOMER. The Solar Portable Alternative Communications Energy

System (SPACES) is a completely renewable system incorporating a small solar panel, a power controller, and a battery for energy storage. The solar panel was tested in a variety of atmospheric conditions to determine performance characteristics and efficiency.

The battery included in SPACES is a Lithium Ion (Li^+) chemistry battery. This chemistry added some interesting layers of complexity to this project. HOMER does not have Li^+ batteries in the component library, and we were not sure if the Kinetic Battery Model (KBM) that HOMER used would be effective for Li^+ batteries. Li^+ batteries have peculiar chemistry tendencies that defy standard models. We believe those behaviors are tied to temperature effects, and if the KBM cannot be used, then perhaps a temperature modified KBM might be effective.

Detailed in Chapter IV is the behavior of solar cells, how they work, and how atmospheric conditions affect them.

Background information on batteries is described in Chapter V, where common chemistries, standard battery models and why Li^+ battery behavior defies standard models.

Testing and evaluation of SPACES are detailed in Chapter VI.

Testing and evaluation of lithium ion batteries is detailed in Chapter VII.

Results and conclusions from testing and analysis of SPACES and batteries, as well as recommendations for future work, are detailed in Chapter VIII.

II. HOMER

A. WHAT IS HOMER

1. Introduction

HOMER is a computer simulation software that models and compares micropower systems to aid in the development of cost effective micro-grids. A micropower system is an electrical generation system that serves a specific load. It may draw power from a grid, or it may be an autonomous power system. HOMER models a power system's physical behavior and incorporates life cycle cost (i.e., costs of purchase, replacement, installation and maintenance) to delineate performance and cost metrics to aid the decision making process.

The information in this chapter is drawn heavily from the documentation published on the HOMER Energy LLC website www.homerenergy.com and conversations with personnel within the company itself. The following information is intended to give the reader a conceptual overview of the capabilities inherent to HOMER.

2. A Brief History

HOMER was developed in the National Renewable Energy Laboratory (NREL) as an outgrowth of the Village Power Program. NREL developed a model to aid the rural electrification program in understanding the trade-offs in different micro-grid designs.

By 1997 NREL understood that there was a need for a publicly available model to enhance grid-connected systems with renewable technologies. HOMER became a Windows based

program written in C++, and additions to the model included economic and emissions constraints. In 2009, NREL executed a commercial license, giving HOMER Energy LLC exclusive rights to develop and market HOMER [7].

B.   HOW HOMER WORKS

1.   Overview

HOMER is a software modeling application that works in three parts: simulation, optimization, and sensitivity analysis. HOMER is particularly useful because of its capacity to model complex systems using a variety of power generation techniques including but not limited to, diesel, solar, wind, hydro and biomass.

When conducting a simulation, HOMER will analyze a system each hour of a year to determine its technical feasibility. It then generates life cycle cost estimates for that system. When optimizing a system, HOMER seeks to determine the most cost effective system arrangement by scaling the various components in the system. The third process is sensitivity analysis, in which HOMER determines the robustness of the optimized system in response to changing variables that are external to the system. For example, a user can ask HOMER to examine how the Net Present Cost (NPC) of the system is affected by fuel prices by analyzing a range of fuel prices that the user defines (i.e., four to ten dollars per gallon). The relationship of these three functions is depicted in Figure 1.
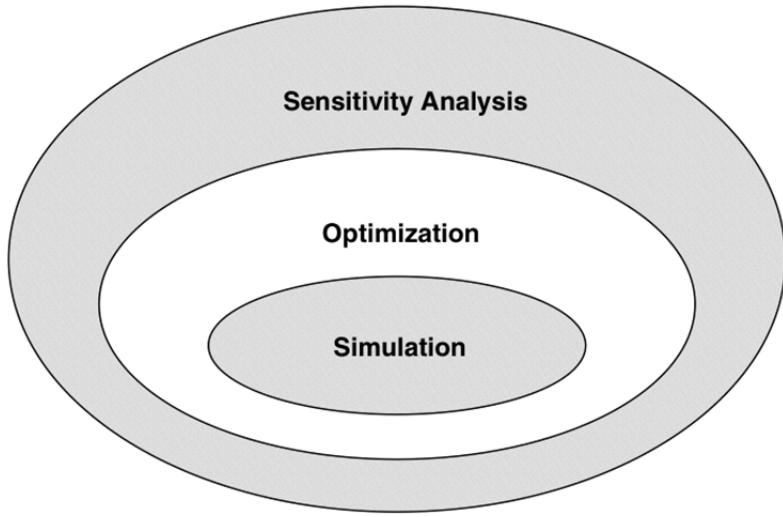
Figure 1. Conceptual relationship between simulation, optimization and sensitivity analysis used in the HOMER software. From [7]

2.   Simulation

HOMER modeling centers on simulating a single micro-grid configuration over a simulation period of one year. Models analyze a single system configuration with specific component sizes and tie in an operating strategy that guides how those system components interact over the simulation period. There are two main questions that this operation seeks to answer: is the system feasible; and how much will it cost as defined by the inputs and constraints? HOMER considers a system feasible if the power produced, captured, or purchased from the grid meets the identified requirements for each time step of a year. Once a system is feasible, HOMER calculates the costs of initial purchase, operation and maintenance, component replacement and fuel to identify the total system cost in today's dollars (NPC).

HOMER can simulate any system configuration the user defines (e.g., diesel, wind, solar, biomass batteries, etc.). The user can design a system that provides power from AC, DC, and thermal load generators or a system that is a combination of power supplies. To do so, HOMER utilizes a cache of historical worldwide data that enables HOMER's algorithm engine to step through an entire year hour by hour for any location on the globe. As the simulation progresses, HOMER decides what to do with excess renewable power or determines how to generate more if there is a shortfall, while operating within the constraints defined by the inputs. If HOMER detects an unresolved shortfall, it will identify the configuration as not feasible [8]

If the system being modeled has a battery bank and one or more generators, then a dispatch strategy is required. A dispatch strategy is a set of rules that govern the use of available power. It can be thought of as disposable income. Once all the bills are paid, where does the rest of the money (power) go? In deciding where to take power from, HOMER will always attempt to minimize the cost per W. To that end HOMER has two types of dispatch strategies, cycle charging and load following.

In cycle charging the batteries are charged by excess power when the generator runs, thereby, allowing the system to take advantage of the generator fuel efficiency curves (depicted in Figure 2). A generator is more efficient in terms of output power vs. fuel burned when it is run at its maximum load, however, it is also burning more fuel per hour, which may be a logistical or economic burden.

Generator operation and maintenance costs tend to be higher than other components in the system; therefore, deciding when, for how long, and at what output level to run a generator is a critical decision point in each time step[6].
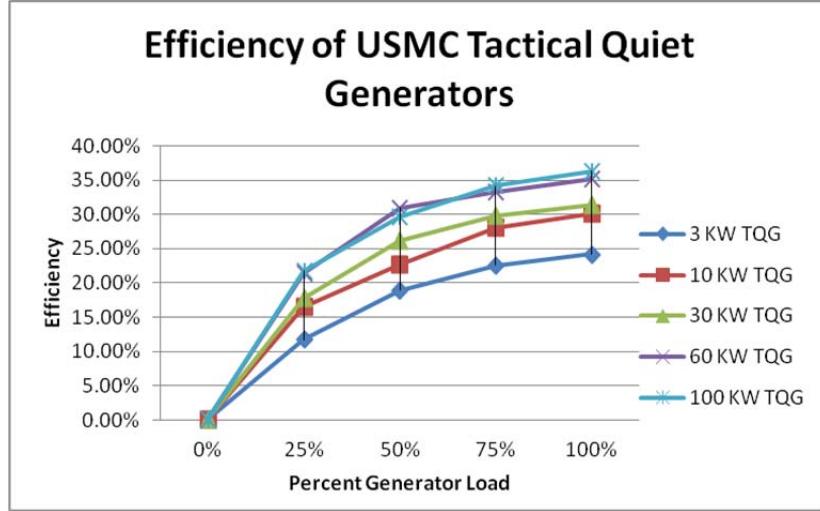
Figure 2.   Efficiency vs. Load of USMC Generators. From [9]

The load following dispatch strategy requires the generator to output only enough power to run the load and not charge the batteries. The batteries are required to be charged from another power source, such as solar or wind. The user selects the dispatch strategy; HOMER enables the user to toggle between both strategies to aid the user in the selection process.

HOMER's designers decided to use one-hour time steps for an annual simulation. A time step too large would miss critical intermittent renewable resources (i.e., solar and wind) and fail to provide the level of detail required for a sufficiently accurate model. Conversely, if the time step

9

is too small, the simulation takes too long to make optimization and sensitivity analysis feasible.

HOMER has a simple graphic interface that enables users to select the system configuration and input system constraints. The simple add/remove feature, depicted in Figure 3, allows the modeler to create a system to supply the prospective load requirements. Additionally, the resources section allows the user to input location specific resource data, either from the Internet, personal files, or from HOMER's library. The user can add economic or system constraints, including how long/often they would like the generator to run.
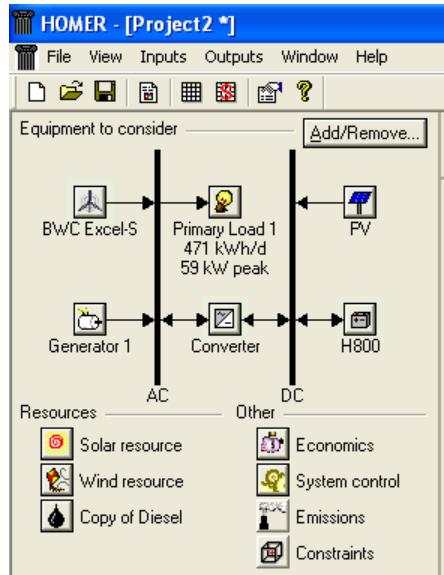
Figure 3.   An example system configuration, a screen shot from HOMER.

HOMER evaluates a system's total cost in today's dollars. The NPC includes: initial purchase, replacement, system maintenance, fuel, and the cost of buying power from

a grid. The NPC also includes any revenue that may be generated by the system configuration by selling extra power back to the grid.

3.   Optimization

In the simulation function, HOMER models a single system configuration. In optimization, HOMER conducts many simulations to determine the optimal system configuration that meets the input constraints at the lowest NPC. In this function, HOMER can be considered a calculator that gives the best output based on the input of decision variables. It is important to remember that the modeler has to ask the right questions to get the optimum results. The advantage of this modeling system is that running multiple scenarios is quick and easy.

Optimization allows the modeler to answer specific questions about a micro-grid that would otherwise be nearly impossible to answer. Due to the complexity of systems interactions, a user who wanted to add renewable energy sources to a diesel generator power system could be overwhelmed trying to determine how much wind, solar, and batteries to add. Would the cost of the investment be worth the upgrade? Will the improvements meet the load needs over the long term? Decision variables that can be addressed by HOMER include but are not limited to:

- The size of a solar array
- The number of wind turbines
- The size and number of generators
- The number and size of batteries
- The size of the AC-DC converter

- The size of a hydrogen storage tank
- The size of the load

The purpose of optimization is to determine the right system components, the sizes and or quantities of each component, and a power dispatch strategy that meets the needs of the micro-grid without producing power shortfalls or excesses [8].

Consider the following example. A modeler would like to update their diesel generator micro-grid with some renewable power, wind, solar or some combination. Figure 3 from the preceding section is an illustration of the HOMER interface for building such a model. The user can ask HOMER to optimize the decision variables using the search space function. In the search space the user can add scaled variables for each component to be analyzed. The search space for this scenario is depicted in Figure 4. The user has specified five generator sizes, five quantities of wind turbines, seven battery bank sizes, and five sizes of solar arrays. The search space, depicted in Figure 4, displays 2625 different system combinations that HOMER will individually simulate. HOMER will disregard any configurations that are not feasible and then rank the remaining configurations from least to most expensive. The tabulated output allows the user to look at decision variables (e.g., project lifetime fuel, project lifetime fuel consumption, operations and maintenance costs). This allows the modeler to look at the trade-offs associated with the each configuration HOMER has determined to be the most effective. An example of HOMER's optimized and tabulated output can be seen in Figure 5. The most cost

effective system is not always the right configuration; other concerns may be carbon emissions, maintenance, or fuel prices.

Figure 4.   The example search space matrix.

Figure 5.   HOMER optimization results from the example.

4.   Sensitivity Analysis

Sensitivity Analysis is a means for the user to cope with uncertainty and to determine the robustness of a given optimal system configuration. While the optimization

process builds the best system configuration under a single set of input assumptions, sensitivity analysis allows the modeler to run optimizations over various sets of input assumptions.

A sensitivity variable is one for which the user has entered multiple values. A sensitivity variable can be anything that is not a decision variable, including but not limited to: diesel prices, grid power prices, expected lifetime of various system components, variable loads, and carbon credits. For each distinct sensitivity case, HOMER will simulate the sensitivity variable and create an optimized output. The user will then be able to determine which sensitivity variables most dramatically affect the costs of a specific system configuration.

While the most obvious advantage of sensitivity analysis is enabling in-depth cost analysis, sensitivity analysis also gives the user a powerful tool for managing uncertainty. Additionally, the user has the ability to answer a variety of specific questions such as:

- What is the cost and benefit analysis of a 50 percent renewable hybrid system?

- What is the optimal combination of technologies for a specific load at a specific location?

- A policy planner can determine what amount of economic incentive is required to make alternative energies appealing to business and residences.

The user can address these types of questions in the constraints and limitations section of HOMER. Both constraints and limitations have search space dialog boxes that can be used to input variables that can effect each simulation outcome[8].

HOMER uses an array of visual tools to help the system designer recognize how each sensitivity variable affects the NPC. A tabular display shows the optimal system configuration as the sensitivity variable changes. A spider diagram compares the sensitivity variables relative to each other so the system designer can see which variable most directly impacts the system. On a spider diagram, the steeper the curve, the higher the impact of that variable on the system.

Another powerful tool is HOMER's ability to conduct sensitivity analysis on hourly data sets, whether that data set is a variable load, or renewable energy source such as solar, wind, hydro or biomass. This enables the system designer to become informed of the impact on the entire system of several low renewable resource days or several high load demand days. The user can then modify the system to minimize the impact to the load during these occasions of intermittent power variation. Without this analysis tool, system designers often err on the side of caution and accept excess electrical supply for 90 percent of the time, which is a waste of both energy and money. This is one of the major problems the Marine Corps faces today.

C. MODELING PHYSICAL SYSTEMS IN HOMER

1. Overview

The focus of this thesis is on the way that HOMER models physical systems most directly relevant to the United States Marine Corps. The following sections will describe in greater detail the way that HOMER models physical system components and the interaction of the power system and the load(s).

2. Electrical Loads

HOMER models two types of electrical loads: primary and deferrable loads. The primary load is the reason the micro-grid exists and is a load that must be met on a set schedule. A deferrable load is one that can be met within a certain window of time. Primary load is an electrical demand associated with communications equipment, lights, computers, or other equipment that consumes a fairly consistent amount of energy. When the demand exceeds the capacity of the system, HOMER classifies it as an unmet load. Each period of unmet load will be noted in the simulation, and the system designer will know where and why the power supply fell short.

The modeler can generate a primary load in a variety of ways: an excel file can be imported, or HOMER can synthesize daily average load data. Load data is specified in kilowatts (kW) for each hour of the day. The user can specify different loads for each month or season as necessary. Additionally, HOMER can introduce random variability in the daily load profile within limits set by the user. The primary electric load also requires an operating reserve, which is also set by the user. The operating reserve, also called a spinning reserve, is specified as an amount of energy not related to a specific device. It is an amount of energy designated to handle periods of excessive loads or power shortage. The user can set the operating reserve to zero if desired.

A deferrable electric load is a demand that can be met anytime within a specified time interval. Battery charging stations and radios are good examples of deferrable load,

as they have internal energy storage capacity. Deferrable loads are advantageous in regions of intermittent renewable resources. Energy storage is always considered the deferrable load in HOMER. The user specifies the size of the deferrable load in kilowatt-hours (kWh). HOMER models a deferrable load as a storage tank of a defined size. When there is excess power being generated by the system, and the primary load is met, excess energy is directed to the storage tank. HOMER continually tracks the level of energy in the tank. When it is full and the primary load is met, HOMER starts tracking excess energy which is in effect wasted unless it is a grid connected system, in which case excess energy can be sold back.

3. Generators

HOMER can model a variety of electric and thermal generators, including internal combustion, fuel cell, Sterling engines, micro-turbines, and thermoelectric engines. When modeling a micro-grid, HOMER can model up to three generators, each with its own fuel efficiency curve, fuel type, and electrical output either Alternating Current (AC) or Direct Current (DC). It is also possible to model a fuel mixture, such as biomass and diesel.

The principle variables HOMER needs to model a generator are:

- Maximum power output (kW)
- Minimum power output (kW)
- Operating lifetime (hours)
- Fuel consumed (liters)
- Efficiency, which is the rate at which fuel is consumed vs. electrical output produced

HOMER assumes a linear fuel curve if given only two points on the efficiency curve; however, given more data, HOMER will create a best fit. HOMER uses the following equation to model fuel consumption:

$$F = F_0 Y_{gen} + F_1 P_{gen}$$
(2.1)

where F_0 is the fuel curve intercept coefficient, F_1 is the fuel curve slope, Y_{gen} is the rated capacity of the generator, and P_{gen} is the electrical output of the generator in kW. The units of F depend on the unit of measure used for the fuel. If the fuel is denoted in liters, then the unit of F is L/h.

The user can specify the intervals during which the generator will run or be shut off. Absent user instructions, HOMER will force the generator on and off based on the needs of the system. According to the dispatch strategy, HOMER will make decisions to set the output of the generator [10].

4. Photovoltaic Cells

Photovoltaic (PV) cells are devices by which incident solar radiation is converted to DC electricity. Commonly known as Solar Cells, PV cells or arrays can vary in size and are characterized in terms of rated capacity. Rated capacity is the maximum power produced by the array in standardized testing conditions. It incorporates the size and efficiency of the array, and therefore, HOMER does not deal with these variables directly. However, it would be a mistake to compile a simulation of a system that claims the best-case power output for all time intervals because PV cells only produce rated capacity output under ideal solar conditions [11]. HOMER uses a modeling tool called a de-

rating factor, which allows the user to scale the available output power from the best case to a more realistic output. The de-rating factor reduces the efficiency of the PV array to take into account things like dust, angle-of-incidence and other factors that may reduce operating performance. HOMER does not automatically account for the fact that PV output decreases as the operating temperature of the cells increase, though the user can incorporate a temperature coefficient when modeling a system in a hot climate.

The voltage at which current is drawn from a PV array significantly impacts the efficiency of the array. This will be discussed in more detail in Chapter IV. For modeling purposes, HOMER assumes that a PV array has a Maximum Power Point Tracker (MPPT) included in the system to ensure that the PV has current drawn at the most efficient voltage and, therefore, is generating the most energy for the time, location, and system configuration [11].

5.   Batteries and Battery Banks

HOMER can model a single battery or an entire bank of batteries, which HOMER treats as a DC storage device. A string of batteries denotes that one or more batteries are connected in series, and a bank of batteries is one or more strings. In the system component library, there are a variety of specific batteries the user can add to their system, mostly variants of a lead acid chemistry or other more common chemistries. The system designer is able to select the number and size of the batteries that HOMER is to consider in its system analysis. If the user is unable to find a suitable battery in the library, HOMER does have

the option of allowing the user to create a battery, and select the way that battery is modeled. Currently, there are two models that HOMER uses in its calculations, the KBM and the simple battery model. The KBM is much more robust and detailed than the simple battery model. The KBM will be discussed in more detail in Chapter V [12].

Batteries are capable of storing a fixed amount of DC electricity at certain round trip efficiencies. Each individual type of battery has limits as to how quickly it can be charged and discharged, how deeply it can be discharged, and how many cycles it can undergo prior to failing. The depth of discharge directly affects the number of cycles a battery can endure. The cycles to failure is inversely related to the depth to which a battery is discharged.

The key parameters HOMER uses to replicate battery behavior are:

- Nominal voltage, which is the rated voltage for each battery.

- The capacity curve, which shows the discharge capacity (available energy) in Ampere-hours (Ah) at a particular discharge current.

- Lifetime curve is the number of cycles to failure verses the depth of discharge.

- Minimum state of charge is the minimum voltage a cell can be discharged to and not suffer permanent damage.

- Round trip efficiency is the amount of energy that can be discharged from a battery compared to the amount of energy it takes to fully charge a battery.

HOMER uses the KBM to track energy going into and out of each battery in the bank. Each of the key parameters enables HOMER to determine the current state of charge and whether energy is stored in or discharged each hour of the year [8].

6. Converters

Converters are devices that can change DC electricity to AC electricity and back. When converting from DC to AC, the process is called inverting, and from AC to DC, the process is called rectifying. The capacity of a converter is always given in terms of AC power throughput (kW). The size of the converter is a decision variable in HOMER. Additionally, output capacity for rectification is a percentage of inversion capacity; the user sets the rectification percentage variable. HOMER assumes that the inversion and rectification capacities are not surge capacities but continuous capacities that the device can withstand for long periods of activity.

When dealing with converters, HOMER does have the capability to model several power sources in parallel. Doing so requires the inverter to have the capability to match AC frequencies, which some converters do not have.

D. ENERGY RESOURCES IN HOMER

1. Defining Resource

The term "resource" is defined in HOMER as something outside the system that provides a means to produce electrical power. Renewable resources include solar, wind, hydro, and biomass. Conventional resources are fuels such as diesel, natural gas, and liquid hydrogen. Renewable resources create a complex problem set for a system modeler because they are location dependent, and highly variable [8].

2. Solar Resources

Solar energy is dependent on several key factors: the latitude, the clearness factor (which denotes how readily the solar energy can traverse the atmosphere) and diffuse radiation (which is sunlight reflecting off nearby surfaces). The user must supply HOMER with the solar data for any given location. HOMER currently has many locations' data already collected, and the correct file need only be imported. If a specific location is not available, there are a variety of websites where the user can find appropriate solar data, such as the NASA website. The data can be inputted in any of three forms: hourly average global solar radiation on the horizontal surface in kW/m^2, monthly average global solar radiation on the horizontal surface in kW/m^2, or monthly average clearness index, which is a ratio of the radiation striking the surface to the radiation striking the upper atmosphere. HOMER synthesizes the data and generates an 8760-hour data set that spans each hour of the year [8].

3.   **Fuel**

There is a library of predefined fuels in HOMER. Should none of the available fuels prove sufficient to match the user's needs, it is possible to create a new fuel. The user need only input the fuel density, the lower heating value, the carbon content, and the sulfur content. The last two values are needed only if the modeler wishes to monitor carbon and other waste emissions.

THIS PAGE INTENTIONALLY LEFT BLANK

III. PROPOSED MODIFICATIONS TO HOMER

A.   INTRODUCTION

HOMER in its current form is an excellent micro-grid modeling tool and economic calculator for determining the most efficient and cost effective system for a user's location. The proposed modifications to HOMER will enable a Marine to design the lightest, smallest, most efficient FOB power system for any location and duration with the tools and systems already in the Marine Corps inventory.

B.   BACKGROUND

1.   Previous Work

Military interest in the capability set of HOMER started in 2010 with a Naval Postgraduate thesis by then-Captain Brandon Newell. His work was intended to demonstrate the viability of using a tool like HOMER to do a thorough pre-deployment energy planning analysis [3]. Since that time HOMER Energy LLC's vision for what its software can do has grown into a more dynamic and user-friendly tool. This, together with the Marine Corps' need to curtail energy waste and simplify the logistics burden of moving fuel around the battle space makes HOMER Energy a meaningful partner moving forward.

2.   Collaborative Partners

There are several stakeholders in this endeavor. The Office of Naval Research (ONR) and the Marine Corps Expeditionary Energy Office are both actively engaged in creating a HOMER application specifically for the military.

Additional help and interest has come from individuals in the Carderock division of the Naval Sea Systems Command (NAVSEA). All parties have worked with HOMER Energy to create a coherent plan to create such a tool.

C.   HOMER FOR MARINES

1.   Marine Corps Power Modifications

The proposed changes to HOMER are intended to create a simple, user friendly tool that any Logistics or Utilities Marine can use to design a micro-grid that can support the Camp Commander and the mission.

The proposed user interface will be a simple, directed set of questions. These questions allow a user without a comprehensive understanding of power systems to design a feasible micro-grid. For more advanced users, such as Utilities Marines who already understand power distribution, a more detailed interface with additional user-specified variables will be created. The intent is that anyone can build a solution to a complex problem set.

The system library will be updated with all current Marine Corps inventory power supplies, such as the Tactical Quiet Generators (TQGs), the next generation power systems Advanced Medium Mobile Power Systems (AMMPS), as well as all renewable systems such as Ground Renewable Expeditionary Energy System (GREENS) and SPACES. Additionally, Jet Propulsion 8 (JP8) must be added to the fuels library because all Marine Corps systems run on that particular diesel blend.

GREENS and SPACES present a unique modeling situation because they are a complete power system already, including

power generation, conversion, and storage[6]. In HOMER's current form, each component is modeled separately. However, the intent is for a user to select GREENS in the component library, and HOMER will know to add each component of the system into the micro-grid.

A load library will also be created. The Marine Corps will need to develop an average 24-hour load profile for each item in its inventory that requires power to operate. The user will be able to specify the load equipment and quantity going to the FOB, and HOMER will synthesize the load profiles into a location and mission-specific primary load. To simplify the process HOMER will have a menu of pre-defined primary loads of varying unit sizes. The predefined loads will be in the form of actual equipment lists from which the user will be able to add and remove items as necessary. Environmental Control Units (ECUs) are seasonally dependant loads that require different profiles for spring, summer, and winter.

While there is renewable resource data available on the Internet for most global locations, the user does have to know where to look if the location profile does not already exist. To simplify this task for the Marine Corps, HOMER will add Marine Corps specific training and operating locations to the resource library, starting with Camp Pendleton, Twenty Nine Palms, and Camp Lejuene.

Other modifications include adding the family of Lithium Ion Batteries to the component library and improving modeling of inverter efficiencies.

2. Logistics Modifications

Currently HOMER does not have any logistics planning tools. HOMER's primary baseline for comparing separate systems is the total NPC, which includes the lifetime cost of fuel, operations and maintenance, and acquisition price of the system. Once a system is through the Marine Corps acquisition process, the NPC is not a driving factor. What is important is how a system is transported to a training area or theater of operations and how it is maintained and supplied. The following modifications seek to provide the Marine Corps with a tool to design an optimal hybrid power system that is as light and lean as possible, as well as an optimal packing method to get the system to the operating area.

Changes in HOMER will start with creating a logistics algorithm that will optimize a system based on logistics requirements. The variables that need to be included are the size (in cubic inches) and weight (in pounds) of each power system. HOMER will also incorporate logistics-specific information about each type of vehicle in the inventory including cargo capacity dimensions, fuel tanker capacity, trailer capacity, and cargo container dimensions.

These proposed modifications will enable the modeler to optimize a system based on logistics concerns and still meet the mission requirements for power generation and distribution. Additionally, the modeler will be able to do sensitivity analysis on the system to determine the best resupply cycle, such as how often a given FOB will require fuel and or batteries.

3. Marine Corps Energy Planning

Currently, the Marine Corps deals with power planning by addressing how much power needs to be produced in order to meet peak loads for a particular FOB. The modified version of HOMER will enable any Marine to consider energy planning as a whole concept. The purpose is a culture shift away from planning for peak power to planning to generate, store, and use only the total energy required to complete the mission. The whole concept approach is the ability to do an analysis quickly each time the Marine Corps needs to erect a camp. The modified version of HOMER enables the user to analyze all the pieces of a system, power sources, loads, and energy resources for any location necessary, based on available equipment and the mission profile. The user will be able to drive the optimization process for each system based on the most pressing concerns of the mission commander, whether those concerns are weight and space or resupply intervals. HOMER will enable the Marine Corps to be lighter, leaner, and more ready for the next fight.

D. AQUISISTIONS ENGINEERING

1. Engineering Analysis

Acquisitions is a complex process that takes many competing ideas for a material solution and prunes them down to a single concept, for which a contract is written to develop a prototype. Often this system lacks the modeling capability to provide direct systems comparisons and a detailed capabilities assessment.

ONR has requested a detailed engineering analysis tool to aid in the assessment of proposed power systems. HOMER is developing an application that will allow the modeler to build a power system from the ground up and then insert it into a micro-grid for performance analysis. The user will be able to build a hybrid system comprised of many different technologies including a diesel generator, PV, solar concentrator, flywheel, wind, hydrogen fuel cell, batteries, and many others. The user will have the flexibility to manipulate variables such as fuel efficiencies, battery depth of discharge, state of charge requirements, power dispatch strategy and much more.

Once the user has designed and "built" the proposed systems in a HOMER file, each power system can be simulated and optimized under actual load profiles to determine which system has the best performance. The acquisitions modeler can even choose the best-proposed system and make modification requests to the system designer to reflect the optimized system HOMER produced.

This application of HOMER will have a separate interface from the Marine Corps Power Planning Tool. The engineering application will retain the user-friendly visual interface, allowing the user to combine the system components in a fashion similar to the proposed item.

E.   PROGRESS REPORT

With the help of ONR and E2O, HOMER Energy has developed a three-phase acquisition strategy. Phase one is prototype development; phase two is bringing the total software system online and conduct fielding tests. Should

this tool have value to the Marine Corps, phase three will be distribution of the software and training for the Marines.

Currently, HOMER is in phase one, at the end of which a functional prototype will be demonstrated to ONR. The prototype will have several basic load profiles; all current power systems programs of record will be in the component library. HOMER will be able to demonstrate design of a FOB power system for a company sized unit or a Marine Expeditionary Unit (MEU). The power system can be optimized for fuel, weight, or size at any of three locations: Camp Lejuene, Camp Pendleton, or Twenty Nine Palms. Finally, HOMER will produce a written report that includes the best packing arrangement for transportation of the system.

THIS PAGE INTENTIONALLY LEFT BLANK

IV. SOLAR CELLS AND POWER SYSTEMS

A. INTRODUCTION

1. PV Basics

A photovoltaic cell is essentially a p-n junction in which electrons and hole pairs, generated by light energy, are separated by the bandgap of the material utilized in making the p-n junction. The visible solar irradiance spectrum is most commonly associated with photovoltaic cells, which is why they are often called solar cells. However, artificial light, infrared light, and even ultraviolet light can be used to generate electricity given the right material in the photovoltaic cell. There are three basic attributes to a functioning PV cell[13]:

- The absorption of incident light generates electron-hole pairs.
- Charge carriers are separated from parent atoms.
- Charge carriers are extracted to an external circuit.

B. SOLAR SPECTRUM AND SOLAR RADIATION

1. Electromagnetic Waves

The electromagnetic (EM) spectrum refers to the entire frequency range of EM radiation. The EM spectrum extends from the Extremely Low Frequency (ELF) bands used for radio communication to gamma radiation, which has a wavelength the size of an atom, and extremely high frequency.

EM waves are generally referred to by three variables; frequency (f), wavelength (λ), and photon energy (E). These three physical descriptive properties are related by the following equations:

$$f = \frac{c}{\lambda} = \frac{E}{h}$$ (4.1)

$$E = \frac{ch}{\lambda}$$ (4.2)

where c is the speed of light and h is Planck's constant (4.135×10^{-15} eVS). These equations relate the wavelength and frequency of EM radiation to the amount of energy each photon has. Grouping wavelengths that behave similarly into "bands" further delineates EM radiation. These bands of EM radiation are shown in Figure 6.
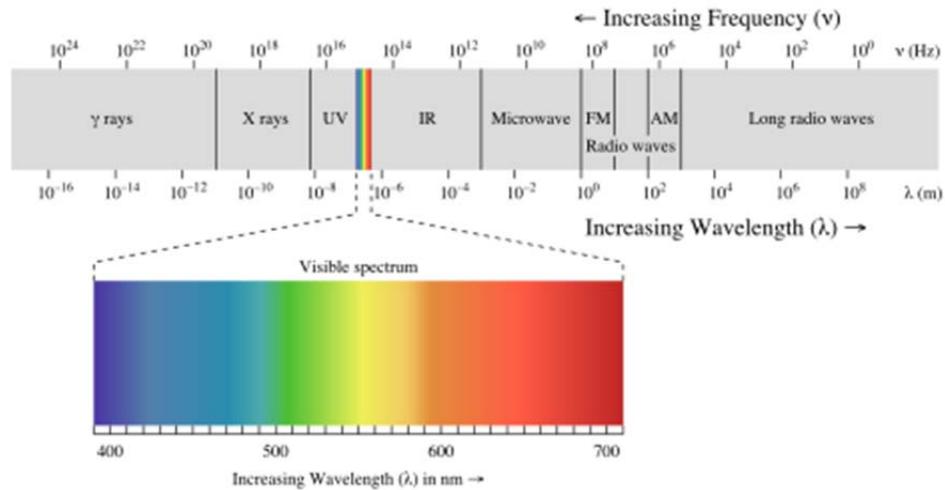
Figure 6.   A diagram of the entire EM radiation spectrum. (From [14])

The bands or classifications of EM energy are sifted into seven categories. From highest energy to lowest, they are:

- Gamma radiation

- X-ray radiation

- Ultraviolet radiation

- Visible radiation

- Infrared radiation

- Microwave radiation

- Radio waves

The bands of EM radiation can be even further broken down into specific EM frequencies. In Figure 7, the specific frequency of radiation is directly associated with wavelength and photon energy. These numbers can be solved for mathematically using Equations 4.1 and 4.2.

Figure 7.   The EM Spectrum, the respective wavelengths and photon energy in eV. From [14]

2.   Solar Radiation

The Sun emits EM radiation across almost the entire spectrum. Gamma radiation photons are created by nuclear fusion within the Sun. They are such high-energy photons that they are converted to a lower energy band by the time they reach the surface of the Sun through interactions with the solar gas. Therefore, the Sun does not emit all EM frequencies, but it is very close to being a blackbody object, which is a theoretical object that does not absorb EM waves and radiates the entire EM spectrum [15].

The EM radiation travels unattenuated through a vacuum in space. Sunlight that strikes the top of earth's atmosphere has a power of 1366 W/m^2, 50% of which is in the infrared band, 40% is in the visible light band, and 10% is in the ultraviolet band. The ultraviolet light is absorbed by the upper atmosphere, specifically the lithosphere. As sunlight travels through the various levels of atmosphere, it is attenuated and refracted; photons reaching the ground are less energetic. Where sunlight has to penetrate the least amount of atmosphere and where the direction the waves are traveling is perpendicular to the surface of the earth, the amount of energy at the surface is about 1000 W/m^2 [16]. The energy breakdown is about 53% in the infrared range, 44% in the visible range, and 3% remains in the ultraviolet range. The variation between the top of the atmosphere and the earth can be seen in Figure 8. In Figure 8 the solid curve is the EM spectrum emitance of a blackbody [15]. The yellow shaded area is the radiated EM spectrum of the Sun in space just outside the earth's

atmosphere, and the red shaded area is the portion of the EM spectrum that reaches the surface of the earth [14].
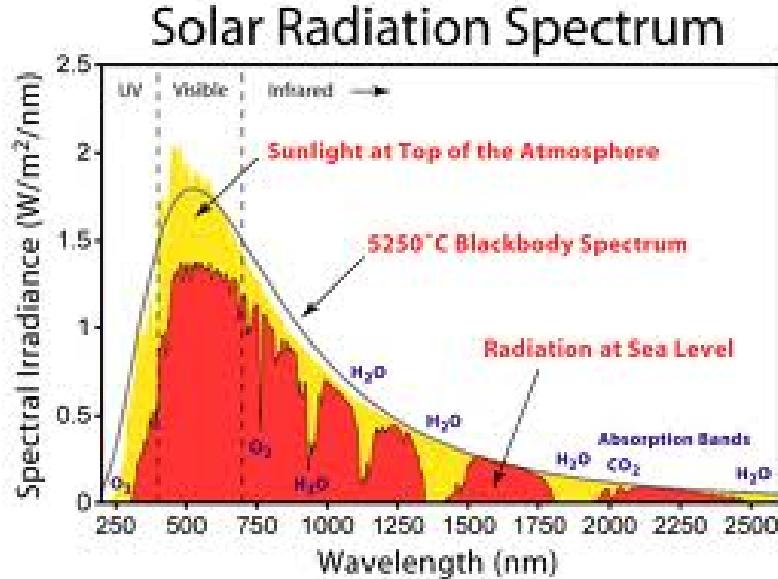
Figure 8.   A comparison of the EM spectrum at the top of the atmosphere and the surface of the earth. From [15]

3.   Air Mass

Air Mass coefficient (AM) is a reference system that assigns a value to the distance sunlight has to travel through the atmosphere. AM is commonly used to characterize solar cell performance at the surface of the earth. At the top of the atmosphere, the reference starts with AM0, where the available power in a square meter is 1366 W. As sunlight travels through the atmosphere, it is scattered, refracted and absorbed by particulates in the atmosphere.

When the Sun is directly overhead, commonly referred to as the zenith, EM radiation travels the shortest distance, defined as AM1. As the angle of the Sun deviates

37

from the zenith, the atmospheric thickness increases, and the AM reference assigned goes up. AM for a specific path length is defined by

$$AM = \frac{1}{\cos z} \tag{4.3}$$

where z is the angle away from the zenith. This is a simplistic model that does not account for the curvature of the earth. A more accurate assessment of the distance sunlight has to travel through a round atmosphere is given by [15]

$$AM = \sqrt{((r\cos z)^2 + 2r + 1)} - r\cos z \tag{4.4}$$

where r is ratio of the radius of the earth over the height of the atmosphere, which is 708. Once the coefficient has been determined for a specific location, the solar intensity can be estimated useing

$$I = 1.1 I_o 0.7^{(AM 0.678)} \tag{4.5}$$

where I_0 is the solar intensity at the top of the atmosphere, 1366 W/m^2. Depicted in Table 1, a sample of various AM coefficients and surface solar intensities can be viewed. The values in Table 1 were calculated using Equation 4.4 [15].

Table 1.   A representation of the AM coefficient and the
            resulting solar intensity at the earth's surface.

Z	AM	W/m^2
	0	1353
0	1	1040
23	1.09	1020
30	1.15	1010
45	1.41	950
48.2	1.5	930
60	2	840
70	2.9	710
75	3.8	620
80	5.6	470
85	10	270
90	38	20

It is important to note that Equation 4.4 is an ideal representation and does not take into account weather, pollutants, humidity and other air mass particulates that may reduce the solar intensity at the surface. Additionally, seasonality affects solar intensity. Monterey is 36 degrees north of the equator; in the summer the Sun is 36 degrees away from zenith at noon providing approximately 1000 W/m^2 of solar energy. However, it is usually overcast during the summer months in Monterey. In October, it is beautifully sunny, and the sun at noon, is significantly closer to the horizon, 23 degrees closer. The best day for solar intensity in Monterey in the winter months is estimated to be 840 W/m^2.

C.   SOLAR CELLS

1.   How Solar Cells Work

Solar cells are a form of PV cell that utilize the visible portion of the EM spectrum. Solar cells are simply

semiconductors, similar in nature to a diode. Elements that are used to make solar cells are those that have only four electrons in the valence band. The most stable atoms are those that have a full valence band of eight electrons. Semiconductors make very structured crystal lattices where each atom in the lattice shares the four electrons in its valence band with four neighbors. Thus, electrons in the valance band are moving between two atoms and are not entirely bound to either. Next, the primary element, most commonly silicon, is doped with impurities [17]. Doping is the addition of an element that has one more or one less electron in the valence band. Therefore, doping adds more charge carriers, either positive or negative. If the silicone is doped with a material that has five electrons in the valence band, then one electron does not have a specific place in the lattice and is free to move through the structure. The lattice is now said to be an n-type material, because the charge carriers are predominantly negative electrons. If the primary element is doped with an element that has three electrons in the valence band, then some atoms are left with an incomplete outer shell, and those atoms appear positively charged. Thus, the lattice is said to be a p-type material [17], [18].

Semiconductors are junctions between n-type and p-type materials in which the excitation of the lattice in one material causes movement of the charge carriers in both materials. These semiconductor junctions require the right amount of energy to break the charge carriers free of the atoms to which they are bound. That specific energy is called the bandgap and is measured in electron volts (eV). The bandgap energy of silicon is 1.1 eV. Refer to Figure 7,

to see that 1.1 eV is the energy of photons in part of the visible light spectrum [18].

2. Factors Affecting Output Power

The size of a solar cell is one of the main factors that determines the current of the particular cell. The voltage is minimally affected by the intensity of the sun. The maximum voltage a solar cell can produce is designated as the open circuit voltage (V_{OC}) and is the potential across the cell when a path for electrons to move does not exist. The intensity of the sunlight is proportional to the amount of current a cell or string of cells produces. The maximum amount of current a cell can produce depends on the intensity of the sun and the area of the cell and is called the short circuit current I_{SC}. The short circuit current is only available when the two terminals of the solar cells are shorted. These characteristics can be seen in Figure 9 [18].
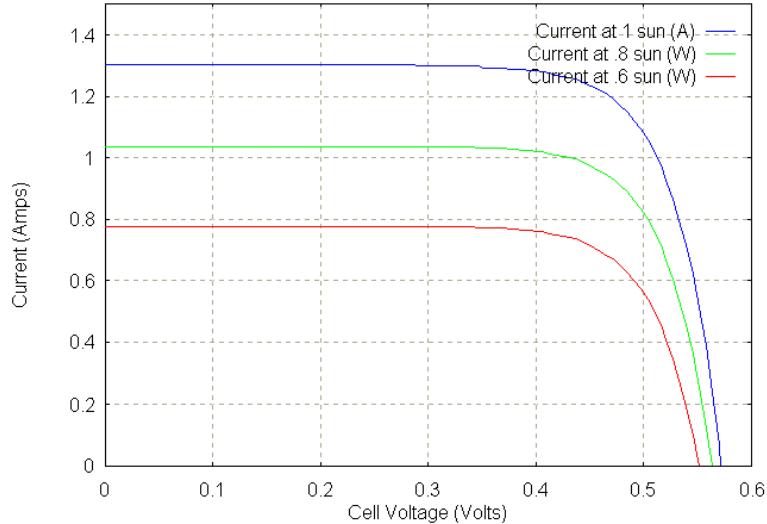
Figure 9.   The behavior of a solar cell at various solar intensities. From [13]

41

Common solar cell behavior is described in the figure above. The current remains relatively set over a range of voltages then drops quickly over the 'knee' of the curve. The solar cells' most efficient operating point is the point on the knee where the current and voltage produce the maximum power. Tracking the Maximum Power (MP) point of a solar cell is the substance of a whole subset of solar research. Figure 9 is an I-V curve; it is a simple matter to measure the V_{OC}, I_{SC}, and MP and then plot the I-V curve [16].

3.   Efficiency and Fill Factor

The efficiency of a solar cell or solar panel is the ratio of the maximum output power of the solar cell to the available input incident power. Solar cell efficiency can be defined as:

$$\eta = \frac{MP}{P_{input}} \qquad (4.5)$$

where η is the solar cell conversion efficiency. The input power is measured in W/m^2, so care must be taken to scale the input power to the array size.[16]

The theoretical maximum output power of a solar cell is $V_{OC}I_{SC}$. Fill Factor (FF) is a ratio of the MP point and the theoretical maximum. Fill factor is defined as:

$$FF = \frac{MP}{V_{oc}I_{sc}} . \qquad (4.6)$$

Other factors that affect the overall efficiency of solar cells are temperature and dirt/dust. To function, a solar cell must absorb light; most of the light is absorbed at the surface of the cell. Those photons, which have

either too much or not enough bandgap energy, generate heat. As the cell temperature increases, the V_{OC} of individual solar cells decreases by approximately 2 mV/C, reducing the overall power output [16].

Solar cells must be cleaned from time to time in order to allow the fully available light spectrum reach the cell surface. This must be done regularly in the desert where dust can quickly build up on a static panel.

Solar cell technology development has been something of a grueling process. Traditional rigid solar cells have been the focus of solar development for 50 years, advancement being driven by satellite power requirements. The most efficient and expensive solar cells on the planet have now broken the 30% efficiency barrier.

D.   THIN FILM SOLAR CELLS

Rigid solar cells that are commonly found on roof and building tops tend to be heavy. They are mounted on an aluminum substrate and encased in glass.

Thin film solar cells are made by depositing layers of semiconductor material on a substrate that is nanometers to micrometers thick. The semiconductor material is deposited as a gaseous vapor onto the substrate and then covered with an anti-reflective coating. There are several material combinations that make effective thin film solar cells; one of the most common is Copper Indium Gallium Selenide (CIGS). Silicon is still a popular choice for thin film, as well as Cadmium-telluride [19].

Thin film solar cells function the same way as rigid solar cells, absorbing light and allowing the energy of a

photon to break an electron free of its valence band bond to move into the higher energy conduction band. However, thin film solar cells tend to have a number of damaged electron bonds that do not allow the electron to break free. Additionally, since there are fewer atoms in the solar cell structure, the net result is there are fewer charge carriers in the structure. Therefore, thin film solar cells tend not to be as efficient as their rigid counterparts. Since 2000 thin film solar cells have struggled to exceed 10% efficiency. Emerging technologies offer the exciting promise of thin film efficiencies in the 16 to 20% range in the near future [20].

Thin film cells are aggressively researched and designed because they are cheaper to make and, even with the reduced efficiencies, are very competitive in the market. The solar cell will be considered ready for mass installation and use when the price per W drops to about one U.S. dollar [21].

E.   ARTIFICIAL LEAF

The concept of modeling nature to produce energy is not new. Scientists and researchers have successfully converted sunlight and water into energy in a variety of ways since the seventies using rare earths and expensive metals as the catalysts for photo-electrochemical reactions. However, the so-called "holy grail" of the artificial leaf is making a system economical and robust enough to enable full-scale competition with fossil fuels and coal burning power plants. A professor at MIT and his research team believe they have done just that.

The last ten years have seen several major leaps forward in this field, and the number of research groups working worldwide on these ideas has ballooned from two to 29 since 2001.[22] Researchers understand the chemical process that takes place in a leaf very well. Leaves utilize the chemical compound chlorophyll as a catalyst that enables the leaf to use sunlight to split water molecules. Freed electrons bind oxygen and carbon dioxide to produce glucose. The remaining electrons from the chemical split are used to repair the chemical makeup of the chlorophyll in the leaf so that it can continue to produce energy. However, chlorophyll itself is a poor choice for the artificial leaf because when directly exposed to Carbon Dioxide in the atmosphere it breaks down rapidly.

An artificial leaf would work in much the same way, simply producing a different chemical output, hydrogen gas. In theory it works like this: a collector is used to gather photons and convert them into electrons, an electrolyzer then uses the energy contained in the electrons to split water molecules, and some chemical or metal catalyst is used to speed the process. According to the Department of Energy, in order for this kind of operation to be scalable to meet National energy demand, each unit will have to last 10,000 hours of use [22].

In 2008 Dr. Daniel Nocera and his team at MIT discovered an inexpensive way to split water molecules using silicon nano-tubes combined with a cobalt/ phosphate catalyst. However, cheap and abundant these materials are, they only freed the oxygen to a gaseous state; the hydrogen

atoms were not able to combine with electrons in order to produce hydrogen gas. At that time Dr. Nocera and his team determined that they would need a separate catalyst for the Hydrogen atoms.

In March 2011, at the National Meeting of the American Chemical Society, Dr. Nocera and his team unveiled a design the size of a playing card that is able to catalyze both oxygen and hydrogen into their gaseous forms ten times more efficiently than a plant can. On one side of the 'card', the cobalt phosphate catalyst drives the chemical reaction for oxygen, and on the other side, a different (undisclosed) catalyst drives the hydrogen chemical reaction. His team asserts that all the materials are cheap and abundant, but the most astonishing news is that the catalysts are self-annealing and that his prototype has lasted for 45 hours of continuous activity thus far [23].

F.   SOLAR CONCENTRATORS

Solar Concentrators are systems or arrays that use mirrors or lenses to amplify the solar intensity a solar cell experiences. They are often used in large solar farms in the southwest. With solar concentrators, a smaller number of more efficient solar cells can be used to produce a large amount of power [16].

G.   DC TO DC CONVERTERS

The SPACES Starpower controller is a DC-to-DC device that enabled the voltage output of the solar panel to be raised or lowered to meet a loads need. The following sections describe the electronics necessary for these conversions. DC-to-DC power converters are a class of

switched mode power electronics that enable voltages to be raised and lowered as necessary. DC-to-DC converters are important in solar cell technology because solar cells tend to provide a varying output, and a DC-to-DC converter can provide a stable output voltage at the required level. Switched mode power supplies have very high conversion efficiencies, generally around 95% or better. The two primary converters will be discussed in the following sections.

1.   Boost Converter

A boost converter is a voltage 'step-up' converter. Boost converters use a switch, either a diode or a transistor, and an energy storage device, a capacitor or an inductor. This device relies on the principle that inductors resist change in current. Figure 10 is a diagram of a typical Boost converter circuit.
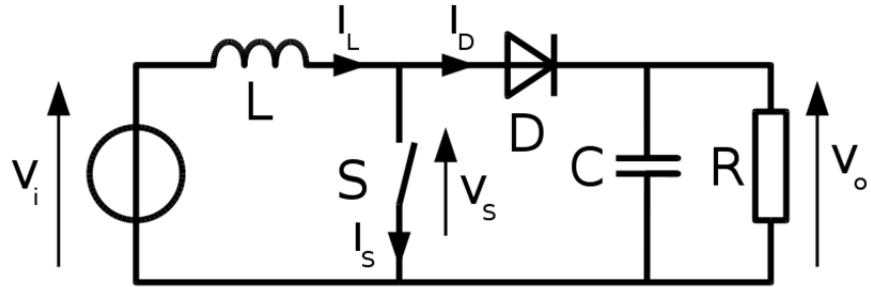
Figure 10.   A typical boost converter circuit configuration. From [24]

When the switch is closed, the load is shorted out of the circuit. The inductor is able to store energy in the magnetic field from the voltage source. When the switch is open the load is reintroduced to the circuit; the rapid addition of a load demands an increase in either voltage or

current. The inductor resists the demand for more current and, therefore, temporarily appears to the load as a voltage source in series with the input voltage, giving the load the higher voltage that is required. If the switch is cycled fast enough, then the inductor will never fully discharge, and the load will always perceive it as a voltage source. Additionally, while the switch is open, the capacitor in parallel with the load is charged to the boosted voltage level. When the switch is closed, the capacitor then becomes a voltage source for the load [25].

The period of time the switch is open compared to the time it is closed is called the duty cycle. Since the duty cycle describes the fraction of time the circuit is on verses the time it is off, the duty cycle is always less than one and can be defined as:

$$D = 1 - \frac{V_i}{V_o} \, . \tag{4.7}$$

When Equation 4.7 is rearranged, it can be seen that the output voltage is always larger than the input voltage: [25]

$$V_o = \frac{V_i}{1-D} \, . \tag{4.8}$$

2. Buck Converter

A buck converter is similar to a boost converter except that it is a voltage 'step-down' converter. Like the boost converter, the buck converter circuit depends on the reluctance of an inductor to change current rapidly. Figure 11 is a representation of a typical buck converter.
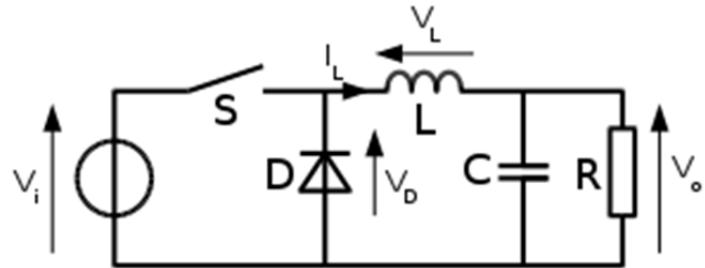
Figure 11.   A typical buck converter circuit.
From [26]

When the switch is open, the circuit is 'off', and there is no current across the load. When the switch is closed, current starts to flow towards the load; however, the inductor resists this increase in current.   In order to maintain the state of energy, the voltage on the load side of the inductor drops. Since the inductor is an energy storage device, as long as the switch opens before the inductor magnetic field is fully charged the load will always perceive a voltage lower than the voltage source. Again the capacitor in parallel with the load ensures the load maintains a constant V_O at a lower voltage than V_i. The buck voltage relationship can be described in terms of the duty cycle: [25]

$$V_O = DV_i .$$ (4.9)

49

THIS PAGE INTENTIONALLY LEFT BLANK

V. LITHIUM ION BATTERIES

A. INTRODUCTION

The Marine Corps is shifting away from disposable energy storage systems to rechargeable batteries in the lithium ion family. The Marine Corps has many mobile communications systems that run on batteries, and the need to understand the capabilities and limitations of our power systems increases with our reliance on them.

1. History of Batteries

The term battery was first used by Ben Franklin to describe a collection of Leyden Jars electrically connected, a reference to an artillery battery. Leyden Jars were the first energy storage devices, and while revolutionary at the time, they were little more than capacitors [27].

An Italian physicist named Alessandro Volta stumbled upon the first known battery in 1799. During some experiments he sandwiched a brine-soaked piece of cardboard between two metal plates and was surprised to discover they conducted electricity when connected [29]. Further work by Volta led to his Voltaic pile; a stack of alternating materials: a zinc plate, brine soaked pasteboard, and a silver plate, repeated several times. This arrangement is depicted in Figure 12. While this was not the first device to produce electricity, it was the first to produce a steady and lasting current. Volta did not appreciate that electricity was created as a result of chemical reactions; he believed the pile to be an inexhaustible power source

that suffered degradation because of the oxidation of the zinc and silver plates. He did not realize that oxidization was the inevitable result of the chemical reactions that enabled electrons to move [27].
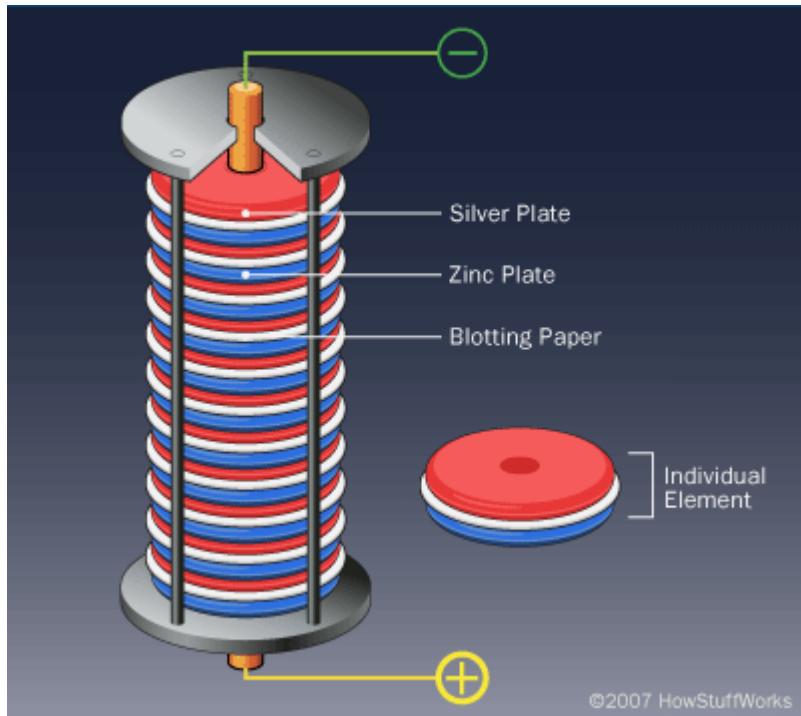
Figure 12.   A depiction of Volta's Voltaic Pile. From [28]

After the Voltaic Pile amazed the world, the race to improve the battery was on. People explored many different chemistries and configurations. The next major breakthrough came from English chemist John Fredrick Daniell. Daniell created his cell using a zinc plate, a copper plate and two chemical electrolytes, zinc sulfate and copper sulfate. Daniell's cell was not very mobile but became a common way to power stationary devices. This cell's primary advantage over previous batteries was its ability to produce a long-lasting reliable voltage source.

2. How Batteries Work

Batteries are electrochemical devices; through a chemical reaction, electrons are freed from their bonds and are able to move through a circuit as a result of a chemical reaction.

Though there are many different battery chemistries, all batteries essentially work same way. A battery has four main components, an anode, a cathode, an electrolyte, and a collector. Most batteries have a positive and negative terminal which, when connected to a load via a circuit, allows electrons to flow from the negative to the positive terminal. The negative terminal is where the anode is located. When a load is connected, the anode experiences an oxidation reaction where ions from the electrolyte combine with the anode freeing electrons to the circuit. The positive terminal has a similar chemical reaction that creates holes, which enable the electrons to recombine as they complete the circuit. The collector allows the electrons to flow from the battery to the circuit [30].

3. Description of Common Battery Chemistries

The sodium-sulfate cell is a rechargeable molten metal battery with a high energy density and a round trip efficiency of 89 to 92 %. It has a long lifetime, up to 2500 cycles, and a shelf life of up to 15 years [29]. A primary disadvantage is that its operating temperature is over 300 C.

Lithium sulfur is a light battery chemistry that has the potential to replace lithium ion and lithium polymer cells due to its extremely high energy density. Experiments

53

so far have been able to create a battery with an energy density of 84% of the theoretical limits, which is four times greater than current lithium ion cells. Another advantage of these cells is that sulfur is a cheap and abundant material [29]. Some issues with lithium sulfur cells include capacity fading over time and limited (about 100) charge/ discharge cycles.

Nickel-cadmium cells have been around for over 100 years. They eventually were enhanced to a sealed battery that responds well to pulse charging and high current rapid discharges. Unlike other batteries, the nickel-cadmium cells require the occasional deep discharge in order to prevent loss of capacity due to memory effects. Modern nickel-cadmium cells have lifetime capacity of over 1000 charge/discharge cycles [29].

Modern nickel-metal-hydride batteries have gained in popularity because of their easily available and environmentally friendly components. These batteries offer an energy density up to 40% higher than nickel-cadmium batteries. However, they are less durable than, and do not handle large loads as well, as nickel-cadmium cells [29].

Lead acid batteries are one of the most commonly known cell chemistries, used in many vehicles for electric turnover of the engine. Lead acid batteries are the oldest rechargeable batteries. They tend to be heavy and have a low energy to weight ratio but can provide very high surge currents. Described in Table 2 are the electrochemical properties of a variety of common battery types.

Table 2.   A comparison of various battery cell chemistries.

Chemistry	Cell Voltage	Specific Energy (MJ/Kg)
Lead-Acid	2.1	0.14
Nickel-Cadmium	1.2	0.14
Nickel-Metal-Hydride	1.2	0.36
Lithium-Sulfer	3	0.35
Lithium-Ion	3.6	0.46
Lithium-Iron-Phosphate	3.3	0.4

B.   LITHIUM ION CHEMISTRIES

Lithium is one of the primordial elements created in the big bang; it is the third element on the periodic table after hydrogen and helium. When trying to store and generate electricity, what is actually occurring is the storage and use of electrons at a relatively high potential. Electrons, however, come with the baggage of the atoms they are attached too. Compare the atomic weight of lead (202.7) to the atomic weight of lithium (6.94). Lithium is 30 times lighter than the material we use to make lead acid batteries. Add to this the fact that lithium, a metal half the density of water, is highly unstable and reacts explosively with water and air. This instability can be perceived as eagerness by a lithium atom to shed its outer electron easily. All of these factors, coupled with its natural abundance, make lithium an excellent element for energy storage devices.

Lithium-ion describes a family of lithium chemistry batteries; they share many qualities, advantages, and disadvantages. Various chemistries differ in performance, cost, and safety considerations.

Lithium Ion Batteries (LIB) operate differently from other batteries. LIBs have similar components to standard batteries, an anode, a cathode and an electrolyte. In the anode, lithium is combined with carbon, most commonly graphite. In the cathode a lithium-metal oxide is used; the metal oxide is what defines the battery chemistry. For example a lithium iron phosphate battery contains lithium and carbon in the anode and lithium iron phosphate in the cathode. The electrolyte used is a lithium salt in an organic solvent [30].

When LIBs are connected to an external circuit a chemical reaction in the anode separates a lithium ion (Li^+) from the carbon, and it migrates through the electrolyte to the cathode. The insertion of the lithium ion into the metal-oxide is called intercalation. The electron that is freed in the process is able to flow to the external circuit. Because the lithium ions move from the anode to the cathode, there is no oxidization in the carbon; this is why lithium batteries do not suffer from memory effects. When the battery is charged, the lithium ions are removed from the metal-oxide and migrate through the electrolyte back to the anode, this process is called deintercalation [31].

The electrolyte is often a liquid lithium salt in an organic solvent. The electrolyte conducts the lithium ions as they migrate. The conductivity of the electrolyte is temperature dependent, making the internal resistance of the battery also a function of temperature.

1. Advantages

Lithium ion batteries can be packaged in a variety of ways, from hard packs of plastic containing multiple cells to very thin and light aluminum. Because they do not necessarily require a metal housing, LIBs are much lighter than other batteries. As mentioned before, LIBs suffer no memory effects. These batteries self-discharge at a much lower rate than lead acid or nickel metal-hydride batteries, prolonging their shelf life. Finally, LIBs generally have a higher open circuit voltage, which provides a higher output power under relatively low current draws. The higher open circuit voltage and lightweight of these batteries contributes to their higher specific power, which is a ratio of the available output power to the weight of the battery [32].

2. Disadvantages

Lithium is an inherently unstable substance; it does not exist in nature in pure form. If overheated a LIB may suffer thermal runaway and cell rupture. Often LIBs contain multiple cells packed into a single battery; if thermal runaway occurs, one or more cells in the pack can rupture violently and in some cases breach the metal or plastic encasement. In extreme cases overheating can lead to combustion. Battery monitoring circuits are included in many cell packs to disconnect the battery in the event unsafe conditions exist, but this adds weight, complexity and expense [32], [33].

During the deintercalation process deposits can form in the electrolyte, which increases resistance over time. Increased resistance reduces the cell's ability to deliver

current, which is more apparent at high current discharges. Internal resistance also increases with age.

C. EXISTING BATTERY MODELS

A variety of battery models exist that predict battery behavior. Each model has its strengths and weaknesses. Models differ in complexity and in the nature of the testing needed to build out and parameterize. The following discussion compares the model that HOMER uses to simulate battery behavior to the electric circuit models, which tend to be simpler and more intuitive for a variety of reasons. Both of these types of models address battery performance and non-linearities such as the relationship of the SOC to VOC, runtime, and state of health [34]. However, neither of these model categories addresses temperature effects; LIBs have performance variations tied to temperature effects.

1. KBM

The kinetic battery model is an analytical model that uses some heuristic or empirical techniques to derive battery behavior [34]. The KBM uses a two-tank reservoir analogy using water to illustrate the flow of electrons to a circuit; this is shown in Figure 13. The KBM depicts the relation effect in batteries in which the open circuit voltage rises after the battery is disconnected from the circuit. This is represented in the analogy by the two tanks returning to equilibrium.
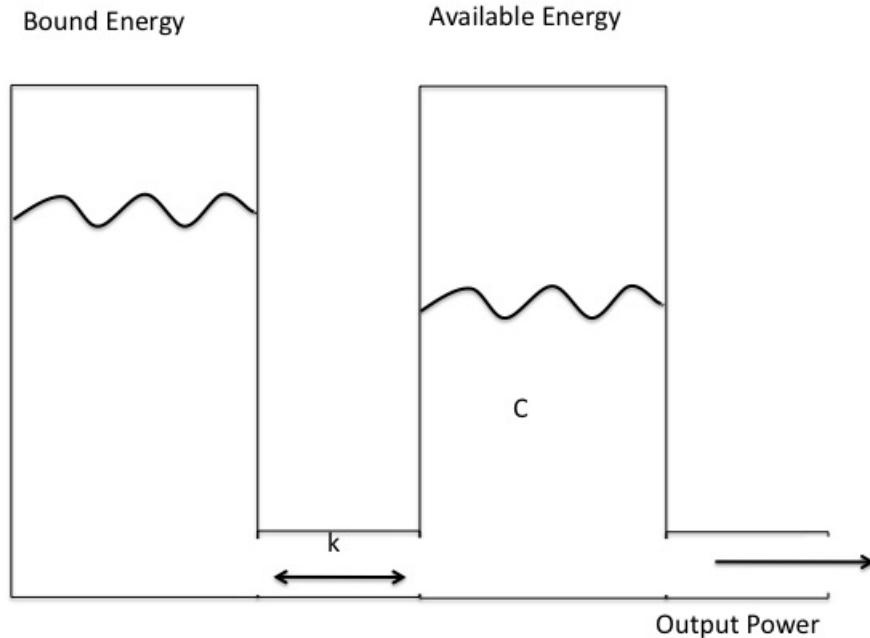
Figure 13.   A visual representation of the KBM.

HOMER uses the KBM to determine the state of charge for the battery, or battery bank, for each time step in a simulation. Manwell and McGowan developed the KBM in 1993; KBM models a battery as a two-tank storage system. Both tanks contain the theoretical maximum capacity of the battery (Q_{max}). The first tank describes the energy that is chemically bound (Q_1), the second tank describes the energy that is available (Q_2) for use. The model connects both tanks with a fixed pipe that enable a controlled amount of bound energy to move to the available energy tank. These two tanks seek to be at equilibrium. The total sum of energy stored in a battery at any time is:[12]

$$Q_{max} = Q_1 + Q_2 .$$ (5.1)

For each simulation hour, HOMER calculates the maximum amount of power that can be discharged from a battery or bank of batteries from: [12]

$$P_{batt,d\max,kbm} = \frac{-kcQ_{\max} + kQ_1 e^{-k\Delta t} + Qkc(1-e^{-k\Delta t})}{1-e^{-k\Delta t} + c(k\Delta t - 1 + e^{-k\Delta t})} \qquad (5.2)$$

where

- Q_1 is the available energy (kWh) in the battery at the beginning of the time step,

- Q is the total energy available in the battery at the beginning of the time step,

- $Q_{\max}$ is the total capacity of the battery (kWh),

- C is the battery capacity ratio (unit-less),

- k is the battery transfer rate constant (h^{-1}), and

- Δt is the length of the time step (h).

The available capacity in each tank at the end of each time step are determined by: [12]

$$Q_{1,end} = Q_1 e^{-k\Delta t} + \frac{(Qkc - P)(1-e^{-k\Delta t})}{k} + \frac{Pc(k\Delta t - 1 + e^{-k\Delta t})}{k} \qquad (5.3)$$

$$Q_{2,end} = Q_2 e^{-k\Delta t} + Q(1-c)(1-e^{-k\Delta t}) + \frac{P(1-c)(k\Delta t - 1 + e^{-k\Delta t})}{k} . \qquad (5.4)$$

HOMER imposes three limitations on charging. The first limitation is to determine the maximum power going into the battery or bank of batteries per time step using:

$$P_{batt,c\max,kbm} = \frac{kQ_1 e^{-k\Delta t} + Qkc(1-e^{-k\Delta t})}{1-e^{-k\Delta t} + c(k\Delta t - 1 + e^{-k\Delta t})} . \qquad (5.5)$$

The second limitation HOMER places on the charging power relates to the manufacture set charge rate. The third

limitation relates to the manufacture limitation set on maximim charge current [35].

2.   Resistive and Capacitive Battery Models

Electric circuit models in which resistive, capacitive and inductive elements are used to represent the circuit offer flexibility and are most suitable for electrical engineering purposes where battery capacity is not the primary modeling concern. A few of the available battery representations are depicted in Figure 14. The electric circuit models can be classified into three main categories: the Thevinin-based, impedance-based, and runtime-based models [34]. These models are unable to describe the dynamic and transient behavior of batteries.

The computer software modeling application SIMULINK uses a Thevinin-based model to describe battery behavior in its simulations. This model was used by Chen, a graduate of the Naval Postgraduate School (NPS), while modeling the impact of adding solar cells to the RAVEN UAV (Un-manned Aerial Vehicle) [29]. SIMULINK is a great tool for circuit analysis and modeling circuit behavior. However, SIMULINK cannot account for the total amount of energy available in a battery.

Impedance-based models are perhaps the most important in this field because they describe dynamic battery behavior the best. An understanding of dynamic behavior is essential for Battery Management Systems (BMS). The impedance of a battery can be used to derive other valuable information about the battery condition such as State of Charge (SOC), temperature, life-cycle, charge and discharge current to name a few [34].
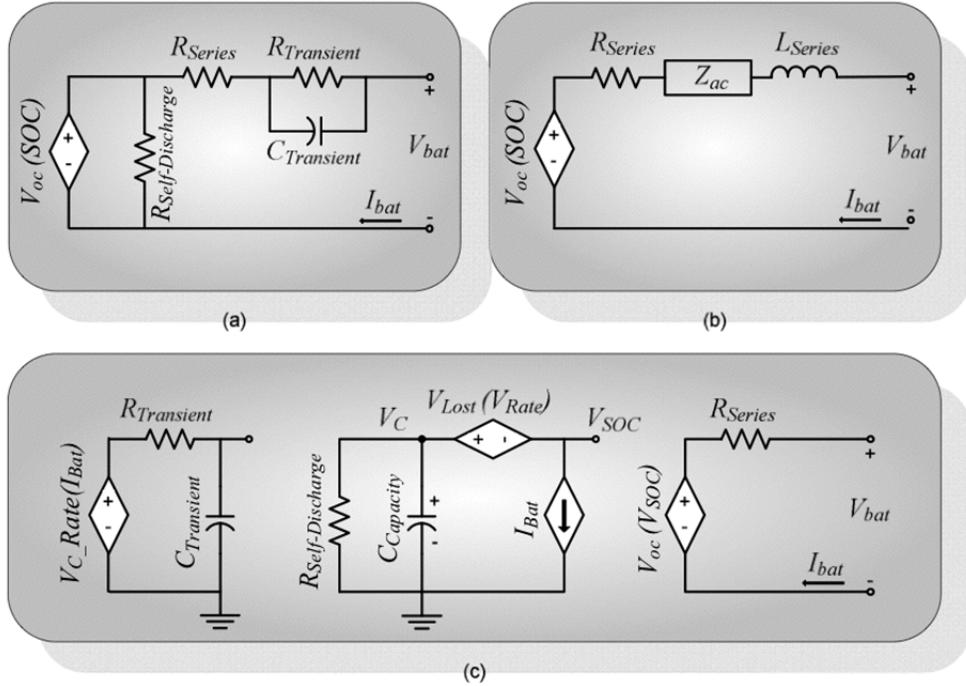
Figure 14.   The three main categories of electric circuit models; (a) Thevinin based, (b) impedance-based, (c) runtime based models. From [34]

Yet another way to use electric circuits to model batteries is the resistive approach. This model breaks the internal resistance of a battery into two categories, ohmic resistance and polarization resistance. Ohmic resistance consists of the electrode resistances and the resistance of the electrolyte. Polarization resistance has to do with the chemical composition of the electrolyte. The ohmic resistance of a battery can give a BMS critical information regarding battery voltage, ohmic loss, discharge time and power available.

3.   Challenges of Lithium Ion Batteries

All models are an approximation; the level of accuracy needed in a simulation determines which model will be used.

62

Both the KBM and the resistive/capacitive models described in this chapter model some battery behaviors and neglect others.

LIBs tend to defy both these standard models for various reasons. LIBs are unique because the Li^+ ions must traverse the graphite lattice, the electrolyte and move into the cathode. The internal lattice structure allows for the relatively free movement of those ions when the battery is fully charged. However, as the battery is depleted the lattice starts to collapse, trapping the ions. This collapse is reversed once the battery is charged. Once a load is attached to a LIB, the SOC drops dramatically; as the battery discharges a slight voltage recovery can be observed, then the battery enters the linear region which the KBM tracks effectively [31]. When discharged at high currents, LIBs have the appearance of additional capacity, something we have termed thermal crossover. Since the parameter 'k' (Equations 5.2-5.4) is largely dependent on battery capacity, this behavior is at odds with the KBM. Initial attempts to parameterize a LIB for the KBM resulted in the chemically bound energy tank appearing much larger than the size available energy tank. It is important to remember that parameter 'c' (Equations 5.2-5.4) is the ratio of the bound energy to the total energy of the battery [33], [37].

The KBM is a good representation of battery behavior for the specific purpose of power modeling as long as the battery is not deep-cycle discharged. We believe that LIB behavior is dependent on the following parameters: temperature, voltage recovery after the initial discharge,

thermal crossover, and the apparent capacity of tank one (available energy). If these behaviors can all be tied to temperature, then it may be possible to create a temperature dependent KBM by adjusting the variable 'k' as the internal temperature of the battery varies [29], [38].

VI. TESTING AND ANALYSIS OF SPACES

A. INTRODUCTION

The Marine Corps has two all renewable power systems in the inventory. Both are solar-based power, with controllers, and energy storage. The large system is the Ground Renewable Expeditionary Energy System (GREENS). GREENS has eight large 200-W solar panels, four Lithium Iron Phosphate (LiFePO$_4$) batteries, and an integrated controller. GREENS is not a man portable system. The solar panels are rigid glass coated and are transported in protective metal cases. The batteries are approximately 80 pounds each. Two complete systems fit into a standard USMC shipping container (quadcon). The second all-renewable system is SPACES, which consists of a single folding solar panel, a DC-to-DC power converter, and a single LIB for energy storage. There are a number of adapters and cables that can be used to power various radios or small systems.

HOMER's current modeling method takes individual components and combines them into a single system to model. HOMER and SPACES are complete systems; however, they physically can be incorporated into larger systems. The intent is to add both SPACES and GREENS to HOMER as complete systems that can be modeled on their own or combined with other power systems and loads. Most importantly, the user will be able to select 'GREENS' or 'SPACES' in the menu, input the number of systems, and HOMER will populate all the components into the workspace.

The following experiments were designed to understand the operating limits of the SPACES system under various

sunlight intensities, with the end goal of making engineering recommendations to the team at HOMER for the inclusion of SPACES into the Marine Corps HOMER model.

B. DESIGN AND METHOD FOR SPACES

1. Design

The Carderock division of NAVSEA loaned a SPACES system to the NPS solar lab. The manufacturer rated the SPACES solar panel at 62 W; the Starpower controller is rated for an input of 9–32 V and will boost the output to 15 to 32 V depending on the load requirements. The controller is compatible with multiple systems, and the complete system comes with many cable adapters. The manufacturer specification for the controller efficiency is 96%. Finally, the energy storage in SPACES is the DS-BT70791A, which is a battery common to many Marine Corps systems. The battery is a LIB, with a nominal voltage of 28.8 V and a 9.4-volt absolute minimum state of charge.

The first step toward modeling this system in HOMER was determining the performance specifications of the folding solar panel in actual light conditions. The second set of tests involved determining whole system performance. Both series of tests would require a control system to compare and validate SPACES performance. All solar testing took place on the roof of Spanagel Hall at NPS.

2. Building a Control System

The solar lab has a small quantity of thin film, flexible solar cells to work with. The first step in building a control system to compare to SPACES was to determine what size array to build. SPACES is approximately

0.73 m^2, and each cell in the control array is 210 cm^2. Using 36 cells, we built an array that is 0.75 m^2. The control panel cells needed to be mounted on a flexible substrate, and we needed to determine how to cover and protect them. In recent laboratory work, thin film solar cells have been attached to rigid boards with simple clear packing tape, which provides both protection from the elements and increases the efficiency of the solar cells by reducing the amount of light reflected. However, using tape to attach cells to a flexible substrate increased the chances of ripples and air pockets trapped in the panel. Our idea was to laminate the cells, sealing them between two flexible sheets of plastic and in the process squeeze all the air out. One big concern was that the cells would not survive the 230 Fahrenheit that is the operating temperature of most laminators.

To heat-test the solar cells, we used three 210-cm^2 cells and tested their output in series. Then they were cut into nine cells that measured 10 cm by 7 cm and were connected in series. We cut the cells to attempt to increase the output and found that the current decreases per cell a little, but now we had nine voltage sources in series, theoretically increasing the output. Once they were mounted on a small flexible substrate, we tested them outside once again to ensure that the cells had not been damaged while being cut. Lastly, the cells were laminated using a standard one-meter wide laminating machine with the thinnest plastic sheeting. Depicted in Figure 15 is the per-single-cell I-V curve before and after laminating the cells. Note the open circuit voltage improves slightly after lamination as expected. The notable drop in short

circuit current is due to the difference in sunlight from 20 September to 21 September. The shape of the two curves are almost identical, there were no discernible losses in the power of the cells due to the heat of lamination.
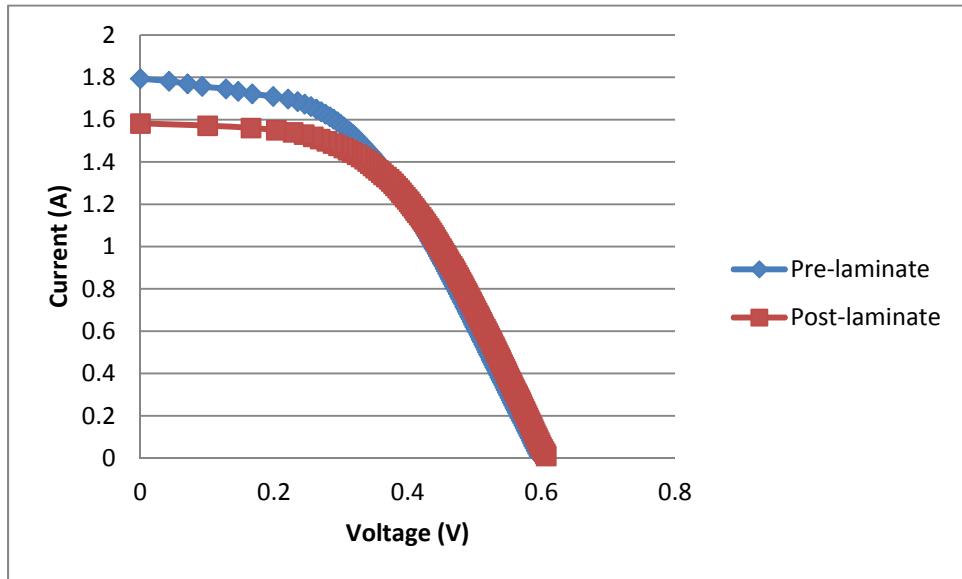
Figure 15.   The I-V curve of the heat test cells before and after lamination per single cell.

The standard laminators available were not large enough to build a control panel the same size as the SPACES, but the idea of heat-sealing solar cells was a valid one. Using two yards of medium thickness flexible plastic sheeting, we built a 36-cell control panel using the standard 210-cm^2 cells.

One yard was stretched and attached to the worktable to prevent wrinkling of the material. The 36 cells were fixed to the plastic sheeting with two-sided tape and connected in series. Mounting the cells in three strings of 12 cells meant the positive and negative terminals were on opposite ends of the panel. To facilitate easier lead

connections, copper tape was run from the negative terminal along the edge to the 'top' of the panel. In Figure 16, the control panel manufacture process is depicted.
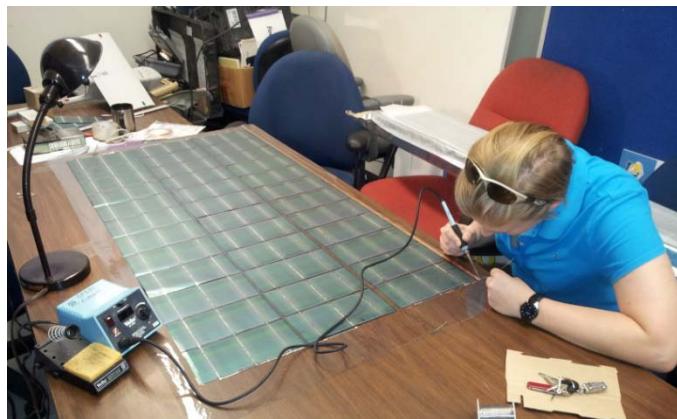
Figure 16.   Manufacturing a control panel
                      in the Solar Lab.

Once the cells were in place, connected and terminal leads attached, it was ready to be covered. We used the second yard of plastic sheeting; we stretched it over the cells and bottom sheeting and attached it to the worktable. It was left overnight stretching on the table to prevent the plastic from shrinking, causing the cells to be warped or uneven. The next day, the two sheets of plastic were sealed together using a clothing iron. While sealing the top and bottom sheets together, we pressed as much air out from between the two sheets as possible.

C.   EXPERIMENTATION AND DATA COLLECTION

1.   Experiment One

October in Monterey is one of the sunniest months of the year. Using the AMPROBE solar meter, we made side-by-side comparisons of the SPACES solar panel and the control

panel over several weeks. The AMPROBE solar meter is a commercial-off-the-shelf device that quickly and accurately measures the open circuit voltage, the short circuit current, and the output power of a solar panel. This piece of equipment collects many data points for a solar array, producing a detailed I-V curve and allowing the users to export the data to a spreadsheet file. The AMPROBE solar meter is depicted in Figure 17. On each day of clear skies, we went out to the roof and measured each panel's output I-V curve.
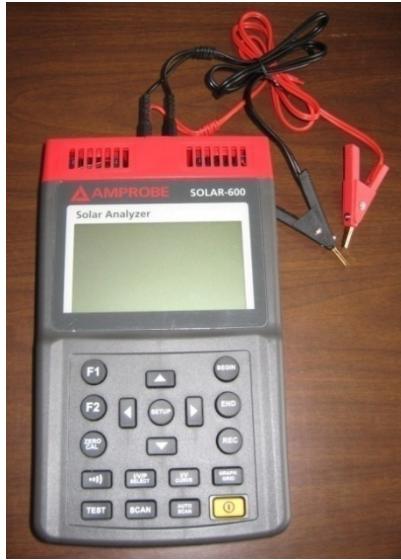
Figure 17.   AMPROBE Solar-600, solar meter.

To evaluate the performance of each panel, it is useful to know the input power per square meter. We know from research that during October in Monterey the best-input power we can expect is roughly 850 W/m^2. By comparing a string of standard cells to a small silicon cell and taking a ratio of the output power at the unit size (1 cm^2), we were able to create a ratio that allows us to estimate each day's solar intensity.

A standard cell is one that was hermetically sealed and measured under laboratory conditions with a known input power. The cells are shipped with an attached data sheet that details the output power, V_{OC}, I_{SC}, FF, I_{MP}, V_{MP}, and their I-V curve. The standard cells we used were measured at 1015 W/m^2 and consisted of a string of nine 210 cm^2, for a total of 1890 cm^2. In 2009, the standard cells produced an MP output of 20.46 W; for at least 5% losses over time, the MP output under an input power of 1015 W/m^2 would be 19.44 W/m^2. When measured on the roof, the standard cells produced only 13.87 W. The ratio of the standard cell's best output under known input power conditions vs. the output power produced in Monterey is:

$$\frac{13.87}{19.44} = \frac{x}{1015} \qquad (6.1)$$

where x is an approximation of the day's solar irradiation input. This approximation does not take into account the variation of the EM spectrum by distortion in the atmosphere or some of the factors that affect cell performance. Knowing the input conditions, the current and voltage of the cell, we can then use a similar ratio to estimate each day's input power.

2. Experiment Two

The second experiment used both the control and SPACES solar panels, the Starpower controller, and two identical Li$^+$ batteries that are the energy storage components of

SPACES. The purpose of this exercise was to see which panel would charge a battery from zero SOC to a full SOC most efficiently.

We used the battery that is included in SPACES, the DS-BT70791A. This particular battery is nominally a 28.2 V (maximum 33.8V) battery arranged in two cell packs. Each cell in a pack has a maximum output voltage of 4.2 V and a minimum voltage of 2.4 V. Internal electronics monitor the state of charge in each cell; when a single cell drops to the minimum voltage the cell pack is disconnected. Each cell pack has a visible meter denoting the percentage of remaining state of charge.

For this set of data collection, we used two identical batteries and drained them until both cell packs were at a zero state of charge. Once the fog cleared at noon on 2 November, we set the systems up on the roof and let the batteries charge.

3. Data

Side-by-side panel data shows that, although the control panel operates at a lower open circuit voltage, it consistently generates a higher maximum power output than the SPACES panel. The control panel performed better under all test conditions. Output power was consistently 5.0 W higher, and the fill factor was consistently better. Shown in Table 3 are the data highlights from the days that measurements were taken. The data in the table show the better performance of the control panel over SPACES blanket with as much as 35% improvement in the output power for the same size blanket.

Table 3.   Performance of both the Control Panel and SPACES
each day of measurement in October, 2012.

Date	Input (W/m^2)	Control					SPACES				
		MP	MP_T	V_O (V)	I_S (A)	FF	MP	MP_T	V_O (V)	I_S (A)	FF
2-Oct	725.00	44.94	96.43	19.89	4.85	0.47	33.16	78.29	25.72	3.04	0.42
4-Oct	678.00	44.31	83.75	21.29	3.93	0.53	32.20	75.49	26.46	2.85	0.43
5-Oct	424.20	30.46	47.92	20.63	2.32	0.64	23.36	53.31	25.74	2.07	0.44
8-Oct	682.00	18.76	44.75	10.62	4.21	0.42	33.65	79.93	26.75	2.99	0.42
13-Oct	725.00	37.27	86.11	21.32	4.04	0.43	33.26	78.72	26.82	2.94	0.42
15-Oct	773.60	37.04	85.13	21.31	4.00	0.44	32.14	76.78	26.53	2.89	0.42
18-Oct	739.00	32.74	73.26	20.83	3.52	0.45	29.13	69.22	26.54	2.61	0.42
24-Oct	784.00	36.75	83.01	21.88	3.79	0.44	31.97	74.87	26.97	2.78	0.43
26-Oct	738.20	33.58	76.26	21.75	3.51	0.44	29.27	69.52	26.78	2.60	0.42

The input power is a rough estimation that was calculated using the ratio mentioned in Section C.2. Depicted in Figure 18 is the solar irradiance measured at the Del Monte costal station over the course of a single day in Monterey. The input power over the course of the month can be seen in Figure 19.
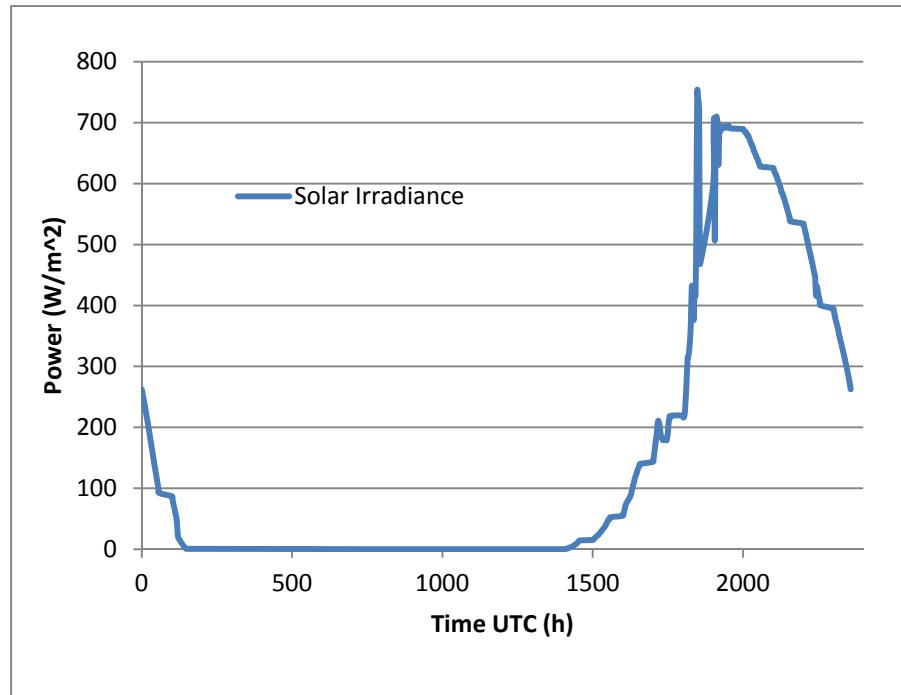
Figure 18.   Measured solar irradiance for 24 hours in Monterey, CA, on 4 October.

73
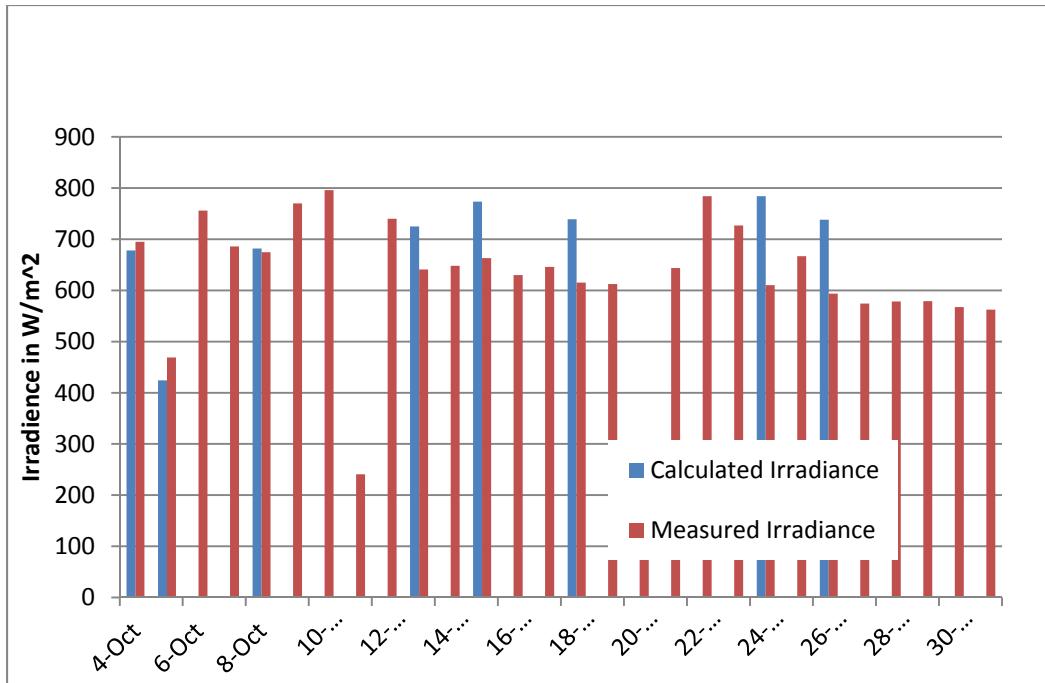
Figure 19.   Calculated and measured solar irradiance
                 in Monterey for the month of October, 2012.

The I-V curves in Figures 20–27 depict the daily
performance of both panels. All measurements were taken
within five minutes of each other. On 8 October, the heat
of the current and the warmth of the day caused the plastic
substrate of the control panel to shrink. The plastic
shrank enough that two columns of solar cells started to
touch. This caused a short circuit, removing half of the
cells and their voltage from the output. As a result of the
short circuit, a minor fire minimally involved six cells.
In order to prevent future short circuits, we opened the
panel and trimmed the cells. This action reduced the
maximum output by approximately three W, and the fill
factor was never as good as my initial measurements. As a
result only the first few days of data collection represent
the true potential of the control panel.
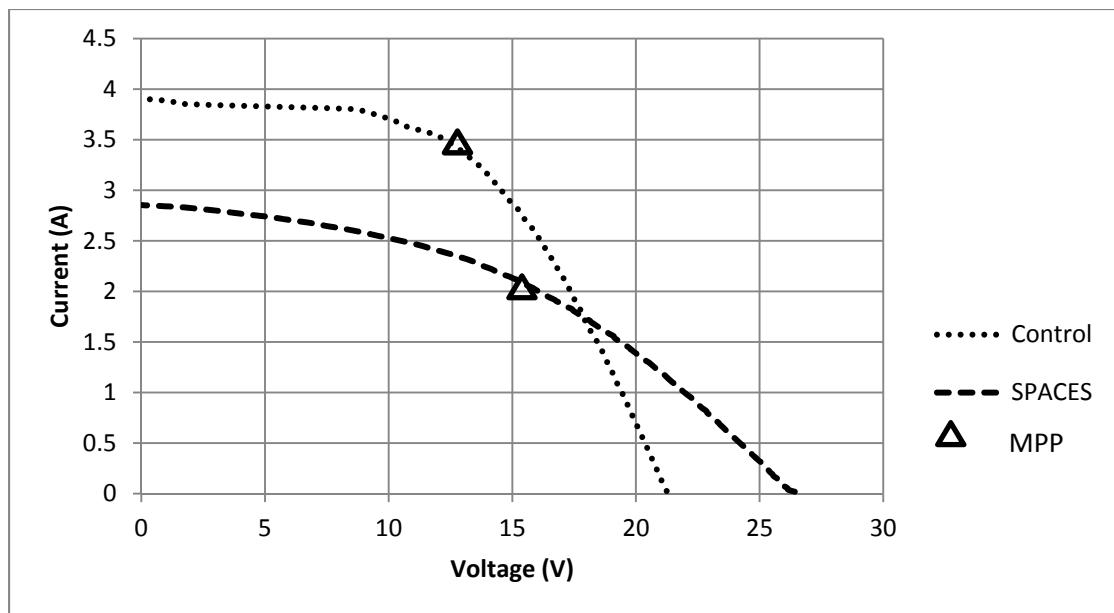
Figure 20.   The I-V curve of both SPACES and the control
                    panel, collected on 4 October.
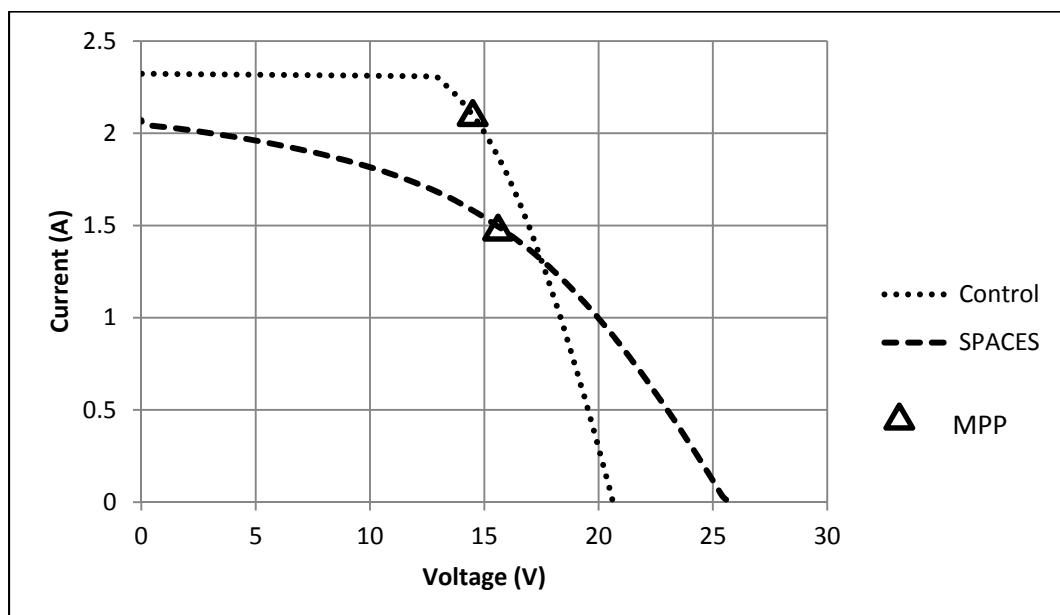
Figure 21.   The I-V curve of both panels on 5 October.

75
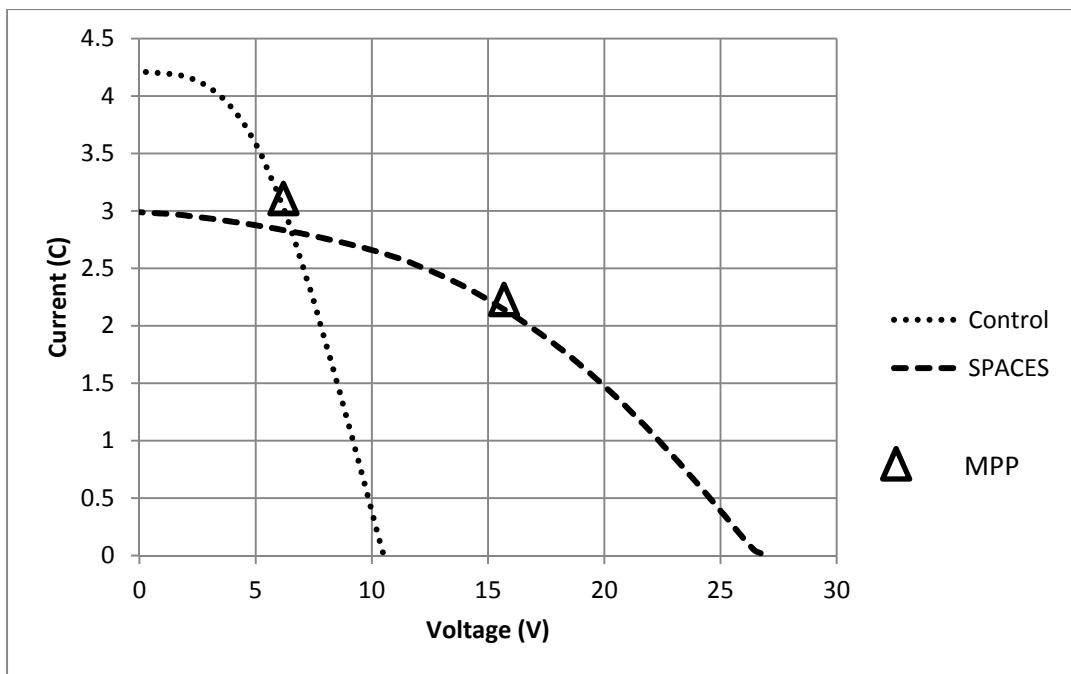
Figure 22.   The I-V curve of both panels on 8 October.
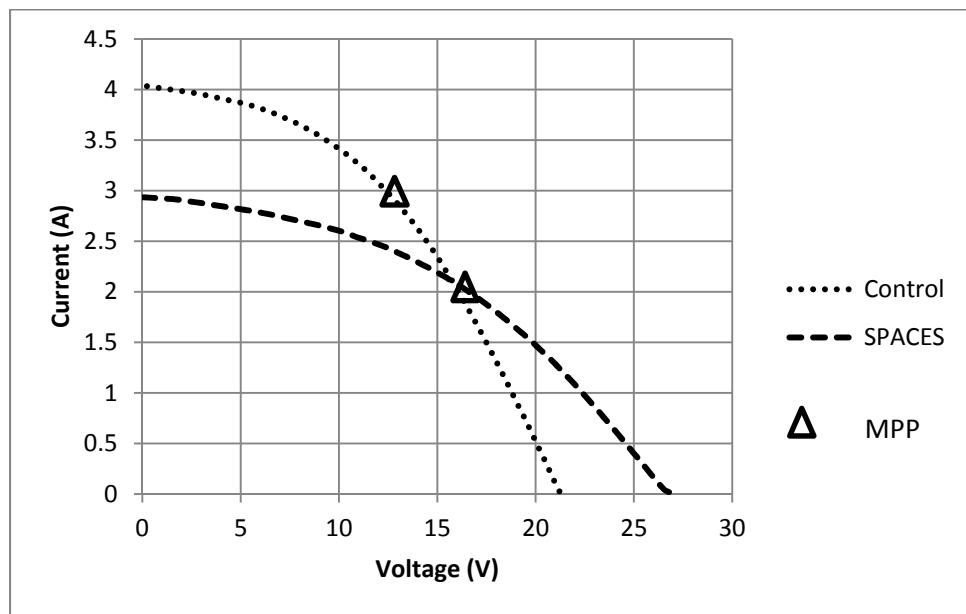
Figure 23.   The I-V curve of both panels on 13 October.
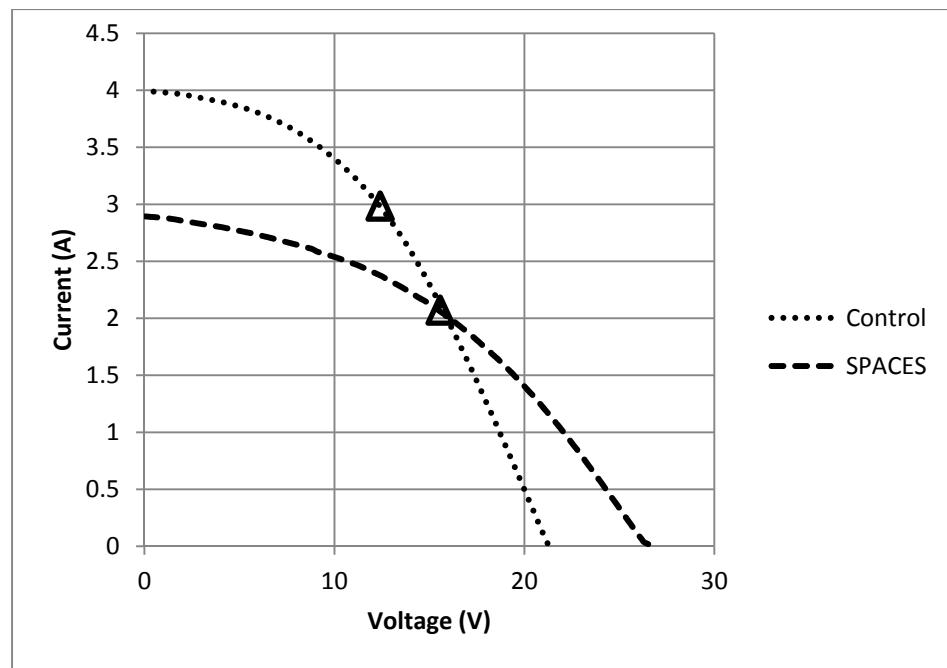
Figure 24.   The I-V curve of both panels on 15 October.
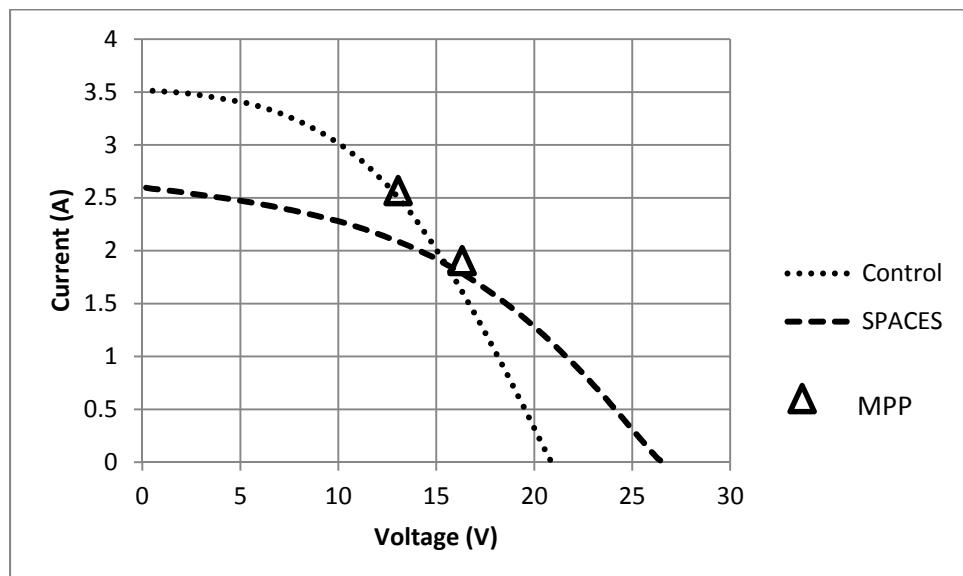
Figure 25.   The I-V curve of both panels on 18 October.
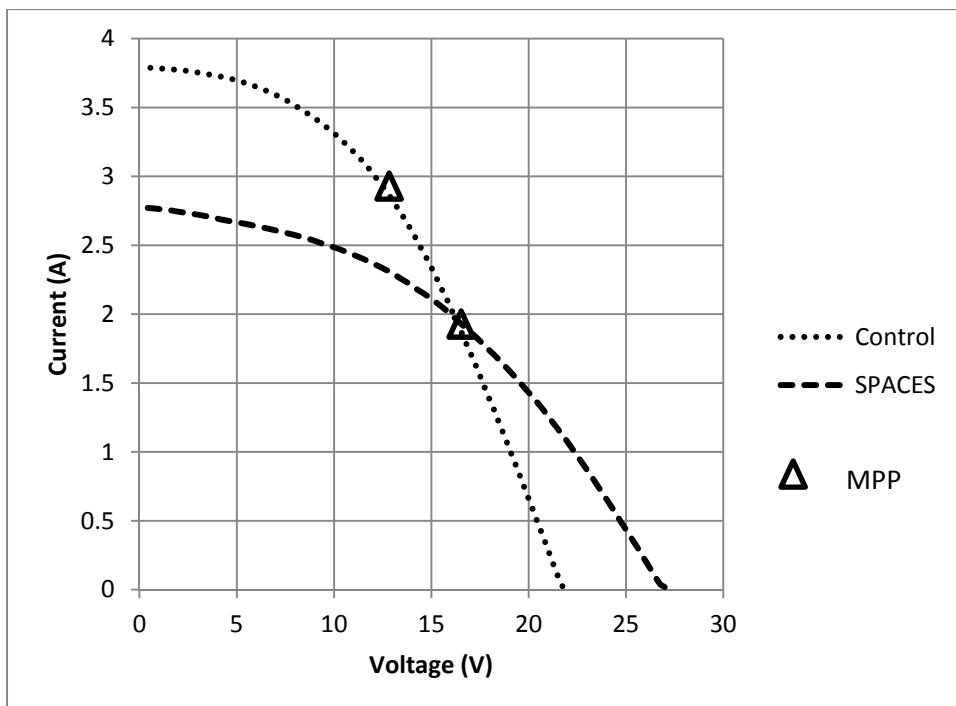
Figure 26.   The I-V curve of both panels on 24 October.
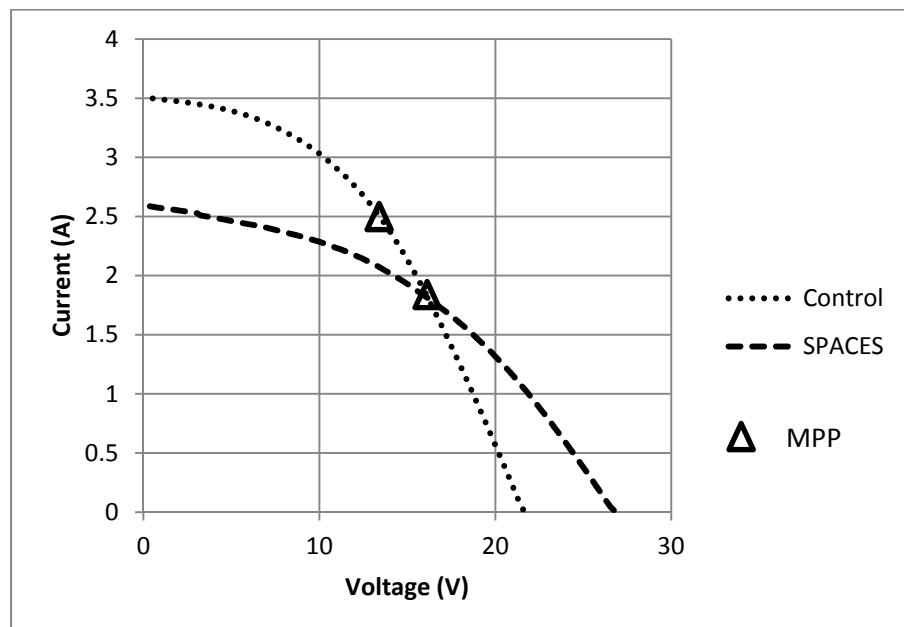
Figure 27.   The I-V curve of both panels on 26 October.
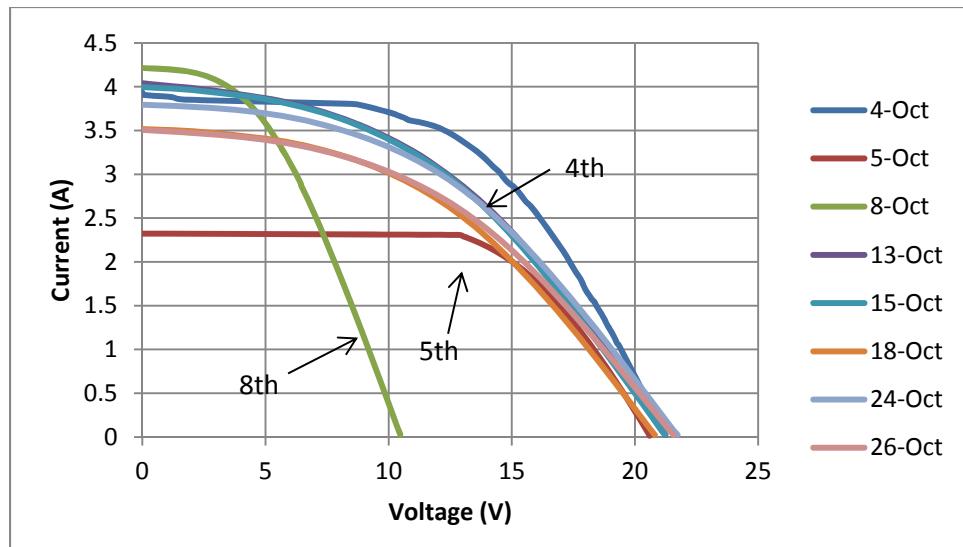
Figure 28.   The control panel performance each day
                 measurements were taken in October.
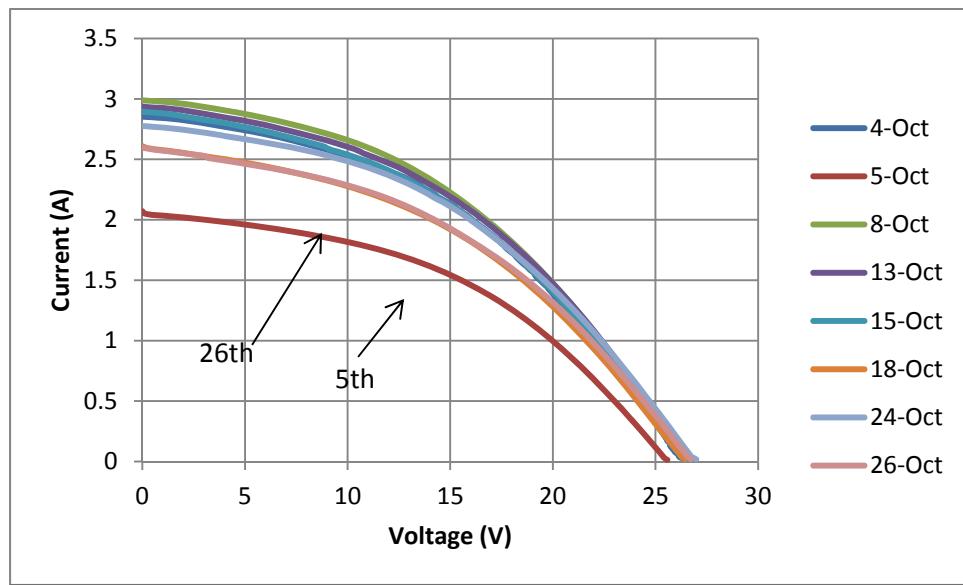
Figure 29.   The performance of SPACES each day
                 measurements were taken in October.

In Figures 20-27, the triangles are located at each
panel's maximum power point. In Figures 28 and 29, each
panel's daily variation and performance is depicted. Note

that in both figures the open circuit voltage does not vary much; it is the current that changes with the light spectrum.
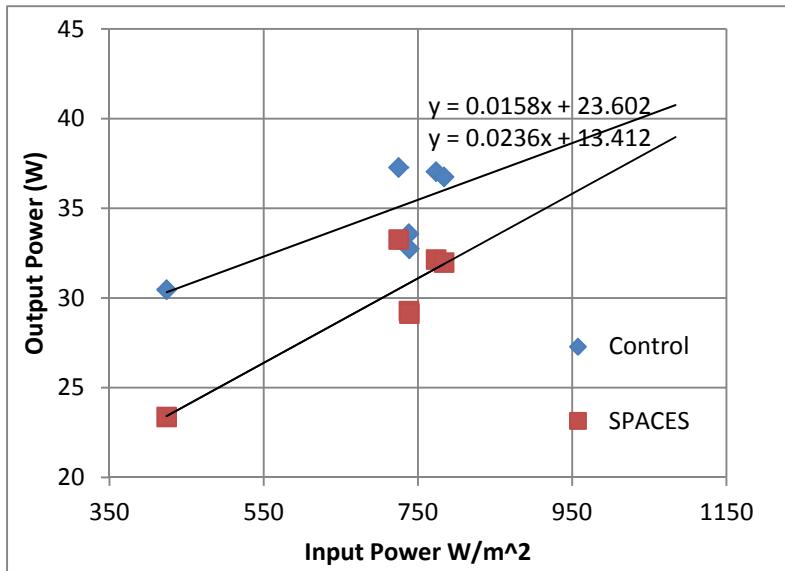
Figure 30.   The output power vs. input power of both panels for the solar spectrum in Monterey, CA.

D.   ANALYSIS OF RESULTS

In Figure 30, we note the pattern of output powers for both panels is very similar. That similarity is due to the panels operating in the same solar spectrum each day. The variation in output power each day when the input power is so similar is due to atmospheric conditions, moisture, and other air particulates. The important take away from Figure 30 is that on the best day in Monterey, SPACES may produce 38 W. If located on the best spot on earth for solar cells, sub-Saharan Africa or some locations in Australia, we expect SPACES would produce as much as 50 W. That estimate is based on the maximum efficiency that SPACES performed at NPS here in Monterey, which was 7.8%. In order to produce

the advertized 62 W at the best solar location on earth, the efficiency of the SPACES panel would have to be 8.8%. The control panel consistently operated at 8.5 to 9.5% efficiency before it was damaged by fire and subsequently being trimmed. After the damage, the control panel consistently performed over 6% efficiency, which was only slightly better than the SPACES panel, which consistently performed at just under 6% efficiency. These efficiencies were calculated taking the size of each array and each day's estimated input power into account. The efficiencies were calculated from:

$$\eta = \frac{P_{Out(W)}}{P_{Input(W/m^2)} Area_{Panel(W)}} \; .$$
(6.2)

Looking at Table 3 (p.73), we see that when the control panel was performing at its peak, it produced 10 to 12 W more power than SPACES with virtually the same area of solar cells.

Using SPACES to charge a battery can be time consuming in Monterey. The lithium ion battery included in the system is a 207 Wh battery. Depicted in Figure 31 is the charge time of the Battery using a controller and battery that are ideal and have zero losses. The second curve depicts charging time accounting for the controller's 96% efficiency and the battery's round trip efficiency of 93.3%. We note that the curves are not significantly different, and the losses in the controller and battery are not significant.
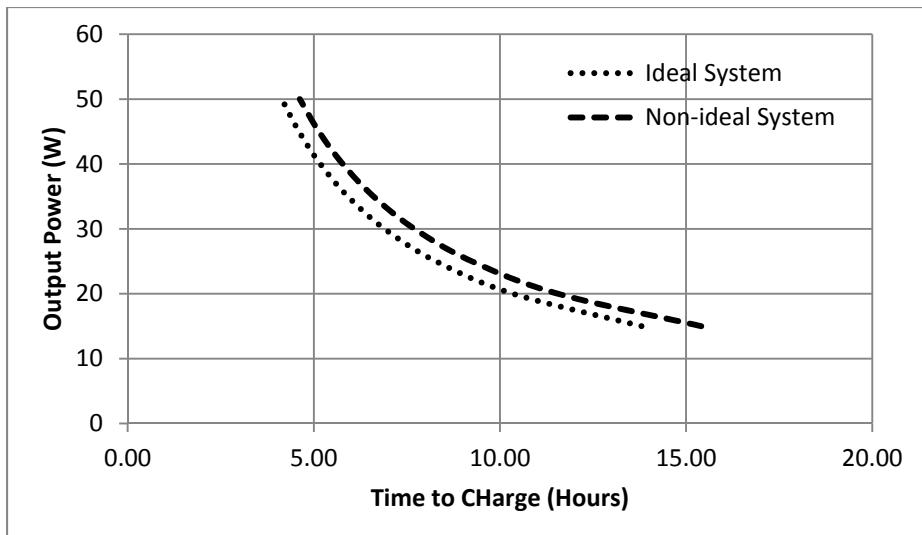
Figure 31.   The time to charge energy storage using the SPACES controller and a solar power input to the controller.

Set up on the roof on three consecutive days, it took SPACES 12.3 hours to fully charge the lithium ion battery that comes with the system. Generating on average 3 to 4 W more took the control system 10.2 hours to charge the same battery.

VII. ANALYSIS OF LITHIUM ION BATTERIES

A.   INTRODUCTION

As discussed in the previous chapter, batteries in the Lithium Ion family have the strange behavior that when discharged rapidly they appear to have increased capacity. As the battery temperature increases, there is often a small voltage recovery in the SOC. This provides the appearance of a higher potential energy in the battery as temperature increases. The experiments outlined in this chapter were designed to discover if there is a deterministic correlation between temperature effects and battery behavior which could be used to develop a simple model. Whether that model could be a modified KBM or a new model is a separate discussion.

B.   DESIGN AND METHOD

1.   Batteries Used

We had three types of lithium ion batteries at our disposal. One 26 V, six cell lithium battery that was current limited to 20 A. We also had one 28.8 V LIB from SPACES. Neither of these were good options for strenuous testing because they did not belong to the Naval Postgraduate School; therefore, we could not destroy them, which was a remote possibility. Additionally, we only had one of each type, and without redundant testing robust conclusions could not be drawn.

The third battery type was $LiFePO_4$ batteries, commercial off-the-shelf products, of which we tested five. These were chosen because they have the same battery

chemistry as the GREENS batteries, though they are significantly smaller. These were single cell 3.2 V, 3.4 Ah batteries, a standard battery capacity (C). The manufacturer rated maximum charge rate is 1.6 A, maximum rated discharge rate is 12 A, and the energy density is 127.2 Wh/Kg. The charge and discharge rates are representative of the capabilities of lithium batteries.

2. Constant Current Circuit

In order to conduct discharge experiments, we needed to be able to control the current. We designed a circuit that used an operational amplifier, two bipolar junction transistors (BJT), several 2.0 W power resistors, and a large power source. The circuit described is depicted in Figure 32.
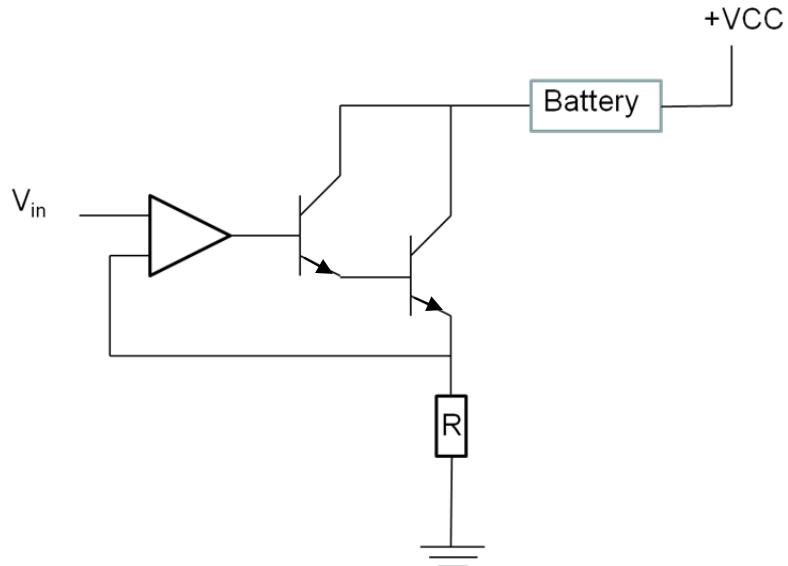
Figure 32.　　The high power constant current circuit used to discharge $LiFePO_4$ batteries.

The circuit in Figure 32 uses the high input impedance and output gain of the operational amplifier to power this

circuit. The input voltage drives the voltage on the feedback loop. Therefore, the input voltage is the voltage on the node above the resistor and forces the current through the resistor to ground. By varying the input voltage, we can set the current to desired levels. Kirchhoff's current law demands that the current through the battery to the BJT collector be essentially the same as the current in the emitter leg. The circuit is governed by the following equations:

$$I_{collector} = I_{emitter} + I_{base} \tag{7.1}$$

$$I_{base} \cong I_R$$
$$I_{collector} \cong I_{battery} \tag{7.2}$$

$$V_R = I_R R = V_{in} \tag{7.3}$$

$$\frac{I_{collector}}{I_{base}} = \beta \tag{7.4}$$

$$I_{battery} = \frac{V_{in}}{R} + I_{base} \tag{7.5}$$

$$\frac{V_{in}}{R} = I_{battery}\left(1 - \frac{1}{\beta}\right) \cong I_{battery} \,. \tag{7.6}$$

Equation 7.1 governs the behavior of BJT's, and Equation 7.2 simply obeys Kirchhoff's law that current in a loop is constant. By following Kirchhoff's Voltage law, we arrive at Equation 7.3. By algebraic rearranging of Equation 7.1 and inserting the substitutions of 7.2, we arrive at Equation 7.5. The symbol β is an operational amplifier constant that relates to amplifier gain; it is usually much greater than one. Substituting Equation 7.4 into Equation 7.5, we arrive at the conclusion that varying the input voltage drives the current through the battery.

Once we determined that the circuit would work, we simulated it in PSPICE and found there would be losses in the BJT's, which are to be expected when discharging a battery's energy and then dissipating that energy as heat. However, the end state of a controlled constant current discharge was feasible. The simulated system is depicted in Figure 33. Additional PSPICE model data is available in Appendix A.
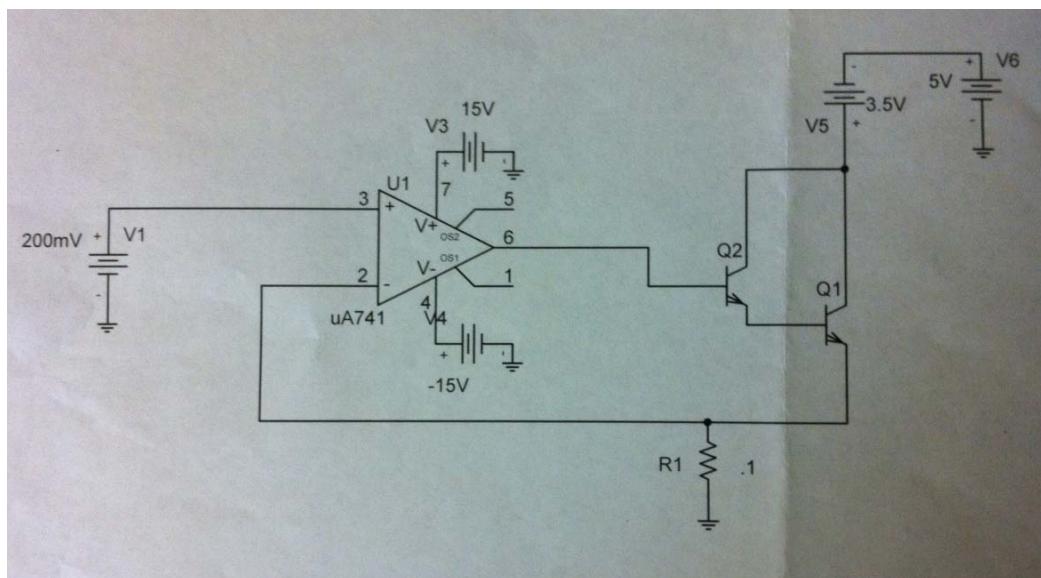
Figure 33.   The PSPICE model of our constant current circuit.

3. Temperature Measurements

Temperature was recorded using a FLIR Systems camera model SC 620. It is a portable long wave infrared camera with a temperature range that extends from -40 C to 500 C. It registers EM waves from eight to twelve μm. The camera has an industry standard 24 C lens and a screen with a resolution of 640 by 480 pixels. This camera takes video and uses an SD memory card slot to store that video.

86

C.   EXPERIMENTATION AND TESTING

The circuit was set up in the power lab on a bench. We kept the battery isolated from the circuit so the heat from the circuit did not interfere with temperature readings from the battery. Depicted in Figure 34 is the laboratory set up.

Figure 34.   The discharge battery test circuit and measurement equipment.

Using a small power supply, we rigged a homemade charging system; in addition we adapted a standard battery charger to fit the size of these particular batteries. We were able to charge four batteries simultaneously; each battery took approximately six hours to charge. The time to charge allowed only a single round of discharges per day, and we set the batteries up for an overnight charge. For these reasons we did not collect charge data. It should be noted though, that as dangerous over-charging a lithium battery is, we never managed to overcharge one. As long as the voltage of the power source remained constant, the

current gradually decreases as the charge on the battery increases until there is no longer any current going into the battery.

The five test batteries were labeled A-E and had positive and negative leads attached. The first test used battery Alpha, the purpose of which was to determine if varying the input voltage did affect the current of the battery. We found that the circuit performed consistently well and that specific input voltage settings would produce consistent current. We found the relationship of V_{in} and the battery current to be linear; therefore, we were able to preset the input voltages for a specific current. After the first experiment, battery Alpha would no longer hold a charge. We suspect that it was a weak battery that had been sitting on the shelf for a few years.

Once the circuit had been tested and was proven to work, we began the tests. Each of the four remaining batteries were discharged at the rate of C, 2C, 3C, and 4C, where 'C' refers to the capacity of the battery; each discharge was recorded using high definition video to record the voltage as the battery discharged, and the FLIR camera was used to record the radiated temperature of the battery. Each of these batteries were discharged once at C (3.4 A), once at 2C (6.8 A), three discharges per battery at 3C (10.2 A), and three discharges per battery at 4C (13.6 A). After each discharge, we collected the voltage data as the battery cooled and returned to equilibrium. To help measure temperature effects, each battery was rapidly cooled using a can of quick-freeze after a 3C and 4C

discharge. Depicted in Table 4 are the number of discharges and rates of discharge for each round of battery testing.

Table 4.   Delineation of battery testing cycles for each battery.

Battery	Variable	RATE OF DISCHARGE				
		C/2=1.7A	C=3.4A	2C=6.8A	3C=10.2A	4C=13.4A
A	X					
B			X	X	XXX	XXX
C			X	X	XXX	XXX
D		X	X	X	XXX	XX

After the second round of discharges, battery Echo would no longer hold a charge, and the data collected with it was deemed suspect. Only batteries Bravo, Charlie, and Delta were discharged at 3C and 4C. For these experiments a total of 25 discharges and cool-downs were observed and recorded

D.   DATA

The following two subsections depict the graphical representation of the data that was collected in the laboratory and the data calculations done to analyze the results of the experiments in Figures 35–45. Each of the figures depicted below are described in the following section along with an explanation of the process calculations and analysis.

1.   Discharge
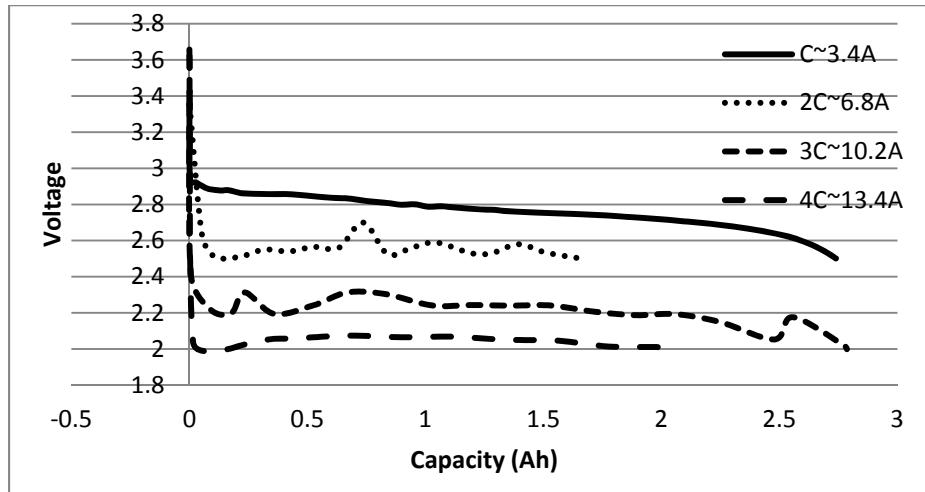
Figure 35.   The discharge curves for battery Bravo at various rates of discharge.
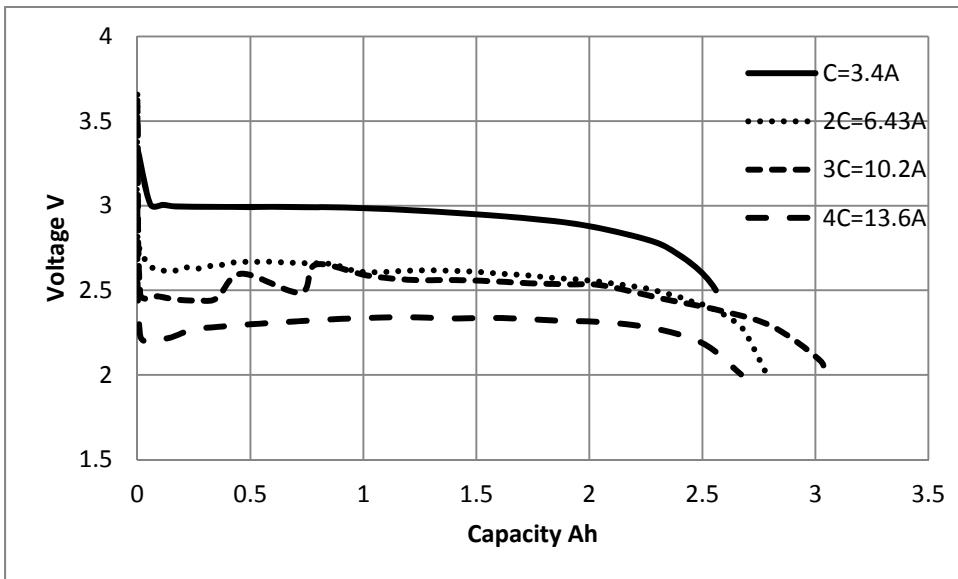
Figure 36.   The discharge curves for battery Charlie at various rates of discharge.
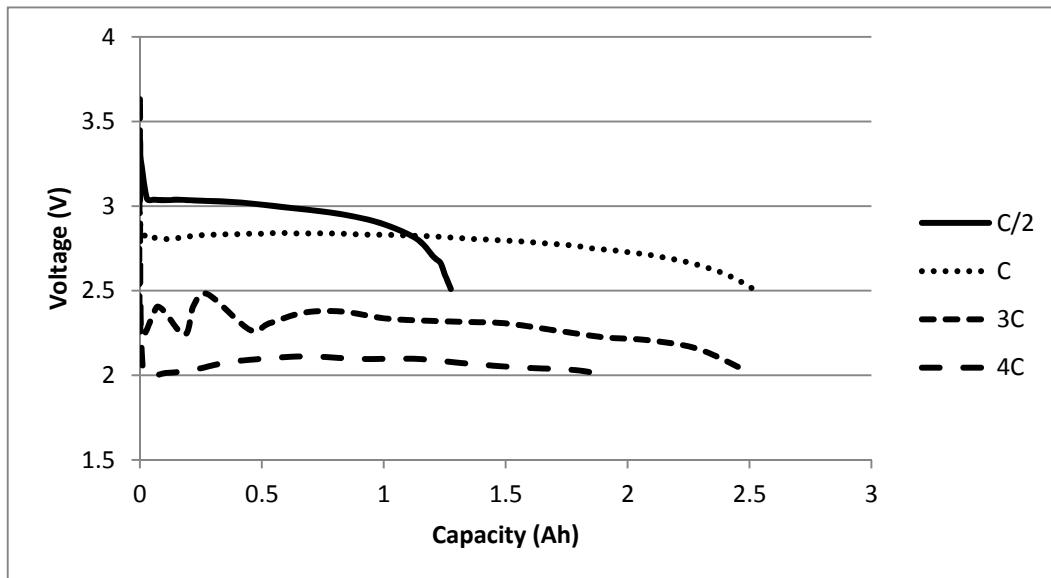
Figure 37.   The discharge curves of battery Delta at
various rates of discharge.

2.   Cool Down
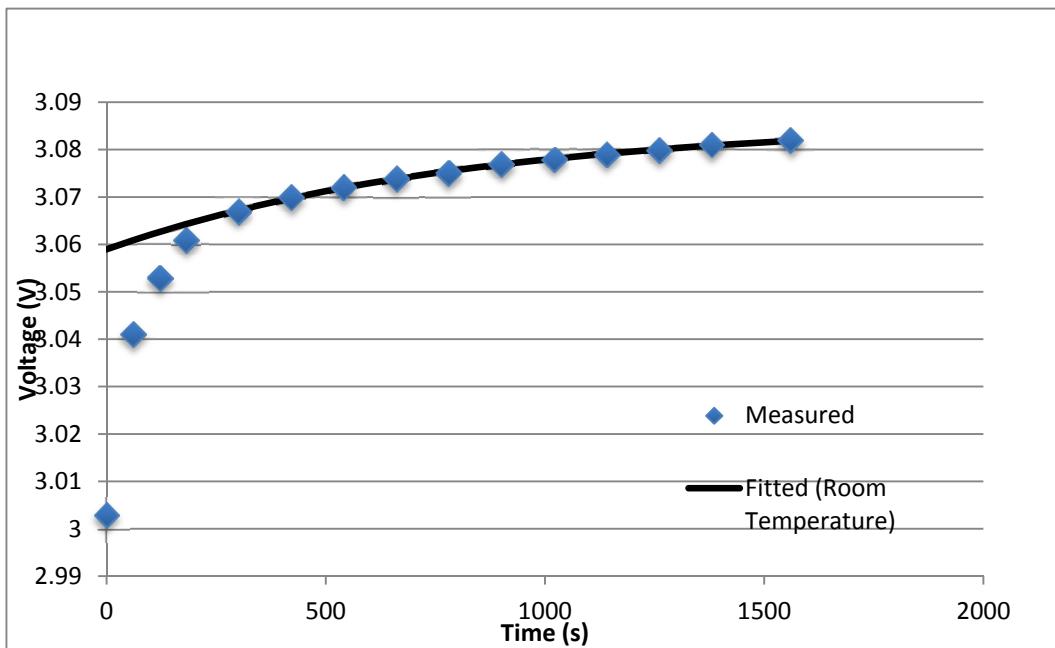
Figure 38.   The KBM fitted curve for battery Charlie 3C
discharge cooled recovery compared to the measured
data.
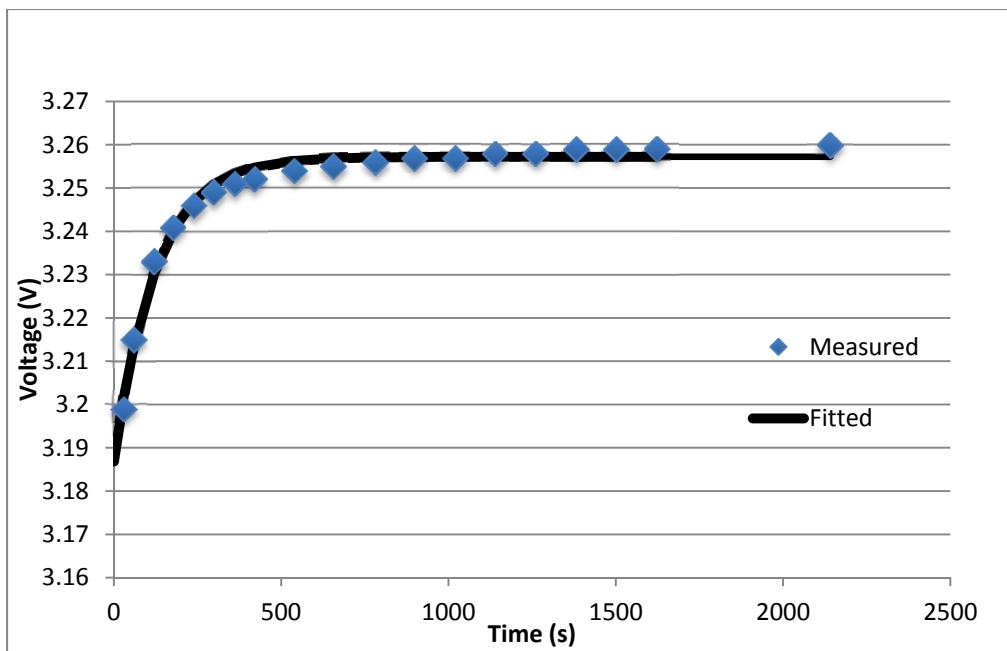
Figure 39.　　The KBM fitted curve for battery Charlie 3C
discharge un-cooled recovery compared to the
measured data.
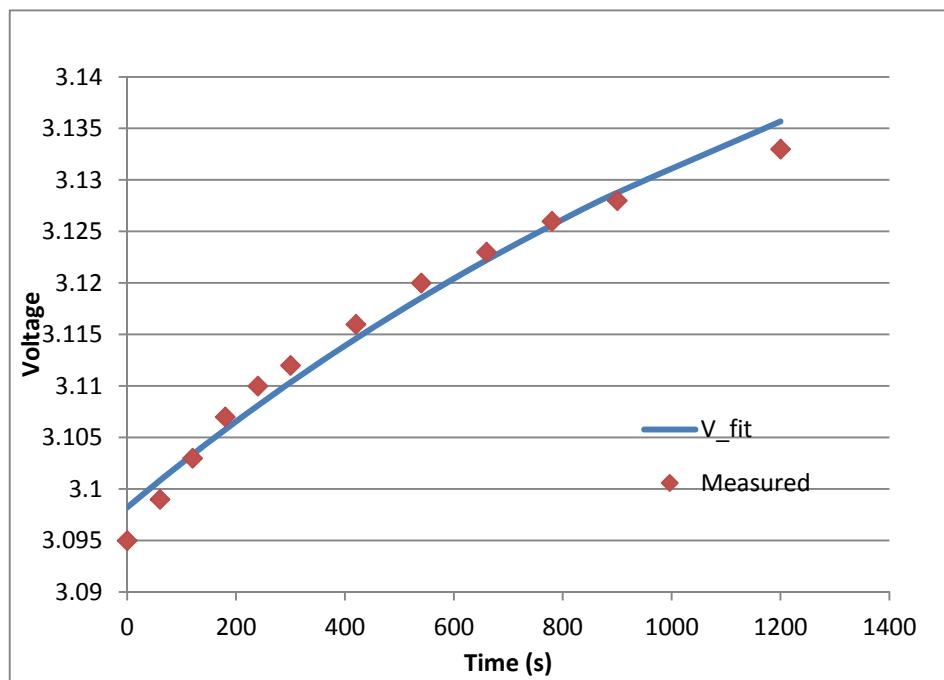
Figure 40.　　The KBM fitted curve for battery Charlie 4C
discharge cooled recovery compared to the measured
data.
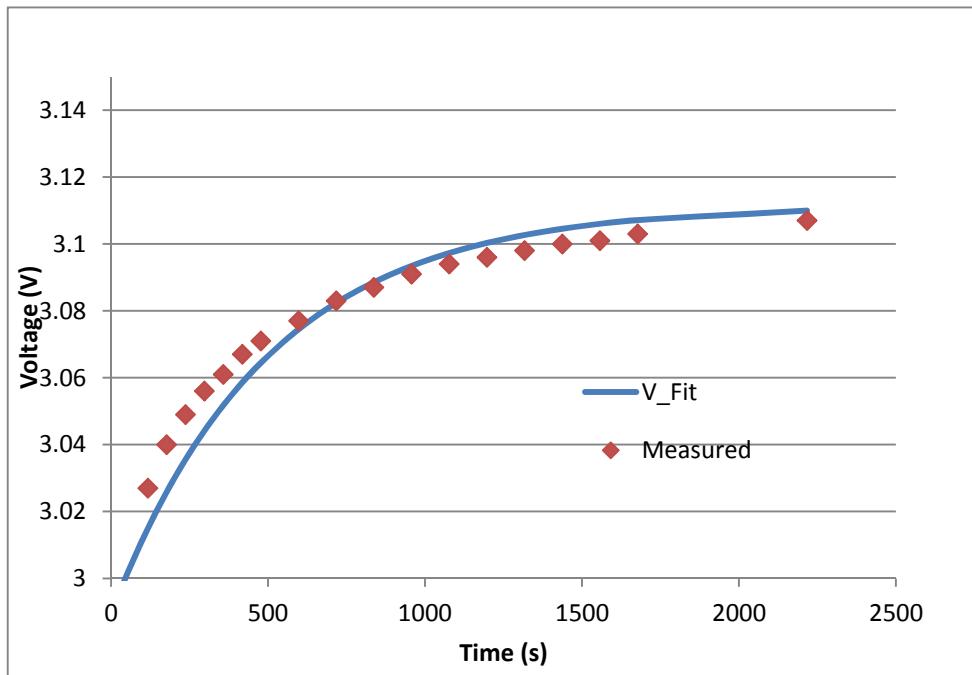
Figure 41.   The KBM fitted curve for battery Charlie 4C discharge un-cooled recovery compared to the measured data.
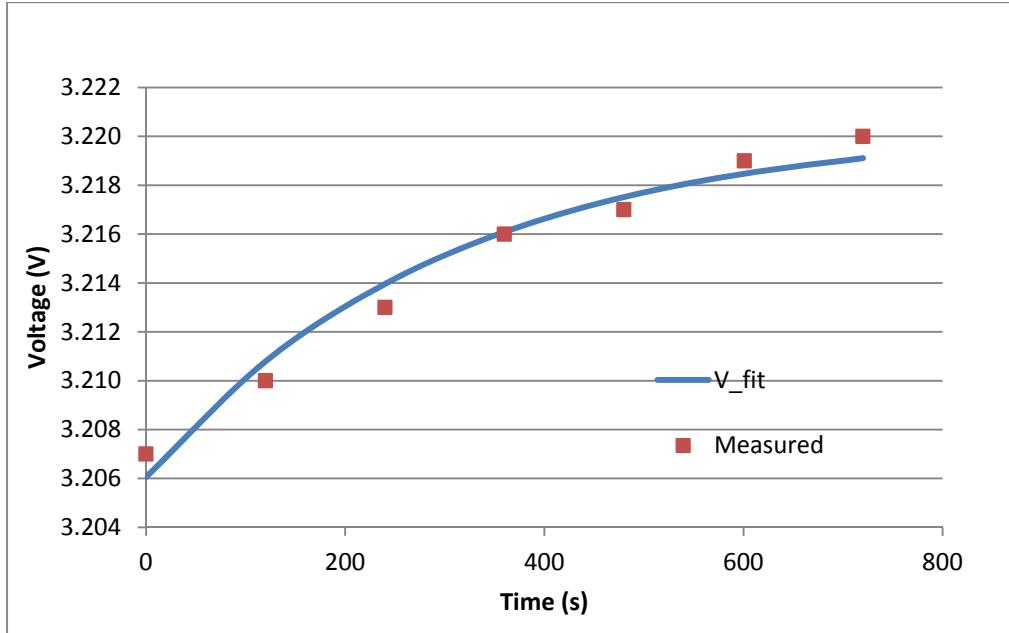
Figure 42.   The KBM fitted curve for battery Bravo 3C discharge cooled recovery compared to the measured data.
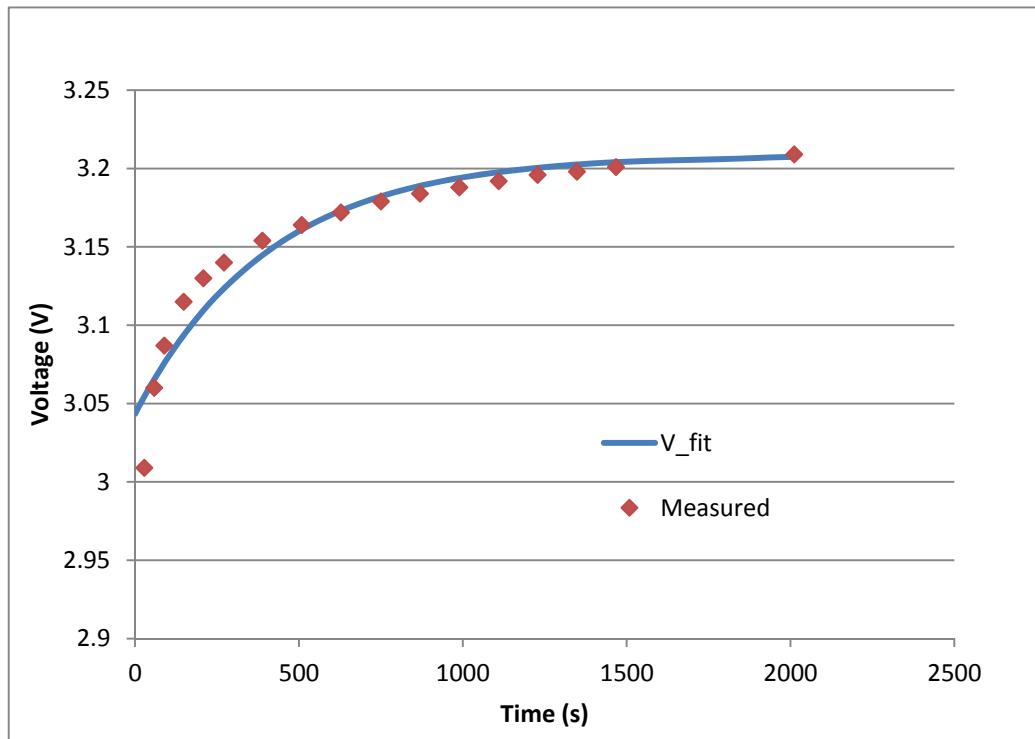
Figure 43.   The KBM fitted curve for battery Bravo 3C
discharge un-cooled recovery compared to the
measured data.
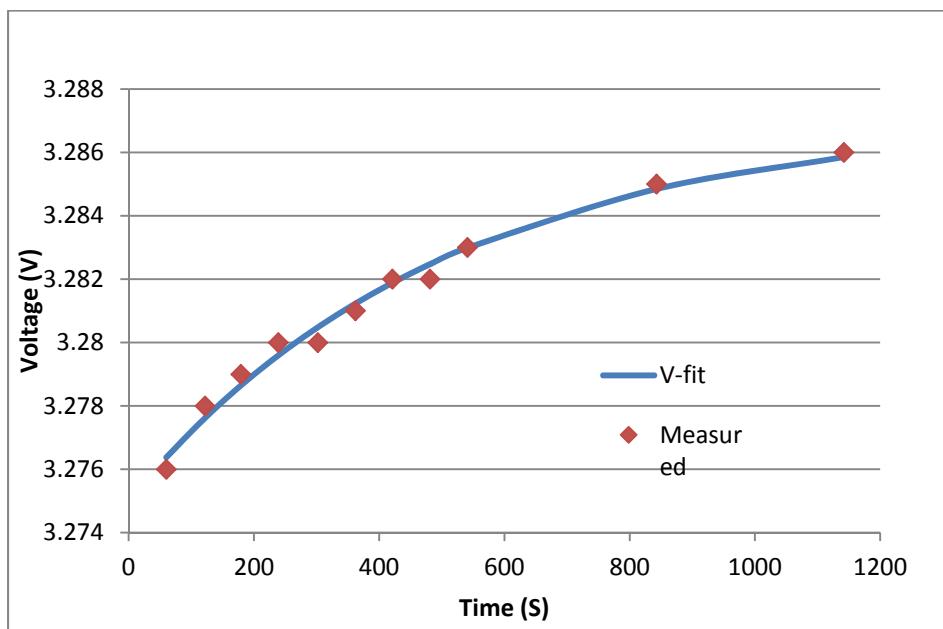
Figure 44.   The KBM fitted curve for battery Bravo 4C
discharge cooled recovery compared to the measured
data.
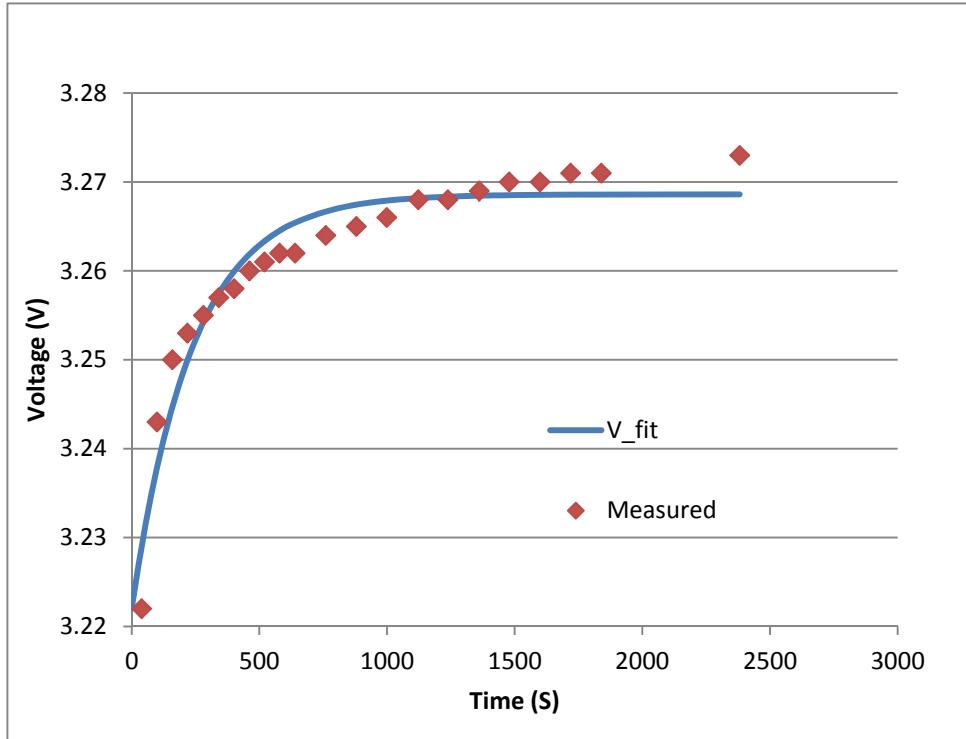
Figure 45.   The KBM fitted curve for battery Bravo 4C
discharge un-cooled recovery compared to the
measured data.

E.   ANALYSIS

1.   Discharge

Of the five batteries we purchased to conduct these experiments, only three were viable in the tests; the other two failed to hold a charge. Of the three that were discharged in the 25 tests only one, battery Charlie, gave reliable and expected results. Battery Charlie provided almost 3 Ah of energy for most discharges and a minimum of 2.6 Ah of energy at worst.

These batteries had been sitting on the shelf for two years, and some degradation was to be expected. Though degraded, each of the three remaining batteries displayed the tendencies toward thermal crossover that has been seen

in so many other Li^+ chemistries. Thermal crossover is the point on Figures 35, 36, and 37 where it seems that more energy can be removed from a battery the faster it is discharged. This behavior does not lend itself to the KBM. The KBM hinges on the value of 'k' which restricts the flow of energy from the chemically bound 'tank' to the available energy 'tank'. When a battery is rapidly discharged, it should not have more energy than when it is discharged slowly.

2. Cool Down

It can be shown that for Li^+ batteries there exists a large region of the discharge curve where the voltage is linearly proportional to the SOC. Therefore, the voltage is linearly proportional to Q_1. This region typically runs from about 98% SOC to 25% SOC. This region can be described by:

$$VOC_{Q_1} = E_0 + E_1 Q_1 - IR \qquad (7.7)$$

where E_0 and E_1 are empirical constants that fit the discharge curve. The internal impedance of the battery is designated R. When the circuit is disconnected and there is no current, Equation 7.7 can be reduced to

$$VOC_{Q_1} = E_0 + E_1 Q_1 \qquad (7.8)$$

For a battery having completed a charge or discharge event and where the voltage and SOC was in the linear region, the equilibrium of Q_1 has the following relationship with voltage:

$$V(t) = VOC_{Q_1}(t) = E_0 + E_1 QC + (Q_1 - Qc)e^{-k\Delta t} \qquad (7.9)$$

Equation 7.9 is obtained by rearranging Equation 7.2 and substituting the result into Equation 7.8. Taking the limit of Equation 7.9, we arrive at the equilibrated voltage of the battery:

$$\lim_{t \to \infty} V(t) = E_0 + EQc = V_{eq} \,.$$ (7.10)

Equation 7.9 can now be rewritten as:

$$V(t) = V_{eq} + V_{conc} e^{-k \Delta t}$$ (7.11)

where V_{conc} is the over/ under potential of the battery at the initial time due to the disequilibrium in the cell. It has a value of:

$$V_{conc} = (Q_1 - Qc) \,.$$ (7.12)

The values of V_{eq}, V_{conc}, and k can be fit to the open circuit equilibration voltage curve of a battery. The resulting value of k can be used as part of the parameterization for the KBM. The benefits of this is that k can be determined at specific SOC using a single curve, and it does not require repeated charge and discharge cycling, which is normally required.

Table 5. The Parameter values of battery discharges using Equation 7.11 from discharge experiments.

	V_{conc}	V_{eq}	k
B 3C Un-cooled	-0.165282293	3.208693719	0.002442694
B 3C Cooled	-0.014353445	3.220411896	0.003333333
B 4C Un-cooled	-0.046607662	3.268605204	0.004192852
B 4C Cooled	-0.012072473	3.287081337	0.002
C 3C Un-cooled	-0.070397154	3.257218754	0.007941791
C 3C Cooled	-0.026957585	3.085923091	0.001212341
C 4C Un-cooled	-0.012072473	3.287081337	0.002
C 4C Cooled	-0.071013631	3.169218963	0.000625

We used Equation 7.11 to fit equilibrium curves to the batteries as they recovered from being rapidly discharged. The batteries that were forced to room temperature rapidly after the discharge was a complete fit to the KBM model within one or two mV for each cooled battery discharged. The cooled fitted models, depicted in Figures 38, 40, 42 and 44, began at the time when the battery reached room temperature. For the each of the batteries that were allowed to cool over time, the fitted voltage recovery followed the general trend of the measured voltage recovery. However, the fitted curve deviated from the measured data by as much as 50 mV. The widest model deviations come at the points on the curve where the temperature of the battery is the warmest. This suggests that the battery cooling off affects the voltage recovery in a dynamic manner. These observations are consistent in all of the recoveries depicted in Figures 39, 41, 43 and 45.

From these results we have concluded that there is a significant temperature effect on battery behavior. Though the 50 mV deviations during recovery are not significant enough to warrant a new model, a temperature corrected KBM could be very useful.

VIII. CONCLUSIONS AND RECOMMENDATIONS

A.   RESULTS

1.   Solar Experiments

In each solar experiment the control panel outperformed the SPACES panel. The solar cells that the control panel is comprised of are three years old and were not properly stored, resulting in some performance degradation. In the process of the experiments, the control panel also caught on fire due to a short circuit. The rated output power of the SPACES is 62 W; the estimated best output of SPACES is approximately 50 W, only 80% of its rated capacity. Systems like GREENS and SPACES are very important to expeditionary power, but the technology is improving constantly. Those systems need to improve as the technology becomes available. In the next two or three years, promising research has the strong potential to yield flexible thin film solar cells that are 16% efficient. Such an improvement would double SPACES output without adding weight or size. A two-fold increase in GREENS output power, while reducing the weight of the system several hundred pounds (by switching ridged cells for new improved thin film cells), will vastly improve expeditionary power systems.

2.   Battery Experiments

A complete tabulation of the data collected can be viewed in Appendix B. These tables depict the behavior of

99

the batteries as they are discharged, including the current at which they are discharged, their temperature rise, and their $V(t)$.

Once all the data was collected, we applied the KBM equations to the equation for the linear region. We found the model fitted a battery voltage recovery nearly perfectly when the battery was at room temperature. Moreover, this behavior was repeated in three different batteries of the same design and chemistry. This suggests a strong correlation between temperature and battery behavior; the internal lattice temperature affects battery voltage.

B.   CONCLUSIONS

The KBM needs to be tested and verified for both charging and discharging. We think there is strong evidence based on work done previously and our work in the lab that the KBM is a valid working model for Li^+ when the battery is operating in the linear region. Additionally, the Marine Corps will not likely be discharging batteries at high enough currents to be concerned with temperature effects. From the data collected, temperature does not appear to affect battery behavior until it is over 40 C. Internal temperature is driven by excessive discharge rates.

SPACES is a well-designed system that provides small units with a micropower system. However, it is important that SPACES improves as solar cell technology improves in order to meet the demands of the modern expeditionary Marine Corps.

C.   RECOMMENDATIONS FOR FUTURE WORK

There is a lot of work left within HOMER to meet the Marine Corps' requirements. We need to collect 24-hour load profiles for our most common FOB structures. A system analysis of GREENS should be conducted in order for that system to be incorporated into HOMER.

The KBM needs to be validated for Li^+ batteries (during both charging and discharging) in order to determine if temperature is the most dynamic variable and, if so, to develop a temperature dependent model.

THIS PAGE INTENTIONALY LEFT BLANK
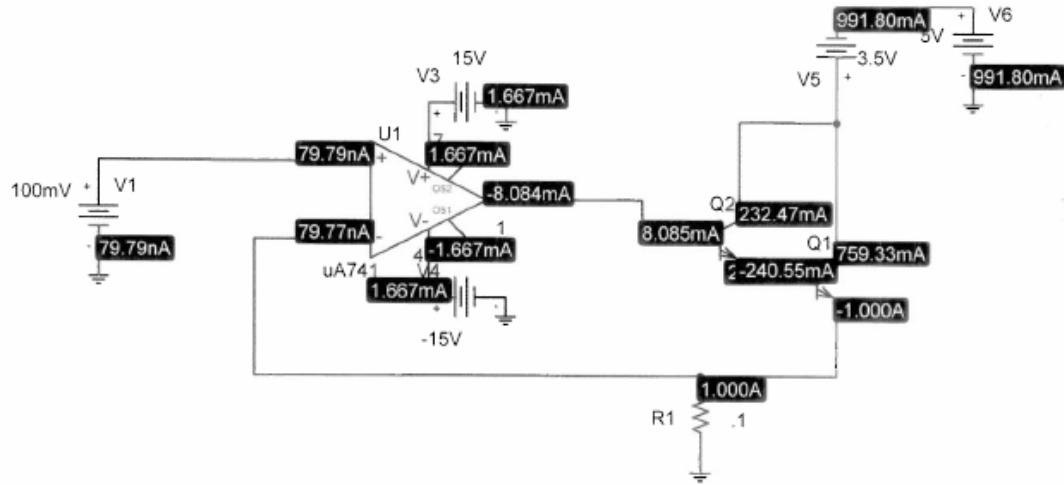
Figure 46.   The constant current PSPICE model with current displayed.
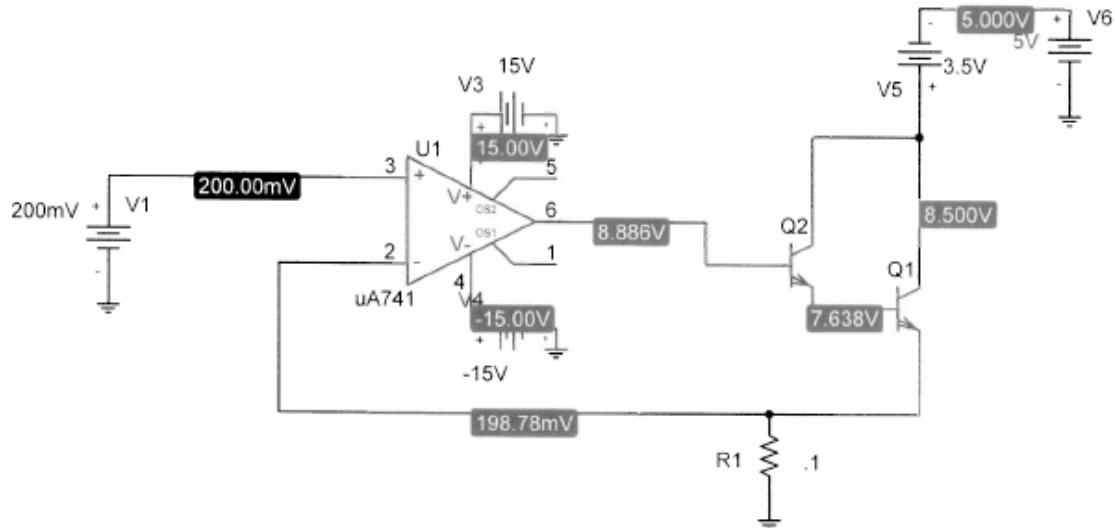
Figure 47.   The constant current PSPICE model with voltage displayed.

THIS PAGE INTENTIONALLY LEFT BLANK

1. BATTERY BRAVO DISCHARGE DATA

17-Oct								
Voc=3.352		Disharge	2C=6.8 A					
						31-Oct		
Time					Drain to 2 V			
Min	Secs	Time	T©	Vcell	V_cell	I_cell	Capacity (Ah)	Power
0	0	0	24.3	3.352	3.648	0	0.000	22.7936
	30	30	24.9	2.63	2.439	6.41	0.053	17.884
1	0	60	25.4	2.51	2.416	6.41	0.107	17.068
2	0	120	25.9	2.51	2.401	6.37	0.212	17.068
3	0	180	26.5	2.55	2.415	6.32	0.316	17.34
4	0	240	27	2.54	2.418	6.34	0.423	17.272
5	0	300	27.3	2.565	2.436	6.3	0.525	17.442
6	0	360	27.6	2.56	2.442	6.33	0.633	17.408
7	0	420	28	2.7	2.445	6.31	0.736	18.36
8	0	480	28.3	2.525	2.448	6.3	0.840	17.17
9	0	540	28.7	2.562	2.446	6.3	0.945	17.4216
10	0	600	28.9	2.589	2.439	6.28	1.047	17.6052
11	0	660	29	2.53	2.405	6.51	1.194	17.204
12	0	720	29.3	2.53	2.426	6.4	1.280	17.204
13	0	780	29.5	2.58	2.425	6.43	1.393	17.544
14	0	840	29.5	2.537	2.406	6.43	1.500	17.2516
15	0	900	33.1	2.511	2.366	6.43	1.608	17.0748
15	33	933	32	2.5	2.363	6.43	1.666	17
16	0	960	31.6	3.2	2.36	6.43	1.715	
17	0	1020	31.3	3.234	2.358	6.43	1.822	
18	0	1080	31	3.251	2.333	6.43	1.929	
19	0	1140	30.6	3.26	2.338	6.43	2.036	
20	0	1200	30	3.268	2.325	6.42	2.140	
21	30	1290	29.4	3.274	2.289	6.42	2.301	
22	0	1320	29.2	3.276	2.275	6.43	2.358	
23	0	1380	28.7	3.278	2.204	6.43	2.465	
24	0	1440	28.5	3.281	2.105	6.43	2.572	
24	33	1473			2.031	6.43	2.631	
25	0	1500	28.2	3.282	1.978	6.43	2.679	
26	0	1560	27.9	3.284				
27	0	1620	27.6	3.285				
28	0	1680	27.4	3.286				
29	0	1740	27.2	3.287				
30	0	1800	27	3.288				
31	0	1860	26.7	3.289				
36	0	2160	25.8	3.29				
41	0	2460	25.3	3.291				
46	0	2760	25	3.292				

18-Oct								
Voc=3.422		Disharge	C=3.4 A					
Time								
Min	Secs	Time	T©	Vcell	I_cell	Capacity (Ah)	Capacity(Ah)	Power
	4	0	28.2	3.422	0	0	0	0
	6	2		2.9341	4.18	0.002	0.002322	
	33	29		2.922	3.4	0.027	0.027389	
1	3	59	29	2.901	3.39	0.056	0.055558	
1	29	85		2.886	3.38	0.080	0.079806	
2	2	118	29.6	2.88	3.37	0.110	0.110461	
2	33	149		2.877	3.36	0.139	0.139067	
3	2	178	30	2.879	3.36	0.166	0.166133	
3	59	235		2.862	3.39	0.221	0.221292	
5	2	298	30.1	2.859	3.39	0.281	0.280617	
6	3	359	30.6	2.857	3.39	0.338	0.338058	
7	1	417	31	2.858	3.39	0.393	0.392675	
8	1	477	31.5	2.855	3.39	0.449	0.449175	
9	1	537	31.7	2.848	3.38	0.504	0.504183	
10	1	597	32.2	2.841	3.38	0.561	0.560517	
11	1	657	32.4	2.836	3.38	0.617	0.61685	
12	1	717	32.8	2.833	3.38	0.673	0.673183	
13	0	776	33.1	2.823	3.38	0.729	0.728578	
14	2	838	33.4	2.814	3.38	0.787	0.786789	
15	0	896	33.6	2.808	3.38	0.841	0.841244	
16	1	957	33.9	2.798	3.38	0.899	0.898517	
17	1	1017	34.1	2.801	3.38	0.955	0.95485	
18	2	1078	34.5	2.787	3.38	1.012	1.012122	
18	59	1135	34.6	2.79	3.38	1.066	1.065639	
20	2	1198	34.7	2.783	3.38	1.125	1.124789	
20	59	1255	34.9	2.778	3.38	1.178	1.178306	
21	59	1315	35.1	2.772	3.38	1.235	1.234639	
23	2	1378	35.2	2.77	3.38	1.294	1.293789	
23	58	1434	35.5	2.762	3.38	1.346	1.346367	
25	1	1497	35.7	2.758	3.38	1.406	1.405517	
26	1	1557	35.8	2.755	3.38	1.462	1.46185	
27	1	1617	36	2.754	3.38	1.518	1.518183	
28	1	1677	36.1	2.751	3.38	1.575	1.574517	
29	1	1737	36.2	2.747	3.38	1.631	1.63085	
30	0	1796	36.4	2.744	3.38	1.686	1.686244	
31	0	1856	36.5	2.74	3.38	1.743	1.742578	
32	0	1916	36.7	2.736	3.38	1.799	1.798911	
33	0	1976	36.7	2.731	3.38	1.855	1.855244	
34	3	2039	36.8	2.726	3.38	1.914	1.914394	
35	2	2098	36.9	2.721	3.38	1.970	1.969789	
36	5	2161	37	2.714	3.39	2.035	2.034942	
37	2	2218	37	2.708	3.38	2.082	2.082456	
38	2	2278	37.2	2.702	3.38	2.139	2.138789	
38	59	2335	37.4	2.695	3.38	2.192	2.192306	
40	5	2401	37.5	2.686	3.38	2.254	2.254272	
41	1	2457	37.6	2.678	3.38	2.307	2.30685	
42	1	2517	37.8	2.666	3.38	2.363	2.363183	
43	1	2577	37.9	2.655	3.38	2.420	2.419517	
44	4	2640	38	2.639	3.38	2.479	2.478667	
45	1	2697	38.2	2.625	3.38	2.532	2.532183	
46	1	2757	38.4	2.601	3.38	2.589	2.588517	
47	3	2819	38.4	2.571	3.38	2.647	2.646728	
48	3	2879	38.7	2.532	3.38	2.703	2.703061	
48	42	2918	38.7	2.501	3.38	2.740	2.739678	
48	50	2926	38.7	2.987	0			
49	0	2936	38.5	3.02	0			
49	30	2966	38.2	3.072	0			

22-Oct									
Voc=3.515	Disharge			3C=10.2A					
Temp=27.4									
Time									
Min	Secs	Time		Temp	V_cell	I_cell	Capacity (Ah)	Capacity %	Power
0	4	0			3.515	0	0		
0	7	3			2.214	11.33	0.009	14.12541	
0	36	32			2.052	11.08	0.098	3.432343	
1	9	65			2.186	9.76	0.176	12.27723	
1	37	93			2.236	9.74	0.252	15.57756	
2	8	124			2.213	10.22	0.352	14.05941	
3	8	184			2.247	10.04	0.513	16.30363	
4	8	244			2.223	10.16	0.689	14.71947	
5	7	303			2.285	9.76	0.821	18.81188	
6	8	364			2.248	9.8	0.991	16.36964	
7	7	423			2.265	9.73	1.143	17.49175	
8	7	483			2.278	9.71	1.303	18.34983	
9	7	543		50.9	2.298	9.59	1.446	19.66997	
10	10	606		52.3	2.261	9.94	1.673	17.22772	
11	7	663		53.7	2.266	9.77	1.799	17.55776	
12	7	723		55.3	2.251	9.9	1.988	16.56766	
13	9	785		57	2.334	9.87	2.152	22.0462	
14	7	843		58.2	2.146	10.26	2.403	9.636964	
15	7	903		59.9	2.035	10.49	2.631	2.310231	
16	7	963	0	62.4	1.827	10.38	2.777	-11.4191	
16	8	964	1	62.4	2.509			33.59736	
16	40	996	33	60.5	3.027			67.78878	
17	7	1023	60	59.3	3.067			70.42904	
18	6	1082	119	56.5	3.109			73.20132	
19	7	1143	180	54.5	3.13			74.58746	
20	7	1203	240	53	3.143			75.44554	
21	7	1263	300	50.9	3.151			75.9736	
22	8	1324	361	49.3	3.158			76.43564	
23	7	1383	420	47.9	3.163			76.76568	
24	7	1443	480	46.4	3.168			77.09571	
25	7	1503	540	45.1	3.172			77.35974	
26	7	1563	600	44	3.175			77.55776	
28	7	1683	720	41.3	3.182			78.0198	
30	9	1805	842	39.6	3.187			78.34983	
32	6	1922	959	38.1	3.191			78.61386	
34	12	2048	1085	36.6	3.195			78.87789	
36	8	2164	1201	35.3	3.198			79.07591	
38	7	2283	1320	33.9	3.201			79.27393	
40	8	2404	1441	33.1	3.204			79.47195	
49	6	2942	1979	29.3	3.212			80	

107

				24-Oct			
Voc=3.621		Disharge			3C=10.2A		
Temp=26.4							
Time							
Min	Secs	Time		Temp	V_cell	I_cell	Capacity (Ah)
0	6	0		26.4	3.621	0	0
0	8	2		26.5	2.408	11.72	0.007
0	38	32		28.1	2.218	10.1	0.090
1	8	62		29.8	2.199	10.3	0.177
1	38	92		31.4	2.313	9.16	0.234
2	8	122		32.7	2.194	10.6	0.359
3	8	182		35.3	2.242	10.41	0.526
4	8	242		37.1	2.313	9.96	0.670
5	8	302		38.8	2.304	9.89	0.830
6	8	362		40.7	2.241	10.22	1.028
7	8	422		42.2	2.243	10.23	1.199
8	9	483		44	2.24	10.2	1.369
9	8	542		45	2.241	10.15	1.528
10	8	602		46.5	2.206	10.28	1.719
11	8	662		47.7	2.187	10.31	1.896
12	10	724		49.1	2.193	10.23	2.057
13	9	783		50.3	2.149	10.34	2.249
14	8	842		51.8	2.053	10.6	2.479
15	8	902		51.5	2.176	10.21	2.558
15	36	930		52.4	2.016	10.75	2.777
15	39	933	0	52.5	1.999	10.75	2.786
15	40	934	1	52.6	2.726	0	
16	8	962	29	50.9	3.009	0	
16	38	992	59	49.6	3.06		
17	9	1023	90	48.8	3.087		
18	8	1082	149	47.1	3.115		
19	8	1142	209	45.7	3.13		
20	11	1205	272	44.4	3.14		
22	8	1322	389	42	3.154		
24	8	1442	509	40.1	3.164		
26	8	1562	629	38.3	3.172		
28	10	1684	751	36.6	3.179		
30	9	1803	870	35.2	3.184		
32	9	1923	990	34	3.188		
34	9	2043	1110	33	3.192		
36	8	2162	1229	32.2	3.196		
38	8	2282	1349	31.4	3.198		
40	7	2401	1468	30.8	3.201		
49	11	2945	2012	28.5	3.209		

24-Oct							
Voc=3.641		Disharge			3C=10.2A		
Temp=25					Cooled		
Time							
Min	Secs	Time		Temp	V_cell	I_cell	Capacity (Ah)
0	7	0		25	3.641		0.000
0	9	2		25	2.262	11.81	0.007
0	39	32		27.4	2.214	10	0.089
1	9	62		29.7	2.223	9.94	0.171
1	39	92		31.7	2.238	10.2	0.261
2	9	122		33.6	2.26	10.09	0.342
3	9	182		37.3	2.264	10.16	0.514
4	9	242		40.8	2.292	9.94	0.668
5	9	302		43.9	2.293	9.99	0.838
6	9	362		46.6	2.291	9.98	1.004
7	9	422		49	2.275	10.08	1.182
8	9	482		51.5	2.29	9.94	1.331
9	9	542		53.8	2.295	9.76	1.469
10	9	602		55.9	2.27	9.89	1.654
11	9	662		58	2.19	10.33	1.900
12	9	722		60.3	2.214	10.07	2.020
13	9	782		62	2.172	10.13	2.200
14	9	842		63.9	2.043	10.69	2.500
15	2	895	0	66.2	1.998	10.23	2.543
15	4	897	2	66	2.295		
15	39	932	37	11.2	3.109		
16	9	962	67	14.6	3.144		
17	9	1022	127	25	3.175		
18	9	1082	187	30.7	3.184		
19	9	1142	247	31.6	3.19		
20	9	1202	307	30.9	3.195		
22	9	1322	427	29.1	3.202		
24	9	1442	547	27.9	3.207		
26	9	1562	667	27.3	3.21		
28	9	1682	787	26.5	3.213		
30	9	1802	907	26.3	3.216		
32	9	1922	1027	26	3.217		
34	10	2043	1148	25.8	3.219		
36	9	2162	1267	26	3.22		

29-Oct							
Voc=3.657		Disharge			4C=13.6		
Temp=26.9							
Time							
Min	Secs	Time		Temp	V_cell	I_cell	Capacity (Ah)
0	5	0		26.9	3.657	0	0
0	9	4		26.9	2.038	14.1	0.016
0	40	35		30.3	1.995	13.24	0.129
1	9	64		34	2.025	13.22	0.235
1	38	93		37	2.054	13.25	0.342
2	8	123		39.9	2.059	13.27	0.453
3	8	183		45.7	2.074	13.29	0.676
4	8	243		50.7	2.065	13.27	0.896
5	8	303		55.5	2.068	13.29	1.119
6	8	363		60.1	2.051	13.27	1.338
7	8	423		64.2	2.046	13.28	1.560
8	8	483		68	2.014	13.22	1.774
9	8	543		71.5	2.01	13.22	1.994
9	20	555	0	72.4	1.995	13.19	2.033
9	28	563	8	71.9	3.146		
10	7	602	47	69.6	3.222		
11	7	662	107	66.1	3.243		
12	7	722	167	63.7	3.25		
13	6	781	226	61.1	3.253		
14	9	844	289	59.1	3.255		
15	9	904	349	56.7	3.257		
16	9	964	409	54.7	3.258		
17	9	1024	469	52.7	3.26		
18	8	1083	528	51.1	3.261		
19	7	1142	587	49.7	3.262		
20	8	1203	648	48	3.262		
22	8	1323	768	45.5	3.264		
24	8	1443	888	42.8	3.265		
26	7	1562	1007	41.2	3.266		
28	10	1685	1130	39.8	3.268		
30	6	1801	1246	37.9	3.268		
32	9	1924	1369	36.3	3.269		
34	6	2041	1486	35.1	3.27		
36	7	2162	1607	34.3	3.27		
38	7	2282	1727	33.1	3.271		
40	7	2402	1847	32.3	3.271		
49	9	2944	2389	29.9	3.273		

30-Oct							
Voc=3.654	Disharge			4C=13.6			
Temp=25.1				COOLED			
Time							
Min	Secs	Time		Temp	V_cell	I_cell	Capacity (Ah)
0	4	0		25.2	3.654	0	0
0	7	3		25	3.301	3.05	0.003
0	37	33		27.1	1.979	13.32	0.122
1	8	64		30.3	1.983	13.23	0.235
1	41	97		34.4	2.023	13.27	0.358
2	8	124		36.8	2.027	13.28	0.457
3	8	184		42	2.03	13.29	0.679
4	8	244		47	2.02	13.27	0.899
5	7	303		51.1	2.019	13.26	1.116
6	8	364		55	2.021	13.27	1.342
7	8	424		58.9	2.007	13.24	1.559
7	43	459	0	60.7	2	13.23	1.687
8	7	483	24	31.8	3.219		
8	40	516	57	15.2	3.248		
9	10	546	87	13.9	3.26		
10	7	603	144	27.3	3.27		
11	7	663	204	24.3	3.274		
12	7	723	264	26.5	3.276		
13	9	785	326	27.2	3.278		
14	6	842	383	27.5	3.279		
15	6	902	443	27.1	3.28		
16	9	965	506	27.1	3.28		
17	9	1025	566	27.1	3.281		
18	8	1084	625	27	3.282		
19	8	1144	685	26.8	3.282		
20	8	1204	745	26.9	3.283		
25	10	1506	1047	26.1	3.285		
30	9	1805	1346	25.9	3.286		

2.   BATTERY CHARLIE DISCHARGE DATA

17-Oct						
Voc=3.340	Disharge	C=3.4 A				
Time						
Min	Secs	Time	T©	Vcell	Capacity Ah	Power
0	0	0		3.34	0	11.356
1	0	60		3.01	0.057	10.234
2	0	120		3.005	0.113	10.217
3	0	180		2.995	0.170	10.183
4	0	240		2.994	0.227	10.1796
5	0	300		2.994	0.283	10.1796
6	0	360		2.993	0.340	10.1762
7	0	420		2.993	0.397	10.1762
8	0	480	24.8	2.993	0.453	10.1762
9	0	540	25.3	2.992	0.510	10.1728
10	0	600	25.7	2.994	0.567	10.1796
11	0	660	26.2	2.993	0.623	10.1762
12	0	720	26.3	2.992	0.680	10.1728
13	0	780	26.6	2.992	0.737	10.1728
14	0	840	26.7	2.991	0.793	10.1694
15	0	900	26.9	2.991	0.850	10.1694
20	0	1200	27.3	2.979	1.133	10.1286
25	0	1500	27.5	2.956	1.417	10.0504
30	0	1800	28.2	2.928	1.700	9.9552
35	0	2100	28.4	2.883	1.983	9.8022
40	0	2400	29.2	2.795	2.267	9.503
42	0	2520	29.3	2.724	2.380	9.2616
44	0	2640		2.61	2.493	8.874
45	0	2700		2.52	2.550	8.568
45	10	2710	30	2.5	2.559	8.5
46	0	2760		2.998		
47	0	2820		3.026		
48	0	2880		3.043		
49	0	2940	28.3	3.052		
50	0	3000	28.1	3.059		
51	37	3097	27.6	3.067		
52	0	3120	27.6	3.068		
53	0	3180	27.4	3.071		
54	0	3240		3.073		
55	0	3300		3.075		
56	0	3360	26.7	3.076		
57	0	3420	26.4	3.077		
58	0	3480	26.2	3.078		
59	0	3540	26.1	3.079		
60	0	3600	26.1	3.08		
65	0	3900	25.7	3.083		
70	0	4200	24.6	3.085		
75	0	4500	24.7	3.086		
76	0	4560	24.7	3.087		
77	0	4620	24.7	3.087		
80	0	4800	24.6	3.087		

18-Oct								
Voc=3.443		Disharge	2C=6.8 A					
					30-Oct			
Time					Drain to 2V			
Min	Secs	Time	T©	V_cell	V_cell	I_cell	Capacity Ah	Power
		0	28	3.443	3.656	0	0	
	1	1		2.967	2.792	5.74	0.002	
	33	33	29.4	2.866	2.643	6.43	0.059	
1	3	63	30.1	2.863	2.617	6.43	0.113	
1	30	90		2.866	2.6143	6.43	0.161	
2	0	120	31.4	2.872	2.635	6.43	0.214	
2	33	153		2.878	2.629	6.43	0.273	
3	1	181	32	2.883	2.644	6.43	0.323	
3	31	211		2.887	2.651	6.43	0.377	
4	3	243	33	2.876	2.666	6.43	0.434	
4	30	270		2.878	2.668	6.43	0.482	
5	2	302	34	2.88	2.668	6.43	0.539	
5	33	333		2.882	2.669	6.43	0.595	
6	0	360	34.6	2.883	2.665	6.43	0.643	
6	58	418	35.5	2.883	2.66	6.43	0.747	
8	1	481	36.4	2.88	2.655	6.43	0.859	
9	0	540	37	2.876	2.614	6.43	0.965	
9	58	598	37.7	2.872	2.607	6.43	1.068	
11	1	661	38.3	2.867	2.615	6.43	1.181	
12	0	720	39	2.86	2.618	6.43	1.286	
13	3	783	39.5	2.853	2.615	6.43	1.399	
14	2	842	40	2.846	2.609	6.43	1.504	
15	0	900	40	2.837	2.598	6.43	1.608	
16	3	963	40	2.825	2.589	6.43	1.720	
17	11	1031	40	2.785	2.573	6.43	1.841	
18	6	1086	40	2.758	2.565	6.43	1.940	
19	4	1144	40	2.725	2.551	6.43	2.043	
20	2	1202	40	2.717	2.532	6.43	2.147	
20	59	1259	40	2.67	2.512	6.43	2.249	
22	3	1323	40.2	2.6	2.473	6.43	2.363	
22	30	1350	40.3	2.56	2.455	6.43	2.411	
22	51	1371	40.3	2.522	2.437	6.43	2.449	
22	57	1377	40.3	2.512	2.424	6.43	2.459	
23	8	1388	40.1	2.938	2.424	6.43	2.479	
23	33	1413	39.4	3.052	2.405	6.43	2.524	
24	0	1440	38.8	3.101	2.373	6.43	2.572	
24	30	1470	38.1	3.13	2.331	6.43	2.626	
25	3	1503	37.4	3.146	2.262	6.43	2.685	
26	2	1562	36.4	3.163	1.991	6.43	2.790	
27	1	1621	35.4	3.173		0		
28	4	1684	34.5	3.18		0		
29	2	1742	34	3.184		0		
30	5	1805	33.5	3.188		0		
33	1	1981	31.9	3.195		0		
36	5	2165	30.9	3.198		0		
39	0	2340	27.9	3.2		0		
42	1	2521	29.4	3.202		0		
45	5	2705	29.1	3.204		0		

21-Oct									
Voc=3.405		Disharge				3C=10.2A			
Temp=25.9									
Time									
Min	Secs	Time		Temp		V_cell	I_cell	Capacity Ah	Power
0	2	0		25.9		3.405		0	
0	3	1		25.9		2.686	10.3	0.003	
0	30	28		26.7		2.531	10.07	0.078	
1	4	62		28		2.539	9.76	0.168	
1	35	93		31		2.455	10.5	0.271	
2	3	121		32		2.578	9.57	0.322	
3	3	181		34		2.579	9.88	0.497	
4	4	242		36.2		2.615	9.58	0.644	
5	5	303		38.2		2.586	9.97	0.839	
6	4	362		39.9		2.558	10.42	1.048	
7	3	421		41.7		2.557	10.49	1.227	
8	5	483		43.7		2.536	10.66	1.430	
9	3	541		45.2		2.54	10.54	1.584	
10	5	603		46.6		2.562	10.55	1.767	
11	4	662		47.9		2.553	10.54	1.938	
12	5	723		49.1		2.52	10.55	2.119	
12	55	773	0	49.1	23.2	2.477	10.72	2.302	
13	5	783	10	48.6	22.7	3.081			
13	35	813	40	48	22.1	3.199			
14	3	841	68	47.3	21.4	3.215			
15	5	903	130	46	20.1	3.233			
16	4	962	189	44.3	18.4	3.241			
17	5	1023	250	43.1	17.2	3.246			
18	4	1082	309	41.9	16	3.249			
19	6	1144	371	40.9	15	3.251			
20	4	1202	429	40.3	14.4	3.252			
22	4	1322	549	37.8	11.9	3.254			
24	2	1440	667	36.3	10.4	3.255			
26	6	1564	791	35.3	9.4	3.256			
28	3	1681	908	33.9	8	3.257			
30	4	1802	1029	33.2	7.3	3.257			
32	4	1922	1149	31.7	5.8	3.258			
34	5	2043	1270	31.1	5.2	3.258			
36	5	2163	1390	30.6	4.7	3.259			
38	6	2284	1511	30.2	4.3	3.259			
40	6	2404	1631	29.7	3.8	3.259			
48	46	2924	2151	28.4	2.5	3.26			

25-Oct								
Voc=3.528		Disharge			3C=10.2A			
Temp=25.8								
Time								
Min	Secs	Time		Temp	V_cell	I_cell	Capacity Ah	Power
0	5	0		25.8	3.528		0	
0	6	1		25.9	2.419	11.98	0.00332778	
0	36	31		27.2	2.473	9.96	0.08576667	
1	8	63		29.1	2.462	10.08	0.1764	
1	35	90		30.9	2.471	10.2	0.255	
2	5	120		32.3	2.434	10.87	0.36233333	
3	5	180		35.1	2.518	10.35	0.5175	
4	8	243		37.2	2.572	10.23	0.690525	
5	5	300		39.3	2.526	10.23	0.8525	
6	8	363		40.9	2.554	10.04	1.01236667	
7	7	422		43	2.539	10.09	1.18277222	
8	5	480		44.2	2.545	10.04	1.33866667	
9	7	542		45.9	2.54	10.07	1.51609444	
10	7	602		46.9	2.541	10.03	1.67723889	
11	7	662		48.4	2.528	10.11	1.85911667	
12	7	722		49.3	2.504	10.19	2.04366111	
13	6	781		50.5	2.46	10.41	2.25839167	
14	6	841		52.1	2.394	10.64	2.48562222	
15	6	901		53.5	2.286	11.04	2.76306667	
16	6	961		55.7	2.089	11.27	3.00846389	
16	48	1003	0	57.7	1.705	11.01	3.06750833	
17	6	1021	18	57.5	2.709			
17	36	1051	48	56.6	2.71			
18	7	1082	79	55.2	2.818			
19	8	1143	140	53	2.845			
20	5	1200	197	51.1	2.859			
21	8	1263	260	49.1	2.87			
22	5	1320	317	47.5	2.877			
23	5	1380	377	45.8	2.883			
24	7	1442	439	44.6	2.888			
26	7	1562	559	41.6	2.896			
28	7	1682	679	39.6	2.901			
30	9	1804	801	37.4	2.905			
32	6	1921	918	36.1	2.909			
34	6	2041	1038	34.4	2.912			
36	5	2160	1157	33.4	2.914			
38	5	2280	1277	32.4	2.916			
40	4	2399	1396	31.3	2.918			
49	6	2941	1938	28.9	2.942			

22-Oct								
Voc=3.623		Disharge			3C=10.2A			
Temp=24.5				COOLED				
Time								
Min	Secs	Time		Temp	V_cell	I_cell	Capacity Ah	Power
0	9	0		24.5	3.623		0.000	
0	13	4			2.476	11.76	0.013	
0	41	32		25	2.465	10.06	0.089	
1	10	61		26.5	2.445	10.2	0.173	
1	41	92		27.6	2.44	10.46	0.267	
2	10	121		29.2	2.453	10.46	0.352	
3	10	181		31.9	2.598	9.16	0.461	
4	10	241		33.9	2.486	10.77	0.721	
5	10	301		35.6	2.652	9.45	0.790	
6	10	361		37.1	2.587	10.17	1.020	
7	10	421		38.5	2.561	10.41	1.217	
8	10	481		40.3	2.561	10.38	1.387	
9	10	541		41.5	2.554	10.42	1.566	
10	10	601		42.8	2.542	10.36	1.730	
11	11	662		44	2.535	10.38	1.909	
12	10	721		45.3	2.529	10.27	2.057	
13	10	781		46.2	2.448	10.75	2.332	
14	10	841		47.7	2.383	11	2.570	
15	10	901		49	2.287	11.22	2.808	
16	10	961		50.5	2.084	11.32	3.022	
16	20	971	0	50.7	2	11.27	3.040	
17	10	1021	50	33	3.003			
18	10	1081	110	22.9	3.041			
19	11	1142	171	27.5	3.053			
20	10	1201	230	21.6	3.061			
22	10	1321	350	24.5	3.067			
24	11	1442	471	25.1	3.07			
26	10	1561	590	24.8	3.072			
28	10	1681	710	24.8	3.074			
30	10	1801	830	24.9	3.075			
32	10	1921	950	24.9	3.077			
34	10	2041	1070	24.8	3.078			
36	10	2161	1190	24.8	3.079			
38	10	2281	1310	24.7	3.08			
40	10	2401	1430	24.7	3.081			
43	10	2581	1610	24.6	3.082			

26-Oct						
Voc=3.607		Disharge		12.4A		
Temp=27.1						
Time						
Min	Secs	Time	Temp	V_cell	I_cell	Power
0	12	0	27.1	3.607		
0	16	4	27.2	2.305	12.15	
0	45	33	30.9	2.298	12.15	
1	15	63	33.7	2.34	11.94	
1	45	93	35.2	2.347	11.96	
2	15	123	37	2.388	12.05	
3	15	183	39.9	2.392	12.44	
4	15	243	43.3	2.383	12.43	
5	15	303	46.3	2.372	12.48	
5	20	308	46.8	2.376	12.48	
5	31	319	46.9	3.158		
6	5	353	46	3.25		
6	32	380	45.2	3.273		
7	1	409	44.5	3.285		
7	34	442	43.7	3.292		
7	40	448	43.7	2.488	13.99	
8	15	483	45.9	2.396	13.98	
9	15	543	49.8	2.381	13.72	
10	15	603	52.6	2.413	12.63	
11	15	663	55.8	2.368	12.67	
12	15	723	58.3	2.4	12.62	
13	15	783	59.4	2.388	12.26	
14	15	843	61.1	2.315	12.3	
15	15	903	63.3	2.144	12.56	
15	41	929	64.4	2	12.71	
15	45	933	64.3	2.831		
16	15	963	63.3	2.991		
17	15	1023	60.5	3.045		
18	15	1083	58	3.06		
19	15	1143	55.8	3.069		
20	15	1203	53.8	3.074		
22	15	1323	50.3	3.083		
24	15	1443	47.1	3.089		
26	15	1563	44.5	3.094		
28	15	1683	42.1	3.097		
30	15	1803	38.9	3.101		
32	15	1923	38.4	3.103		
34	15	2043	36.8	3.105		
36	15	2163	35.5	3.107		
38	15	2283	34.5	3.109		
40	15	2403	33.6	3.12		
49	15	2943	30.2	3.114		

29-Oct								
Voc=3.524		Disharge			4C=13.6A			
Temp=27.4								
Time								
Min	Secs	Time		Temp	V_cell	I_cell	Capacity	Power
0	6	0		27.4	3.524		0	
0	9	3		27.5	2.235	14.54	0.012	
0	39	33		30.6	2.215	13.75	0.126	
1	9	63		35	2.267	13.75	0.241	
1	40	94		37.2	2.284	13.76	0.359	
2	11	125		39.2	2.297	13.78	0.478	
3	11	185		43.2	2.317	13.81	0.710	
4	9	243		46.8	2.333	13.83	0.934	
5	11	305		50.5	2.341	13.85	1.173	
6	9	363		54.2	2.334	13.83	1.395	
7	6	420		57.3	2.336	13.84	1.615	
8	9	483		60.1	2.321	13.81	1.853	
9	9	543		62.7	2.31	13.79	2.080	
10	10	604		65.2	2.27	13.73	2.304	
11	10	664		67.9	2.182	13.6	2.508	
12	9	723	0	70.6	2.003	13.3	2.671	
12	12	726	3	70.6	2.695			
12	39	753	30	70.4	2.953			
13	9	783	60	69.1	2.999			
14	9	843	120	66	3.027			
15	9	903	180	63.2	3.04			
16	9	963	240	60.5	3.049			
17	9	1023	300	58.1	3.056			
18	9	1083	360	55.8	3.061			
19	10	1144	421	53.7	3.067			
20	9	1203	480	51.8	3.071			
22	9	1323	600	48.2	3.077			
24	9	1443	720	45.4	3.083			
26	9	1563	840	42.9	3.087			
28	9	1683	960	43.4	3.091			
30	9	1803	1080	41.5	3.094			
32	9	1923	1200	39.5	3.096			
34	9	2043	1320	38	3.098			
36	9	2163	1440	36.4	3.1			
38	9	2283	1560	35.3	3.101			
40	9	2403	1680	34.2	3.103			
49	9	2943	2220	31	3.107			

30-Oct							
Voc=3.618	Disharge			4C=13.6A			
Temp=27.4				COOLED			
Time							
Min	Secs	Time		Temp	V_cell	I_cell	Capacity	Power
0	6	0			3.618	0	0	
0	9	3			2.218	14.39	0.011992	
0	41	35			2.231	13.62	0.132417	
1	10	64			2.206	13.55	0.240889	
1	39	93			2.246	13.61	0.351592	
2	9	123			2.262	13.66	0.466717	
3	9	183			2.297	13.69	0.695908	
4	9	243			2.312	13.69	0.924075	
5	9	303			2.3	13.67	1.150558	
6	9	363			2.295	13.66	1.377383	
7	11	425			2.294	13.66	1.612639	
8	9	483			2.284	13.64	1.830033	
9	8	542			2.28	13.65	2.055083	
10	9	603			2.25	13.6	2.278	
11	10	664			2.179	13.49	2.488156	
12	5	719			1.992	13.17	2.630342	
12	7	721	2		2.726	0		
12	39	753	34		3.019			
13	8	782	63		3.054			
13	39	813	94		3.073			
14	9	843	124		3.084			
15	9	903	184		3.095			
16	9	963	244		3.099			
17	9	1023	304		3.103			
18	9	1083	364		3.107			
19	9	1143	424		3.11			
20	9	1203	484		3.112			
22	9	1323	604		3.116			
24	9	1443	724		3.12			
26	9	1563	844		3.123			
28	9	1683	964		3.126			
30	9	1803	1084		3.128			
35	9	2103	1384		3.133			

THIS PAGE INTENTIONALLY LEFT BLANK

LIST OF REFERENCES

[1]   J.T. Conway, "Opening Remarks," presented at USMC
        Energy Summit, Washington DC, August 2009.

[2]   USMC, "Memorandum 11/09: Establish the Marine Corps
        Expeditionary Energy Office," November 2009.

[3]   B. Newell, "The Evaluation of HOMER as a Marine Corps
        Energy Pre-deployment Tool." M.S.E.E. thesis, Naval
        Postgraduate School, United States of America, 2010.

[4]   Expeditionary Energy Office, "USMC Expeditionary
        Power Systems." 8 Nov, 2011.

[5]   M. Gallagher, "USMC Acquisitions Initiatives in
        Tactical Electrical Power." Internet:
        http://www.dtic.mil/ndia/2011power/GeneralSession_Gal
        lagher.pdf 3 May, 2011, [accessed 5 Aug 2012].

[6]   Expeditionary Energy Office, NAVSEA. "Current Power
        and Energy Requirements of Forward Deployed USMC
        Locations." 24 January 2012.

[7]   HOMER Energy LLC, "History page," June 2010,
        http://homerenergy.com.history.html [Accessed: 5
        September 2012].

[8]   T. Lambert, P. Gillman, and P. Lilienthal, in
        "Micropower system modeling with HOMER," Integration
        of Alternate Sources of Energy, F.A. Farret, M.G.
        Simoes, John Wiley and Sons, December 2005, pp. 379–
        416.

[9]   E. Shields, Carderock Division, NAVSEA, (private
        communication), August 2012.

[10]   HOMER Energy, HOMER Help Menu: Generator, HOMER
        Energy, 2010.

[11]   HOMER Energy, HOMER Help Menu: Photovoltaic Cells,
        HOMER Energy, 2010.

[12]   HOMER Energy, HOMER Help Menu: Kinetic Battery Model,
        HOMER Energy, 2010.

[13]   Wikipedia, "Solar Cells," November 2010, [Online].
        Available: http://en.wikipedia.org/wiki/Solar cells.
        [Accessed 4 April 2012]

[14]   Wikipedia, "Electromagnetic Radiation," November
        2010, [Online]. Available:
        http://en.wikipedia.org/wiki/Electromagnetic radiatio
        n. [Accessed 4 April 2012]

[15]   Wikipedia, "Air Mass (Solar Energy)," November 2010,
        [Online]. Available:
        http://en.wikipedia.org/wiki/Air Mass. [Accessed 4
        April 2012]

[16]   "EC3230 Space Power and Radiation Effects." Class
        notes for EC3230, Department of Electrical and
        Computer Engineering, Naval Postgraduate School,
        Summer 2011.

[17]   A. S. Sedra and K. C. Smith, *Microelectronic
        Circuits*. Oxford University Press, USA, pp. 50–200,
        2009.

[18]   "EC3200 Advanced Electronics Engineering." Class
        notes for EC3200, Department of Electrical and
        Computer Engineering, Naval Postgraduate School,
        Summer 2011.

[19]   "EC4950 Emerging Nanotechnologies." Class notes for
        EC4950, Department of Electrical and Computer
        Engineering, Naval Postgraduate School, Fall 2011.

[20]   M. Pagliaro, R. Ciriminna, and G. Palmisano, (2008,
        July) "Flexible Solar Cells." ChemSusChem. [Online]
        1, 11 pp. 880–891. Available:
        http://onlinelibrary.wiley.com/doi/10.1002/cssc.20080
        0127/abstract. [Accessed: 4 April 2012]

[21]   "New Solar Cell Technology Greatly Boosts
        Efficiency." Science Daily, 29 April, pp. 1–3, 2011.

[22]   A. Regaldo, "Reinventing the Leaf" Internet:
        http://www.scientificamerican.com/assets/zemi/files/p
        df/Reinventing the Leaf.pdf. [Accessed: 4 April 2012]

[23] D. Nocera et al., (2011, November) "Wireless Water Splitting Using Silicon-based Semiconductors and Earth Abundant Catalysts." Science Magazine [Online] 334 pp. 645–648. Available: www.sciencemag.org [Accessed: 4 April 2012]

[24] Google, "Boost Converter Images," 2010, [Online]. Available: http://www.google.com/images?hl=en&biw=1276&bih=598&gbv=2&tbs=isch%3A1&sa=1&q=boost+converter+circuitry&aq=f&aqi=g1g-m1&aql=&oq=&gs_rfai=. [Accessed 22 October 2012]

[25] "EC3150 Solid State Power Electronics Conversion." Class notes for EC3150, Department of Electrical and Computer Engineering, Naval Postgraduate School, Summer 2011.

[26] Google, "Buck Converter Images," 2010, [Online]. Available: http://www.google.com/images?hl=en&source=imghp&biw=1276&bih=598&q=buck+converter&btnG=Search+Images&gbv=2&aq=f&aqi=&aql=&oq=&gs_rfai=. [Accessed 22 October 2012]

[27] S. Fletcher, "Bottled Lightning: Super Batteries, Electric Cars and the New Lithium Economy." New York, NY: Hill and Wang, pp. 38–59,2011

[28] "How Batteries Work," http://electronics.howstuffworks.com/everyday-tech/battery.htm, [Accessed 15 August 2012].

[29] C. C. Keen. "Extending the Endurance, Missions and Capabilities of Most UAVs Using Advanced Flexible/Ridged Solar Cells and New High Power Density Batteries Technology" M.S. thesis, Naval Postgraduate School, United States of America, 2011.

[30] Wikipedia, "Lithium Ion Batteries," November 2010, [Online]. Available: http://en.wikipedia.org/wiki/Lithium_ion_batteries. [Accessed 15 August 2012].

[31] S. Miller, Carderock Division, NAVSEA, (private communication), August 2012.

[32] S. X Chen,., K. J Tseng,., and S. S. Choi, "Modeling of Lithium-Ion Battery for Energy Storage System Simulation," Power and Energy Engineering Conference, pp.1-4, 27-31 March 2009

[33] Y. K. Tan, J. C. Mao, and K. J. Tseng,"Modeling of battery temperature effect on electrical characteristics of Li-ion battery in hybrid electric vehicle," IEEE Ninth International Conference on Power Electronics and Drive Systems pp.637-642, 5-8 Dec. 2011.

[34] A. Shafiei, et. All. "Battery Modeling Approaches and Management Techniques for Plug-in Hybrid Electric Vehicles." http://ieeexplore.ieee.org/xpls/abs_all.jsp?arnumber=6043191&tag=1, September 2011 [Accessed 15 August 2012]

[35] HOMER Energy, HOMER Help Menu: Charging, HOMER Energy, 2010.

[36] HOMER Energy, HOMER Help Menu: Discharging, HOMER Energy, 2010.

[37] M. Cervi, Carderock Division, NAVSEA, (privet communication), August 2012.

[38] E. House, Carderock Division, NAVSEA, (privet communication), August 2012.

INITIAL DISTRIBUTION LIST

1. Defense Technical Information Center
    Ft. Belvoir, Virginia

2. Dudley Knox Library
    Naval Postgraduate School
    Monterey, California

3. Marine Corps Representative
    Naval Postgraduate School
    Monterey, California

4. Director, Training and Education,
    Quantico, Virginia

5. Director, Marine Corps Research Center,
    Quantico, Virginia

6. Marine Corps Tactical Systems Support Activity
    (Attn: Operations Officer)
    Camp Pendleton, California

7. Dr. R. Clark Robertson, Chair
    Department of Electrical and Computer Engineering
    Naval Postgraduate School
    Monterey, California

8. Dr. Sherif Michael
    Department of Electrical and Computer Engineering
    Naval Postgraduate School
    Monterey, California

9. Dr. Daniel Nussbaum
    Department of Operations Research
    Naval Postgraduate School
    Monterey, California

10. CAPT Kline, USN Ret
    Department of Operations Research
    Naval Postgraduate School
    Monterey, California

11. Dr. H.S. Coombe
    Office of Naval Research
    Arlington, Virginia

12. Maj Brandon Newell
    United States Marine Corps
    Expeditionary Energy Office

13. Dr. Peter Lilienthal
    HOMER Energy LLC
    Boulder, Colorado

14. Dr. Steve Miller
    Philadelphia, PA

15. Maj Nora Pencola
    San Diego, California

16. Cynthia Harvey
    Stafford, Virginia

17. Alexis R. Harvey
    Naval Postgraduate School
    Monterey, California